INDUCING NEURAL PLASTICITY AFTER SPINAL CORD INJURY TO RECOVER IMPAIRED VOLUNTARY MOVEMENT

By

Jordan Alexander Borrell

Submitted to the graduate degree program in Bioengineering and

the Graduate Faculty of the University of Kansas in partial fulfillment of the

requirements for the degree of Doctor of Philosophy.

Dissertation Committee:

_____

Chairperson Randolph J. Nudo, Ph.D.

_____

Paul D. Cheney, Ph.D.

_____

Jessie M. Huisinga, Ph.D.

_____

Carl W. Luchies, Ph.D.

_____

Arvin Agah, Ph.D.

Date Defended: Friday, September 27th, 2019

The Dissertation Committee for Jordan Alexander Borrell
certifies that this is the approved version of the following dissertation:

INDUCING NEURAL PLASTICITY AFTER SPINAL CORD INJURY TO RECOVER IMPAIRED VOLUNTARY MOVEMENT

_____

Chairperson Randolph J. Nudo, Ph.D.

Date Approved: Friday, September 27th, 2019

ABSTRACT

Spinal cord injury (SCI) is often an incapacitating neural injury most commonly caused by a traumatic blow to the spine. A SCI causes damage to the axons that carry sensory and motor signals between the brain and spinal cord, and in turn, the rest of the body. Depending on the severity and location of a SCI, many corticospinal axons and other descending motor pathways can remain intact. Moderate spontaneous functional recovery occurs in patients and animal models following incomplete SCI. This recovery is linked to changes occurring via the remaining pathways and throughout the entire nervous system, which is generally referred to as neuronal plasticity. It has been shown that plasticity can be induced via electrical stimulation of the brain and spinal cord targeting specific descending pathways, which can further improve impaired motor function. Most importantly, it has been shown that activity dependent stimulation (ADS), which is based on mechanisms of spike timing-dependent plasticity, can strengthen remaining pathways and promote functional recovery in various preclinical injury models of the central nervous system.

The purpose of this dissertation was to determine if precisely-timed stimulation of the spinal cord triggered by the firing of neurons in the hindlimb motor cortex would result in potentiation of corticospinal connections as well as enhance hindlimb motor recovery after spinal cord contusion. In order to achieve this, we needed to determine the optimal neurophysiological conditions which would allow activity dependent stimulation (ADS) to facilitate enhanced communication between the cerebral cortex and spinal cord motor neurons. Thus, this dissertation project investigated three specific aims.

The first study determined the effects of a contusive spinal cord injury on spinal motor neuron activity, corticospinal coupling, and conduction time in rats. It was discovered that spinal cord responses could still be evoked after spinal cord contusion, most likely via the cortico-

reticulo-spinal pathway. The second study determined the optimal spike-stimulus delay for increasing synaptic efficacy in descending motor pathways using an ADS paradigm in an acute, anesthetized rat model of SCI. It was discovered that bouts of ADS conditioning can increase synaptic efficacy in intact descending motor pathways, as measured by cortically evoked activity in the spinal cord, after SCI. The third study determined whether spike-triggered intraspinal microstimulation (ISMS), using optimized spike-stimulus delays, results in improved motor performance in an ambulatory rat model of SCI. It was determined that ADS therapy can enhance the behavioral recovery of locomotor function after spinal cord injury.

The results from this study indicate that activity-dependent stimulation is an effective treatment for behavioral recovery following a moderate spinal cord contusion in the rodent. The implications of these results have the potential to lead to a novel treatment for a variety of neurological disease and disorders.

ACKNOWLEDGEMENTS

I wish to express my deepest appreciation to my advisor, Dr. Randy Nudo, for his constant support and guidance throughout my graduate career and this study. He has given me the opportunity to work on a project that holds my interest to the highest degree and has a direct benefit to a population in need. I am thankful to my committee, Dr. Paul Cheney, Dr. Jessie Huisinga, Dr. Carl Luchies, and Dr. Arvin Agah for their input and support in this work. I especially would like to thank them for taking time out of their busy schedules to review and guide this project.

I also would like to thank Dr. Shawn Frost for his ongoing support, training, and guidance during my graduate career. His teaching of surgical and histological techniques was critical to the success of this study. I wouldn't be where am I today without his assistance. Additionally, I would like to thank Erica Hoover, the research assistant for this project, and Brad Lamb, a current graduate student in the lab, for their assistance in behavioral training and testing. Their aid in this aspect allowed me to successfully complete this study on the appropriate timeline.

Similarly, I am grateful for the collaborative support and assistance. Special thanks go to Dr. Domenico Gattozzi, a current neurosurgeon resident, and Dr. Dora Krizsan-Agbas. Dr. Gattozzi's assistance and guidance during the spinal cord implantation procedure was critical to the success of this project. I am grateful for the time he took out of his busy schedule to share his knowledge of surgical techniques and help perform a crucial step in the study. Dr. Krizsan-Agbas's conduction of the spinal cord contusion procedure was imperative for a reproducible injury model. I want to thank her as well for the time she took out of her busy schedule to perform this procedure. This study would not have gone so smoothly without their help.

I am especially thankful for the constant support and guidance of the Nudo lab. For listening to my frustrations and allowing me to bounce ideas off them, I am very much indebted.

Special thanks go to Dr. Scott Barbay, Dr. Heather Hudson, and Dr. David Guggenmos, the senior researchers in the lab, for their additional guidance and advice during the day-to-day tasks and issues that would arise. I am thankful for the amazing graduate students, Max Murphy and Page Haley, in the lab who have kept me focused along the way. The comradery and easy-nature of the lab is something that made my time in the lab that much easier and enjoyable, and I thank the entire Nudo lab for the memories and fun times.

Finally, I would like to thank my parents, Art and Evonne Borrell, for their continued support and encouragement as I battled through the ups and downs of my graduate studies. Their love and support kept me on track to successfully completing and earning my doctoral degree. I credit them for my success, as I couldn't have done it without such amazing parents.

TABLE OF CONTENTS

LIST OF TABLES

CHAPTER 3

CHAPTER 4

CHAPTER 5

LIST OF FIGURES

CHAPTER 2

CHAPTER 3

CHAPTER 4

CHAPTER 5

LIST OF ABBREVIATIONS

ADS	Activity Dependent Stimulation
BBB	Basso, Beattie, and Bresnahan
BCSC	Brain-Computer-Spinal Cord
CST	Corticospinal Tract
EMG	Electromyography
EPSP	Excitatory Post-Synaptic Potential
FL-HL	Forelimb-Hindlimb
FR	Firing Rate
HLA	Hindlimb Area of Motor Cortex
ICMS	Intracortical Microstimulation
ISMS	Intraspinal Microstimulation
L1	First Long-Latency Response
LTD	Long-Term Depression
LTP	Long-Term Potentiation
M1	Primary Motor Cortex
MEP	Motor Evoked Potential
Peak	Peak Long-Latency Response
POA	Probability of Activation

RbST	……	Rubrospinal Tract
RtST	……	Reticulospinal Tract
SCI	……	Spinal Cord Injury
SD	……	Standard Deviation
SE	……	Standard Error
Short	……	Short-Latency Response
STDP	……	Spike Timing-Dependent Plasticity
StTA	……	Stimulus-Triggered Average
TMS	……	Transcranial Magnetic Stimulation

CHAPTER ONE: Introduction

Motivation

The leading causes of paralysis include stroke, spinal cord injury, multiple sclerosis, cerebral palsy, and accidental injury which together affect roughly 5.3 million people in the United States (Foundation 2012). Spinal cord injury (SCI) is a devastating neurological trauma that affects approximately 291,000 people in the United States (National Spinal Cord Injury Statistical Center 2019). In addition, there are approximately 17,730 new cases of SCI reported each year (National Spinal Cord Injury Statistical Center 2019). A SCI can be caused by a car accident, sports injury, work related trauma, fall, or war wound (Migliorini, Tonge et al. 2008, Foundation 2009). In the United States, alcohol has been found to be a large contributing factor resulting in 25% of spinal cord injuries (Prevention 2010). Most notably, for returning USA military service members, the most common war injury is a spine fracture representing 83% of all wounds and occurring in 91% of all casualties (Schoenfeld, Laughlin et al. 2013). With increasing amounts of people living with paralysis due to a SCI, there is a need for treatment options for spinal cord injured patients.

When living with a SCI, the cost for treatment and care can be overwhelming. The cost of living for someone with SCI increases exponentially depending on severity and location of injury on the spinal cord. Depending on the severity of the SCI, the average yearly expense for each subsequent year is anywhere from $120,000 to $200,000 per year (National Spinal Cord Injury Statistical Center 2019). For an incomplete motor functional injury at any level of the spinal cord, the estimated lifetime cost for a 25 year old is approximately $3.7 million; however, for a high tetraplegia (C1-C4) injury, the estimated lifetime cost for a 25 year old is approximately $5.0 million (National Spinal Cord Injury Statistical Center 2013, National Spinal Cord Injury Statistical Center 2019). In addition to the costs, 87.9% of all SCI patients are discharged from hospitals to private homes where renovations to their living space need to be made for handicap accessibility (Foundation 2009). In essence, the cost of a SCI is a financial burden for which few people are readily prepared and can arise at any moment.

In addition to the financial burden, SCI patients also endure a mental burden. From the moment a person obtains a SCI, their life changes dramatically. In a study conducted by Migliorini, Tonge, and Taleporos, nearly half of the population (48.5%) with SCI suffered from depression (37%), anxiety (30%), clinical-level stress (25%), or post-traumatic stress disorder (8.4%) (Migliorini, Tonge et al. 2008). In addition to the patient, the caretaker and support network of the patient bears the mental and financial burden, as SCI patients may or may not need some form of assistance. Depending on the severity of the injury, a caretaker may have to feed, bathe, dress, and aid the patient every day and night. As a result, a SCI affects the patient and their support network in multiple ways. With a SCI, there is a potential loss of income, loss of employment, loss of freedom, and loss of support (Foundation 2009, National Spinal Cord Injury Statistical Center 2013), which could have a detrimental impact the mental state of a SCI patient.

With these issues in mind, researchers have focused on various avenues of recovery after a SCI. However, most rehabilitation and treatment strategies can only improve function to varying degrees. As a result, studies are now looking to reorganize and strengthen neuronal pathways (i.e., induce plasticity) via electrical stimulation. Plasticity is a natural ability of the central nervous system that researchers are now coming to understand. From the studies of Shahdoost, et al. (Shahdoost, Frost et al. 2014a, Shahdoost, Mohseni et al. 2014b), an exciting development of brain-computer-spinal cord (BCSC) interface devices seeks to confirm the idea that a SCI injury can be bypassed with a BCSC interface device and motor function can be restored by inducing plasticity on the central nervous system. With the likelihood of some functional recovery, there is a possibility to alleviate some of the burden a SCI imposes on the patient and caretaker.

Specific Aims

Depending on the severity and location of a SCI, many corticospinal axons and other descending motor pathways can remain intact. As a result, an alternative approach to treatment may be to use neurophysiological principles of synaptic potentiation to condition spared corticospinal fibers. This approach, called activity-dependent stimulation (ADS), utilizes devices that record and digitize extracellular neural activity from an implanted microelectrode, discriminates individual action potentials in real time, and delivers small amounts of electrical current to another microelectrode implanted in a distant population of neurons, essentially artificially bypassing the injury. This ADS paradigm results in enhanced synaptic efficacy, and thus, may provide more effective control of spinal cord motor neuron activation from control signals in the motor cortex (M1), aiding in the restoration of motor function. In this proposal, we will test the central hypothesis that precisely-timed stimulation of the spinal cord triggered by the firing of neurons in M1 will result in potentiation of corticospinal connections as well as enhanced motor recovery after SCI.

Prior results demonstrated the effect of ADS in restoring skilled motor function after traumatic brain injury (Guggenmos, Azin et al. 2013). Intraspinal microstimulation (ISMS) has been used to derive a three-dimensional map of hindlimb motor representations in the lumbar spinal cord of the rat (Borrell, Frost et al. 2017), demonstrating our ability to target selected motor neuron pools. The proposed project will determine the optimal neurophysiological conditions which will allow ADS to facilitate enhanced communication between the cerebral cortex and spinal cord motor neurons. We will utilize our extensive experience and understanding of neurophysiological recording, microstimulation, and behavioral assessment in a preclinical model to assess the role of synaptic plasticity in response to ADS in motor recovery after SCI. Three specific aims are proposed:

Aim 1: Determine the effects of a contusive spinal cord injury on spinal motor neuron activity, corticospinal coupling, and conduction time in rats. After an SCI, intracortical microstimulation (ICMS) will be administered in the hindlimb area of M1 and extracellular single-unit activity will be recorded in the lumbar spinal cord to assess the efficacy of corticospinal control of spinal cord motor neurons. Results will be compared to pre-injury ICMS-evoked activity. Hypothesis 1: ICMS-evoked unit activity in the spinal cord will decrease and conduction time will be altered after a spinal cord contusion injury.

Aim 2: Determine the optimal spike-stimulus delay for increasing synaptic efficacy in descending motor pathways using an ADS paradigm in an acute, anesthetized rat model of SCI. Single-unit spikes will be detected in real time in the hindlimb area of M1 and used to deliver precisely-timed electrical stimulation (10–25 ms spike-stimulus delay) in the spinal cord ventral horn. Synaptic efficacy will be measured by the number of ICMS-evoked spikes in the matched site in the lumbar spinal cord in one 5-minute pre-ADS period and three 5-minute test periods following each 1-hour ADS conditioning bout. Fine-wire EMG recordings derived from hindlimb muscles will validate the optimal parameters as a secondary measure. Hypothesis 2: Synaptic efficacy of corticospinal connections will vary as a function of ISMS current spike-stimulus delay. The optimal stimulus delay will be used in Aim 3.

Aim 3: Determine whether spike-triggered ISMS, using optimized spike-stimulus delays, results in improved motor performance in an ambulatory rat model of SCI. Optimized parameters derived from Aim 2 will be utilized to determine if these results can be extended to ambulatory, tethered rats with SCI. A battery of behavioral tasks will be used to document motor performance before and after the ADS treatment. Hypothesis 3: Spike-triggered ISMS will result in improved motor performance.

Our long-term research goal is to use novel neurotechnological approaches to restore impaired motor function in the lower limbs following spinal cord injury. The proposed studies will establish a new SCI rat model of ADS that will overcome current limitations in SCI research and provide novel approaches to potentiate synaptic efficacy in the spared fibers descending to the spinal cord. It is likely that these neurophysiological results will allow greater insight into plasticity mechanisms underlying motor recovery after SCI. These studies in rats will provide an entirely new approach to restorative treatment after SCI. Future studies will test the ability of spike-triggered ISMS to improve motor performance in a larger preclinical animal model, eventually leading to human clinical trials.

Dissertation Content

This thesis document contains six chapters. Chapter 1 consists of an introduction and motivation to the dissertation topic. Chapter 2 contains an extensive background search of relevant published literature related to the dissertation topic. Chapter 3 is the first of 3 manuscripts, this one reporting the background, methods, and results of Aim 1 of this dissertation study investigating the effects of a contusive spinal cord injury on spinal motor neuron activity, corticospinal coupling, and conduction time in rats. The Aim 1 manuscript has been submitted for publication and is currently under review. Chapter 4 is the second manuscript reporting the background, methods, and results of Aim 2 of this dissertation study investigating the optimal spike-stimulus delay for increasing synaptic efficacy in descending motor pathways using an ADS paradigm in an acute, anesthetized rat model of SCI. Chapter 5 is the third manuscript reporting the background, methods, and results of Aim 1 of this dissertation study investigating whether spike-triggered ISMS, using optimized spike-stimulus delays, results in improved motor performance in an ambulatory rat model of SCI. The Aim 2 and Aim 3 manuscripts are currently in the early draft stages. Chapter 6 is a summary of this dissertation document.

References

Borrell, J. A., S. B. Frost, J. Peterson and R. J. Nudo (2017). "A 3D map of the hindlimb motor representation in the lumbar spinal cord in Sprague Dawley rats." J Neural Eng **14**(1): 016007.

Foundation, C. D. R. (2009). "One Degree of Separation: Paralysis and Spinal Cord Injury in the United States." from www.christopherreeve.org.

Foundation, C. D. R. (2012). Christopher & Dana Reeves Foundation - Policy Data Brief: Paralysis in the US.

Guggenmos, D. J., M. Azin, S. Barbay, J. D. Mahnken, C. Dunham, P. Mohseni and R. J. Nudo (2013). "Restoration of function after brain damage using a neural prosthesis." PNAS **110**(52): 21177-21182.

Migliorini, C., B. Tonge and G. Taleporos (2008). "Spinal cord injury and mental health." Aust N Z J Psychiatry **42**(4): 309-314.

National Spinal Cord Injury Statistical Center, B., Alabama (2013). Spinal Cord Injury Facts and Figures at a Glance.

National Spinal Cord Injury Statistical Center, B., Alabama (2019). Spinal Cord Injury Facts and Figures at a Glance.

Prevention, C. f. D. C. a. (2010). "Spinal Cord Injury (SCI): Fact Sheet." from http://www.cdc.gov/traumaticbraininjury/scifacts.html.

Schoenfeld, A. J., M. D. Laughlin, B. J. McCriskin, J. O. Bader, B. R. Waterman and P. J. Belmont, Jr. (2013). "Spinal injuries in United States military personnel deployed to Iraq and Afghanistan: an epidemiological investigation involving 7877 combat casualties from 2005 to 2009." Spine (Phila Pa 1976) **38**(20): 1770-1778.

Shahdoost, S., S. B. Frost, G. M. Van Acker, 3rd, S. DeJong, C. Dunham, S. Barbay, R. J. Nudo and P. Mohseni (2014a). "Towards a Miniaturaized Brain-Machine-Spinal Cord Interface

(BMSI) for Restoration of Function after Spinal Cord Injury." IEEE Eng Med Biol Soc.: 486-489.

Shahdoost, S., P. Mohseni, S. B. Frost and R. J. Nudo (2014b). A Multichannel Coricospinal Interface IC for Intracortical Spike Recording and Distinct Muscle Pattern Activation via Intraspinal Microstimulation. 2014 IEEE 57th International Midwest Sympsium on Circuits and Systems (MWSCAS). College Station, TX**:** 310-313.

CHAPTER TWO: Background

Spinal Cord Injury

Spinal cord injury (SCI) results in damage to the axons that carry sensory-motor signals between the brain and the spinal cord, and in turn, the rest of the body. A SCI is defined as *anatomically complete* if all of the ascending and descending neuronal tracts are severed and prognosis for recovery is very poor. Even in the case of an anatomically complete injury, the neuronal circuitry and pathways above and below the lesion generally remain intact, except for axons severed from their cell bodies. While it is possible for such axon fragments to persist for weeks, severed myelin sheaths generally retract and then axons degenerate distal to the injury through a process known as Wallerian degeneration (Chen, Nabavizadeh et al. 2016). This effectively disconnects the spared neural circuits that remain intact both above and below the site of injury.

The devastating sensory-motor deficits incurred by anatomically complete injuries persist for multiple reasons. Axon growth-inhibitory proteins such as NOGO-A prevents axonal regeneration in the central nervous system (Buss, Pech et al. 2005). Scar tissue at the site of injury may also make it difficult for any sprouting axons to traverse the injury site (Guth, Zhang et al. 1999). Fortunately, about half of all new SCIs are *incomplete* based on neurological criteria (National Spinal Cord Injury Statistical Center 2019). An incomplete SCI renders hope for partial to full recovery of sensory and motor function with appropriate post-operative care and rehabilitation. The most common form of incomplete SCI seen in the clinic occurs after contusion of the spinal cord from the dorsal aspect. If the force and penetration of the contusion is limited, a subset of the neuronal tracts may be spared. Typically, neuronal tracts along the dorsal surface are damaged, while the ventral and lateral neuronal tracts may remain intact. For restorative approaches, spared descending fibers represent a promising neural substrate that is targeted for neurophysiological enhancement. Through the ablation and sparing of specific descending motor pathways, research can help identify the functional role of each

motor pathway and their participation in various spinal cord injuries, guiding therapy for rehabilitation.

Furthermore, even when spinal cord injuries are diagnosed as complete based on neurological criteria, they are not necessarily anatomically complete, and some sensory and motor fibers remain intact below the level of injury. Throughout an individual's life, dendrites and spines branch and proliferate, synapses form and degenerate, and the efficacy of synaptic contacts is modulated within a complex network of ascending and descending connections between the brain and spinal cord. Thus, it is not surprising that after a SCI, the structure and function of these interconnected regions are drastically altered (i.e., neuroplasticity occurs). Since neuroplasticity and the gradual replacement of lost synapses by the sprouting of undamaged axons may contribute to recovery after SCI (Bareyre, Kerschensteiner et al. 2004), it is critical to understand how plasticity might be directed to optimize recovery.

Descending Motor Pathways of the Rat

In order to direct plasticity and enhance functional recovery of locomotion, it would first be beneficial to identify and understand the specific descending pathways normally involved in the initiation and maintenance of locomotion. There are three well-studied descending pathways normally involved in the initiation and maintenance of locomotion in the rat, which will be described here: the corticospinal tract, reticulospinal tract, and rubrospinal tract (Figure 2.1). These three tracts combine to allow the execution of normal gait in intact rats: the corticospinal tract (CST) allows for voluntary control of limb movement; the reticulospinal tract (RtST) is involved in the initiation of limb movement, during phase control, and postural responses to coordinate sustained stepping and adjustments to perturbation; and the rubrospinal tract (RbST) is most active during swing phase of gait. In the following sections, their anatomy and function are described in greater detail.

The Corticospinal Tract

The corticospinal tract (CST) is the principal pathway that allows for voluntary control of limb movement (Nudo and Masterton 1990, Oudega and Perez 2012). The CST in the rat (Figure 2.1A) originates in the motor cortex and terminates mainly in the deep dorsal horn and intermediate grey matter (Casale, Light et al. 1988, Akintunde and Buxton 1992, Mitchell, McCallum et al. 2016). Corticospinal neurons residing in layer V of the hindlimb motor cortex are known to converge at the corpus callosum, course through the internal capsule, cross the midline in the pyramidal decussation (~90% of corticospinal axons in the rat), and descend predominantly in the contralateral dorsal funiculus and to a lesser extent in the ipsilateral ventral funiculus and in the contralateral lateral funiculus (Brown 1971, Terashima 1995, Lemon 2008, Fink and Cafferty 2016). Of the descending funiculi in the spinal cord, the rat CST has three bilateral components that descend in the ventral part of the dorsal funiculus, the dorsal aspect of the lateral funiculus, and the medial aspect of the ventral funiculus. These CST fibers have been found at all rostro-caudal levels of the spinal cord (Lemon 2008). Similarly, the CST in non-human primates and humans (Figure 2.1B) originates in the motor cortex, courses through the internal capsule, and crosses the midline in the pyramidal decussation (~90% cross in non-human primates and ~75% cross in humans). In contrast to the rat CST, the CST of non-human primates and humans has two bilateral components descending in the dorsolateral funiculus and medical aspect of the ventral funiculus (Oudega and Perez 2012).

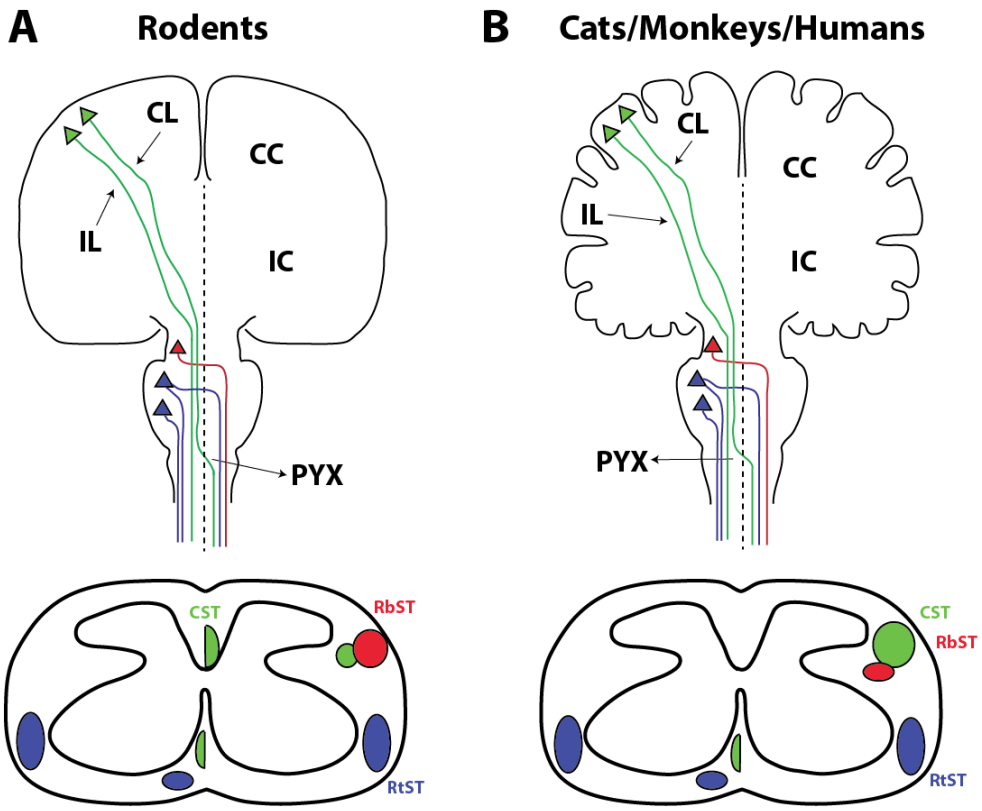

Figure 2.1. Schematic drawings of the brain and spinal cord illustrating the course of the descending motor pathways in A) adult rodents and B) cats/monkeys/humans. In rats, cats, monkeys, and humans, descending motor pathways originate from the same structures in the brain. Differences occur in the location (i.e., funiculi) of the descending pathways in the spinal cord. Corticospinal tract (CST; green), rubrospinal tract (RbST; red), reticulospinal tract (RtST; blue), corpus callosum (CC), internal capsule (IC), pyramidal decussation (PYX), contralateral (CL), ipsilateral (IL), and midline (dashed line). Figure was modified from previously reported figures by Oudega and Perez and are not drawn to scale (Oudega and Perez 2012).

In humans, the CST has direct cortico-motoneuronal connections which allow for skilled movements of the hand and figures and helps mediate and adjust gait. As a result, bilateral lesions to the CST have devastating effects on walking in humans (Nathan 1994). These connections and impairments are similarly seen in non-human primates. At first, it was shown via anatomical tracing and electrophysiology that rats, much like non-human primates and humans, have direct cortico-motoneuronal connections (Liang, Moret et al. 1991). However, it was later shown that there are no such connections in the adult rat (Yang and Lemon 2003, Alstermark, Ogawa et al. 2004). In the mouse, corticospinal neurons in the forelimb motor

cortex synapse onto spinal cord interneurons while corticospinal neurons in the sensory cortex synapse onto different interneurons, suggesting that corticospinal neurons in the motor and sensory cortices differentially control skilled movement through distinct corticospinal interneuron circuits (Ueno, Nakamura et al. 2018). The fact that different populations of corticospinal neurons project in a segregated manner suggests that the CST is composed of subsystems controlling different spinal cord circuits that modulate motor outputs and sensory inputs in a coordinated manner (Olivares-Moreno, Moreno-Lopez et al. 2017).

Functional Role of the Corticospinal Tract

It is generally accepted that the CST in the rat, located in the dorsolateral funiculus, has an important role for reaching and digit grasping (i.e., fine motor skills) (Whishaw, Pellis et al. 1993, Alaverdashvili and Whishaw 2008) and has less important role in gait (Schucht, Raineteau et al. 2002). However, studies of CST transection have shown the importance of the CST in the rat during gait. Bilateral ventral transections, as compared to bilateral dorsal transections, have demonstrated the importance of the ventrolateral funiculus in the control of open-field locomotion (BBB scores); however, bilateral dorsal transections demonstrated the importance of the dorsolateral funiculus for precise limb control to locomote on the grid walk (Schucht, Raineteau et al. 2002). Additionally, in quadrupedal animals, recordings of CST neurons have shown that the corticospinal pathway is directly involved in skilled movements and gait modifications (Beloozerova and Sirota 1993, Drew, Jiang et al. 1996). These neuronal recordings and lesion studies further suggest that the CST in the rat has an important role in fine motor placement and voluntary control of movements in both the forelimbs and hindlimbs.

Regardless of lesion severity, corticospinal axons are severely damaged following a contusion SCI in rats (Basso, Beattie et al. 2002). This type of bilateral moderate contusion has shown deficits during overground walking as measured by decreased BBB scores and impairments on the treadmill recorded via the DigiGait Imaging System (Krizsan-Agbas, Winter

et al. 2014). Similarly, following a unilateral transection of the pyramidal tract, severe impairments were observed including hypermetria, trunk instability, lateral shifts in weight support, toe dragging, and hindlimb exo-rotation but recovered rapidly within the first week post-SCI (Metz, Dietz et al. 1998). Although there is a rapid recovery of hindlimb deficits after a unilateral injury to the CST, the initial deficits show the importance of the CST. Additionally, after damage to the crossed CST alone, rats have difficulty traversing a horizontal ladder, a task that requires accurate placement of the feet (Metz and Whishaw 2002). These lesion studies show the importance of the corticospinal system in the regulation of hindlimb locomotor activity, where it has been shown that there is a requirement for precise modification of limb trajectory (Drew, Jiang et al. 2002).

The Reticulospinal Tract

In addition to the CST, the reticulospinal (RtST) (Waldron and Gwyn 1969, Zemlan, Behbehani et al. 1984) plays an important role in voluntary movement. The RtST originates in the gigantocellular and pontine nuclei, bilaterally projects, and terminates primarily within the intermediate grey matter of lamina VII and VIII in the rat (Matsuyama, Mori et al. 1999, Mitchell, McCallum et al. 2016). These RtST fibers are located primarily in the ventral and ventrolateral funiculi and are found at all rostro-caudal levels of the spinal cord (Waldron and Gwyn 1969, Mitchell, McCallum et al. 2016).

It has been shown that the fastest excitatory pathways from motor cortex in the rat are mediated disynaptically via a cortico-reticulospinal-motoneuronal pathway, while the slower excitatory pathways are mediated polysynaptically via corticospinal fibers and segmental interneurons (Alstermark, Ogawa et al. 2004). The RtST has a larger number of terminals on local commissural interneurons and long descending propriospinal neurons as compared to the CST (Mitchell, McCallum et al. 2016). Since forelimb-hindlimb (FL-HL) and left-right coordination (i.e., interlimb coordination) is controlled via long descending propriospinal

pathways (Frigon 2017), these terminals suggest that left-right activity in the rat spinal cord is not influenced directly via CST systems but is strongly controlled by the RtST pathway and could contribute to functional recovery following damage to the CST

Functional Role of the Reticulospinal Tract

Following a CST lesion in the C1-C2 spinal segments which spares the cortico-reticulospinal pathways, marked deficits were not seen in reaching and grasping, which implicates an important role of the RtST in their control within the rat (Alstermark and Pettersson 2014). In rats with mild and moderate T8 spinal cord contusions, it was shown that spared RtST fibers from different origins exist in both the dorsolateral funiculi and the ventrolateral funiculi (Basso, Beattie et al. 2002). Rats with spared RtST fibers recover 7 to 8 points in the BBB locomotor score as compared to those with only spared CST fibers, further implicating the RtST as an important player in the initiation and control of open-field locomotion (Schucht, Raineteau et al. 2002).

The role of RtST in locomotor ability may be enacted through the mediation of phase-specific control of individual limbs, postural adjustments to ensure sustained stepping, and limb and postural responses to perturbations (Basso, Beattie et al. 2002). Furthermore, forelimb-hindlimb and left-right coordination are controlled via long descending propriospinal pathways (Frigon 2017), which receive a larger number of terminals from reticulospinal neurons as compared to corticospinal neurons; this suggests that left-right activity is strongly controlled by the reticulospinal pathway (Mitchell, McCallum et al. 2016).

The Rubrospinal Tract

The rubrospinal tract (RbST) originates from magnocellular neurons in the red nucleus of the midbrain and terminates primarily in the intermediate grey matter of laminae V, VI, and VII in the rat (Brown 1974). More specifically, the distribution of neurons in the red nucleus consists

of large cells in the caudal, magnocellular division as well as small densely packed cells in the rostral, parvocellular division (Basso, Beattie et al. 2002). These RbST fibers are located primarily in the contralateral dorsolateral funiculus and have been shown to project to all rostro-caudal levels of the spinal cord , while the other 20% of the fibers descend in the ipsilateral dorsolateral funiculus (Brown 1974, Kuchler, Fouad et al. 2002).

Functional Role of the Rubrospinal Tract

To determine the functional role of the RbST, most studies have focused on lesion studies in the cat since the RbST has a more prominent role in gait in the cat as compared to rats. It has been shown that the rubrospinal rather than the corticospinal tract is associated with recovery of inclined plane performance in rats with compressive injuries to the thoracic cord (Fehlings and Tator 1995). Specifically, it has been shown in the cat that the rubrospinal tract excites hindlimb flexor motoneurons via polysynaptic pathways (Hongo, Jankovska et al. 1969) and that stimulation of the red nucleus during locomotion enhances flexor activity during the swing phase (Orlovsky 1972). With this notion, it was further shown in the cat that the majority of rubrospinal neurons descending to the lumbosacral spinal cord are modulated in phase with the locomotor cycle, with maximal discharge at the swing phase when flexors are active (Orlovsky 1972).

Additionally, unilateral excitotoxic lesions of the red nucleus in rats produced asymmetric gait during braking and propulsion between the contralateral forelimb and ipsilateral hindlimb, which provides evidence that the red nucleus plays a role in ongoing overground locomotion in the rat (Muir and Whishaw 2000, Webb and Muir 2003). Conversely, after bilateral pyramidal tract lesions in rats, some dorsolateral funiculus pathways, including the RbST, were able to compensate for loss of CST input during skilled reaching but not during overground or skilled locomotion (Kanagal and Muir 2009). Even with these disparate results, it has been shown that the ventrolateral funiculus is important while the dorsal funiculus is relatively insignificant in the

control of open-field locomotion; however, for precise limb control to locomote on the grid walk sparing of the dorsolateral or dorsal column is also required (Schucht, Raineteau et al. 2002). Additionally, in rats with mild and moderate T8 spinal cord contusions, it has been shown that the recovery of forelimb-hindlimb coordination is also associated with the number of rubrospinal axons spared after injury, especially if long descending propriospinal axon sparing is insufficient (Basso, Beattie et al. 2002). As a result, the RbST has no role in the initiation of open-field locomotion but plays a role in ongoing, flat surface overground locomotion in the rat.

The Vestibulospinal Tract

Most studies of the vestibulospinal tract (VST) have been conducted in the cat. However, recent studies have shown that the pattern of organization of the vestibulospinal tracts in the mouse is very similar to that in the cat (Liang, Paxinos et al. 2011, Liang, Bacskai et al. 2014). Thus, it can be assumed that this organization in the rat is very similar. The VST originates in the vestibular complex which is composed of the lateral, medial, and spinal vestibular nuclei and terminates primarily in the ventromedial spinal gray mater (Nudo and Masterton 1988, Basso, Beattie et al. 2002). The vestibulospinal fibers are located primarily in the ventromedial and ventrolateral funiculi and terminate in all rostrocaudal levels of the spinal cord. More specifically, a study in the rat found that the ventrolateral VST arises from the lateral vestibulospinal nucleus, ipsilaterally descends to all rostrocaudal levels of the spinal cord, and terminates predominately in the lumbosacral segments (Shamboul 1980). However, it was shown in the cat that the fibers arising from the medial and spinal vestibular nuclei descend in the ventromedial VST and project to both sides of the spinal cord (Hayes and Rustioni 1981).

Functional Role of the Vestibulospinal Tract

The VSTs are the main initiators of coordinated postural extensor activity in the limbs and trunk. The lateral VST was shown to be responsible for initiating extensor tone in the limbs (Pompeiano 1972). The medial VST has been shown to coordinate head position with the

position of the body in space and mediate the vestibulocollic reflex in the cat (Wilson, Boyle et al. 1995).

Plasticity After Spinal Cord Injury

Disruption of the CST, as often occurs in SCI, results in a substantial loss of motor function. Moderate spontaneous functional recovery occurs in patients and animal models following incomplete SCI. This recovery can occur at various timepoints after initial injury and is linked to changes occurring throughout the entire nervous system, which is generally referred to as neuronal plasticity (Fouad and Tse 2008). For many years the central nervous system was thought to be rigid and hard-wired and thus could not self-repair. Luckily, researchers have discovered that this was not the case as a myriad of changes encompassing modifications that range in scale from synaptogenesis to large scale axonal outgrowth and sprouting may occur at various timepoints following the initial injury.

Nonetheless, the functional implication of spinal cord plasticity following injury is not well understood and remains complicated. The mechanisms underlying functional recovery after SCI (Raineteau and Schwab 2001, Darian-Smith 2009) are thought to include reversal of spinal shock, remyelination, axonal outgrowth and sprouting, increased spine density, motor map reorganization, synaptic strengthening/weakening, and synaptogenesis. As a result, many neural repair strategies to improve motor function after SCI have sought to augment restoration of function in the CST due to its importance in voluntary control, especially in humans.

Most importantly, uninjured descending motor pathways have been shown to compensate after injury to the CST (Fouad, Krajacic et al. 2011). After an incomplete C3/C4 dorsal column transection in the mouse, uninjured dorsolateral corticospinal pathways have been shown to substantiate remarkable motor cortical plasticity and partial recovery after SCI (Hilton, Anenberg et al. 2016). This was accomplished by the transient silencing of uninjured

dorsolaterally projecting corticospinal neurons by activating the inhibitory DREADD receptor hM4Di. This activation abrogated spontaneous recovery which resulted in a greater change in skilled locomotion than in control uninjured mice using the same silencing approach. These data demonstrate the pivotal role of a minor dorsolateral corticospinal pathway in mediating spontaneous recovery after SCI and support a focus on spared corticospinal neurons as a target for therapy. Similarly, following complete lesions of the dorsal CST in adult rats, sprouting from an uninjured ventral CST occurred onto medial motoneuron pools in the cervical spinal cord; this sprouting was paralleled with functional recovery (Weidner, Ner et al. 2001). Extensive spontaneous structural plasticity was discovered as a mechanism correlating with functional recovery in motor systems in the adult central nervous system of the rat. However, an ablated dorsomedial CST has been shown to sprout rostral to the injury (Fouad, Pedersen et al. 2001, Hill, Beattie et al. 2001) and to further contact with short and long propriospinal neurons (Bareyre, Kerschensteiner et al. 2004). The data presented here demonstrate that various forms of plasticity can occur in the injured dorsomedial CST and in the uninjured dorsolateral and ventromedial CSTs.

Similarly, an uninjured RtST has been shown to play a major role in recovery. In adult rats with bilateral injury to the CST at the level of medullar pyramids and bilateral ablation of rubrospinal axons at C4, the density of RtST processes increased and acquired the role of the damaged tracts by promoting task-specific recovery (Garcia-Alias, Truong et al. 2015). Following unilateral C4 spinal hemisection in adult rats, RtST fibers formed close appositions onto descending, double-midline crossing C3-C4 propriospinal neurons, which crossed the lesion site in the intact half of the spinal cord and recrossed to the denervated cervical hemicord below the injury, which was accompanied by substantial locomotor recovery (Filli, Engmann et al. 2014). Follow a lateral hemisection at T8 in the rat, recovery of weight-bearing stepping in the hindlimb ipsilateral to the injury occurs in parallel with increased numbers of collaterals of

spared reticulospinal fibers entering the intermediate lamina below the injury at L2; however, sprouting of injured reticulospinal fibers was not found above the lesion (Ballermann and Fouad 2006).

In summary, there is a solid basis for substantial plasticity that occurs with specific descending motor pathways after injury. Understanding these naturally occurring adaptations has helped derive the research in this dissertation and is essential in mediating the design of new, functionally meaningful treatments for SCI. Most importantly, with the notion that the central nervous system has the ability to naturally reorganize after injury, research has focused on treatments that help promote and drive plasticity to help further promote functional recovery after spinal cord injury.

Severity of Spinal Cord Injury

An important criterion to consider when determining the efficacy of plasticity promoting therapies is the severity of the spinal cord lesion. It is well understood that the amount of functional recovery correlates with the amount of spared white matter that remains after injury (Krizsan-Agbas, Winter et al. 2014). In extreme cases of complete spinal transection, plasticity will fail to reestablish descending control of muscles below the level of injury despite the intact circuitry that remains distal to the injury site. Because the presence of intact axons is the only way to transmit voluntary central nervous system motor commands below the site of the injury, this means that the total volume of spared white matter is the most important determinant of spinal cord injury severity. Similarly, plasticity capable of driving rehabilitation of the descending motor pathways depends on the location of the sparing as well as the degree of axonal sparing (Loy, Magnuson et al. 2002, Schucht, Raineteau et al. 2002).

Another challenge regarding lesion size when studying plasticity or the efficacy of plasticity promoting treatments is the choice of lesion model. For example, mild injuries, which

result in an extensive amount of sparing, allow for a substantial amount of spontaneous plasticity and concurrent recovery. Conversely, a severe injury may not be followed by any behavioral improvements after intervention due to the excessive amount of tissue loss. Recognizing that many treatments have yet to result in extensive recovery leads to the notion that many treatments may have been dismissed prematurely simply due to an unsuitable lesion model. The choice between mild or severe lesion model might undervalue or completely mask the potential of a plasticity promoting treatment. As a result, moderate lesions will most likely produce better outcomes for plasticity promoting treatments due to viable tissue/axon sparing and were deemed appropriate for this study.

Electrical Stimulation Promotes Plasticity After Injury

Electrical stimulation is one therapeutic intervention after injury that has been shown to promote plasticity and axonal sprouting (Brus-Ramer, Carmel et al. 2007). After injury, new connections form spontaneously but are subsequently lost if they do not project below the lesion and become functionally relevant (Bareyre, Kerschensteiner et al. 2004). To reduce the pruning of spontaneous connections after injury, direct stimulation of specific pathways that remain intact after injury may be key for functional recovery. For example, electrical stimulation of spared corticospinal pathways from the motor cortex after a unilateral transection resulted in axonal sprouting into the denervated side of the spinal cord, which was associated with improved motor function that persisted beyond the period of stimulation (Carmel, Berrol et al. 2010). Despite the distance between the electrical stimulus and the site of sprouting, increased sprouting of CST axons was observed following electrical stimulation of motor cortex, leading to the partial reconstruction of the lost CST. This was coupled with sprouting that increased the density of the cortical projections to the magnocellular red nucleus, strengthening the cortico-rubrospinal connection (Carmel and Martin 2014). Electrical stimulation of intact pathways after injury appears to strengthen the connection of intact pathways. This augmentation could

additionally result in new cortico-cortico or cortico-spinal connections that could branch into injured/disconnected or neighboring/intact pathways.

Epidural Stimulation and Rehabilitation

One form of neurological rehabilitation for an SCI is epidural stimulation (Figure 2.2). Epidural stimulation is an invasive technique where a stimulating electrode is attached to the epidural surface of the spinal cord. This technique may or may not involve the removal of the dura matter of the spinal cord; however, it does require a laminectomy of the vertebrae. An epidural stimulating electrode, usually thin and flat, is then placed on the spinal cord directly below the lesion and fixed in place through various techniques. The placement and pattern of epidural stimulation is designed to recruit the lumbosacral motoneurons in combination with the weak excitatory activity from the remaining descending axons of the spinal cord below the lesion (Gad, Choe et al. 2013). This technique has been successful in rats (Tresch and Bizzi 1999, Ichiyama, Gerasimenko et al. 2005, Gad, Choe et al. 2013), cats (Musienko, Courtine et al. 2012, Lavrov, Musienko et al. 2015), non-human primates (Sharpe and Jackson 2014), and humans (Harkema, Gerasimenko et al. 2011).

Recently, completely paralyzed human patients have been implanted with an epidural stimulating electrode for pain suppression purposes (Harkema, Gerasimenko et al. 2011). These patients were able to generate full weight-bearing standing and recover some voluntary control of the toe, ankle, and entire lower limb during epidural stimulation. According to Harkema et al., movement was able to be generated due to the epidural stimulation in combination with sensory information from the lower limbs related to bilateral extension and loading. This is a promising step toward neurological recovery and suggests that stimulation therapy paired with rehabilitation training may be necessary in order to further the recovery of voluntary motor function.

Intraspinal Microstimulation

There are various forms of electrical stimulation that have been used to activate and modulate the circuitry below the lesion. However, there is one form of electrical stimulation that is gaining traction and seems to have greater benefits over other forms: Intraspinal microstimulation (ISMS; Figure 2.2). The development of novel devices using ISMS continues to evolve through the use of animal models of SCI. ISMS has been used to evoke functional motor responses in nonhuman primates (Moritz, Lucas et al. 2007, Zimmermann, Seki et al. 2011, Sharpe and Jackson 2014), cats (Mushahwar, Collins et al. 2000, Mushahwar and Horch 2000, Saigal, Renzi et al. 2004), and rats (Tresch and Bizzi 1999, Bamford, Putman et al. 2005, Kasten, Sunshine et al. 2013, Sunshine, Cho et al. 2013). More recently, there has been increased interest in the development of ISMS as a therapeutic option for treatment of SCI. This may be because the stimulation amplitudes with ISMS are typically magnitudes lower than in other functional electrical stimulation techniques (Sharpe and Jackson 2014). ISMS, as compared to other forms of electrical stimulation, involves penetrating the spinal cord in order to directly target neurons in the ventral regions of the spinal cord. This high spatial specificity of ISMS allows it to avoid recruitment of cells in the dorsal spinal cord, while targeting spared spinal circuits within the ventral horn directly, which allows for the previously described low stimulus amplitude. Although ISMS is more invasive than epidural stimulation, implantation of microwires and the chronic application of ISMS has been shown to be well tolerated by spinal cord tissue (Bamford et al. 2010). To date, ISMS has been studied in animal models for potential recovery of both forelimb (Kasten, Sunshine et al. 2013, Sunshine, Cho et al. 2013) and hindlimb (Tresch and Bizzi 1999, Bamford, Putman et al. 2005) motor outputs.

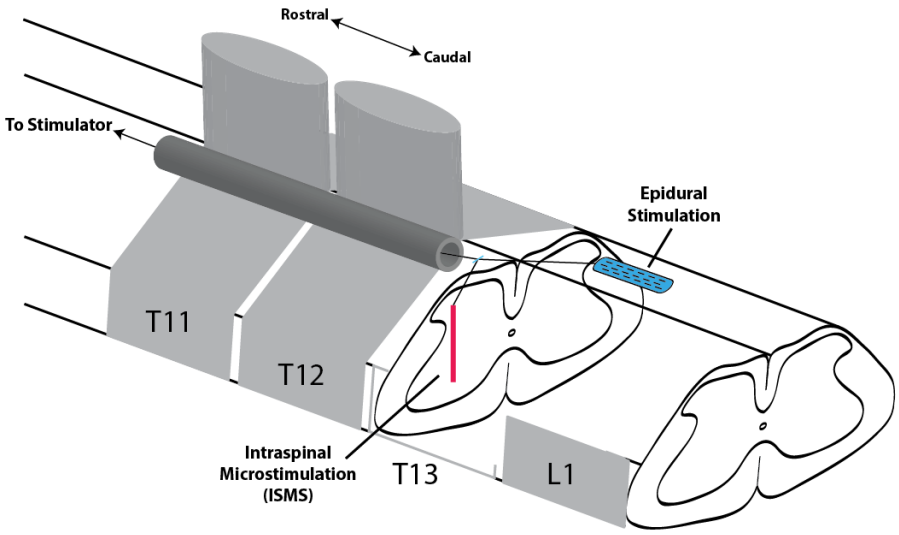

Figure 2.2. Schematic illustration of the placement of intraspinal microstimulation (ISMS) electrodes and epidural stimulation electrodes. ISMS electrodes (highlighted in red) penetrate the spinal cord to target the intermediate and ventral gray matter. Epidural stimulation electrodes reside on the dorsal surface (highlighted in blue) of the spinal cord.

In this dissertation project, ISMS directly targets the motoneuron pools in the lumbar enlargement, which contain large proportions of the neural networks involved in locomotion in the rat (Kiehn 2006). Within the ventral region, ISMS activates fibers in passage composed of afferent projections in the ventral horn and propriospinal neurons. These fibers in turn activate motor neurons trans-synaptically. This last point is critical, as it means that ongoing activity within the spared spinal circuit can adapt to influence the recruitment of motor neurons in a near normal physiological order. In turn, this allows for the graded production of force with increasing amplitude as well as the co-activation of synaptically linked inhibitory antagonistic neurons. As a result, plasticity at the level of the intact spinal center is able to recalibrate the “disconnected” circuit, leading to the generation of coordinated, multi-joint movements and reducing the challenge of coordinating the activity of individual muscles.

Spike Timing-Dependent Plasticity

When stimulating the central nervous system, it is beneficial to understand the effects the stimulation has on the synaptic connections between neurons. An influential hypothesis, that neurons could modulate the relative strength that they exerted at a given synapse, was set forth by Donald Hebb (Hebb 1949). Since Hebb's postulate, there have been various demonstrations of how synaptic strength might be influenced by electrical stimuli in the nervous system. For example, a persistent enhancement of the evoked potentials recorded in response to a test stimulus pulse was observed when tetanic stimulation was applied to the hippocampus (Bliss and Lomo 1973). This phenomenon, known as long-term potentiation (LTP), suggests that the synapses involved in relaying the test stimulus became stronger due to the electrical stimuli. Similarly, the efficacy of synapses can be reduced, resulting in a phenomenon known as long-term depression (LTD) (Levy and Steward 1983).

Evidence from experiments that studied the synaptic currents of two cells linked by a single synapse provided the most compelling evidence that the mechanism driving such phenomena as LTP and LTD was likely based on the relative timing of the pre- and post-synaptic cells' action potentials. An action potential is the electrical process through which a cell releases the contents of its axon terminal in order to propagate signals within the nervous system in an electrochemical fashion. As it turns out, many kinds of neurons have an intrinsic mechanism that allows them to modify synaptic strength: in order to strengthen a synaptic connection, there is a critical window preceding the firing of an action potential in the post-synaptic cell during which the arrival of a pre-synaptic action potential at the synapse improves the relative influence of future pre-synaptic action potentials on the post-synaptic cell's membrane potential. This window, and the relative order of pre- and post-synaptic action potentials depends upon the cell type and location, but in general the window between pre- and post-synaptic spiking that leads to LTP is when the presynaptic cell's action potential leads the

post-synaptic cell's action potential by tens of milliseconds (Figure 2.3)(Bi and Poo 1998). This is now referred to as spike timing-dependent plasticity (STDP).

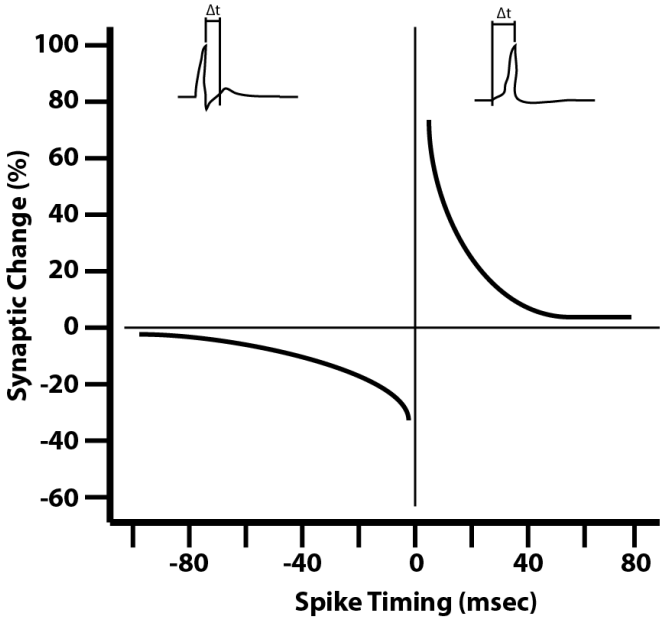

Figure 2.3. Critical window for the induction of synaptic potentiation and depression. The percentage change in the excitatory post-synaptic current amplitude at 20-30 min after repetitive correlated spiking (pulses at 1 Hz) was plotted against spike timing, which is defined as the time interval (Δt) between the onset of the EPSP and the peak of the postsynaptic action potential during each pair of correlated spiking, as illustrated by the traces above. Figure was modified from previously reported figures by Bi and Poo (Bi and Poo 1998, Bi and Poo 2001).

Activity Dependent Stimulation

In order to direct spike timing-dependent plasticity, one innovative device-based approach utilizes activity-dependent stimulation (ADS) in a brain-computer spinal cord interface. ADS paradigms record and digitize extracellular neural activity from one location, discriminate individual action potentials in real time, and deliver small amounts of electrical current to another population of neurons. This approach is based on the recruitment of a STDP-like mechanism that allows the facilitation of synapses based on an optimal fixed latency between the detection of action potentials and the delivery of the current pulse (Hebb 1949, Jackson and Zimmermann 2012). The ability of the nervous system to alter the strength of synaptic connections underlies

learning and memory in healthy organisms, and is a potential mechanism for recovery after injury (Guggenmos, Azin et al. 2013).

In animal models, potentiation of synaptic activity can be accomplished with short bursts of electrical stimuli in an open-loop fashion (i.e., pre-programmed stimulation rates and amplitudes) (Bliss and Lomo 1973). Open-loop ISMS has been shown to improve motor function after cervical contusion injury in rats (Bareyre, Kerschensteiner et al. 2004, Jackson, Mavoori et al. 2006, Kasten, Sunshine et al. 2013, Mondello, Kasten et al. 2014). However, investigators are now exploring closed-loop stimulation, or ADS paradigms, to replicate the natural timing of pre- and post-synaptic events, and thus potentiate, or condition, specific neuronal pathways (Jackson, Mavoori et al. 2006).

It is now believed that the use of ADS to replicate the natural timing of pre- and post-synaptic events may contribute to strengthening the synaptic efficacy of spared fibers/pathways after injury and may enhance functional recovery. Using this conditioning approach, we have previously demonstrated in a traumatic brain injury model that conditioning of a corticocortical pathway enhanced synaptic efficacy between the cortical regions of interest and resulted in rapid behavioral recovery (Guggenmos, Azin et al. 2013). In cortical ADS applications, connections are artificially enhanced by using neural recordings in one cortical area to trigger precisely-timed electrical stimulation in another cortical area (Guggenmos, Azin et al. 2013), to muscles (Moritz, Perlmutter et al. 2008), or to the spinal cord (Nishimura, Perlmutter et al. 2013, Zimmermann and Jackson 2014) in real time. Specifically, in ADS applications across SCIs, cortical activity has traditionally been used to trigger epidural stimulation (Capogrosso, Milekovic et al. 2016), ISMS (Nishimura, Perlmutter et al. 2013, Zimmermann and Jackson 2014); however, one study used EMG recordings to trigger ISMS (McPherson, Miller et al. 2015).

Although these proof-of-concept studies demonstrate that neural interface systems can effectively bridge damaged neural pathways and promote recovery after injury, in preclinical SCI

models, these systems have been limited to improving motor function of the upper limb. If similar approaches can be used after SCI to improve lower limb function to *strengthen spared descending pathways* from the brain to the spinal cord, it may be possible to *enhance voluntary control of movement* after incomplete spinal cord injuries. Since some fibers may remain intact even after neurologically complete SCI, such a conditioning approach may have application in an even broader SCI population. Such a treatment approach could augment concomitant physical and occupational therapy, *potentially reducing rehabilitation time*. Ultimately, patients *might regain some voluntary movement* due to the increased synaptic efficacy in descending fibers.

References

Akintunde, A. and D. F. Buxton (1992). "Differential sites of origin and collateralization of corticospinal neurons in the rat: a multiple fluorescent retrograde tracer study." Brain Res **575**(1): 86-92.

Alaverdashvili, M. and I. Q. Whishaw (2008). "Motor cortex stroke impairs individual digit movement in skilled reaching by the rat." Eur J Neurosci **28**(2): 311-322.

Alstermark, B., J. Ogawa and T. Isa (2004). "Lack of monosynaptic corticomotoneuronal EPSPs in rats: disynaptic EPSPs mediated via reticulospinal neurons and polysynaptic EPSPs via segmental interneurons." J Neurophysiol **91**(4): 1832-1839.

Alstermark, B. and L. G. Pettersson (2014). "Skilled reaching and grasping in the rat: lacking effect of corticospinal lesion." Front Neurol **5**: 103.

Ballermann, M. and K. Fouad (2006). "Spontaneous locomotor recovery in spinal cord injured rats is accompanied by anatomical plasticity of reticulospinal fibers." Eur J Neurosci **23**(8): 1988-1996.

Bamford, J. A., C. T. Putman and V. K. Mushahwar (2005). "Intraspinal microstimulation preferentially recruits fatigue-resistant muscle fibres and generates gradual force in rat." J Physiol **569**(Pt 3): 873-884.

Bareyre, F. M., M. Kerschensteiner, O. Raineteau, T. C. Mettenleiter, O. Weinmann and M. E. Schwab (2004). "The injured spinal cord spontaneously forms a new intraspinal circuit in adult rats." Nat Neurosci **7**(3): 269-277.

Basso, D. M., M. S. Beattie and J. C. Bresnahan (2002). "Descending systems contributing to locomotor recovery after mild or moderate spinal cord injury in rats: experimental evidence and a review of literature." Restor Neurol Neurosci **20**(5): 189-218.

Beloozerova, I. N. and M. G. Sirota (1993). "The role of the motor cortex in the control of accuracy of locomotor movements in the cat." J Physiol **461**: 1-25.

Bi, G. and M. Poo (1998). "Synaptic Modifications in Culutured Hippocampal Neurons: Dependence on Spike Timing, Synaptic Strength, and Postsynaptic Cell Type." The Journal of Neuroscience **18**(24): 10464-10472.

Bi, G. and M. Poo (2001). "Synaptic modification by correlated activity: Hebb's postulate revisited." Annu Rev Neurosci **24**: 139-166.

Bliss, T. V. P. and T. Lomo (1973). "Long-Lasting Potentiation of Synaptic Transmission in the Dentate Area of the Anesthetized Rabbit Following Stimulation of the Preforant Path." J. Physiol. **232**: 331-356.

Brown, L. T. (1971). "Projectsions and Terminations of the Corticospinal Tract in Rodents." Exp. Brain Res. **13**: 432-450.

Brown, L. T. (1974). "Rubrospinal projections in the rat." J Comp Neurol **154**(2): 169-187.

Brus-Ramer, M., J. B. Carmel, S. Chakrabarty and J. H. Martin (2007). "Electrical stimulation of spared corticospinal axons augments connections with ipsilateral spinal motor circuits after injury." J Neurosci **27**(50): 13793-13801.

Buss, A., K. Pech, D. Merkler, B. A. Kakulas, D. Martin, J. Schoenen, J. Noth, M. E. Schwab and G. A. Brook (2005). "Sequential loss of myelin proteins during Wallerian degeneration in the human spinal cord." Brain **128**(Pt 2): 356-364.

Capogrosso, M., T. Milekovic, D. Borton, F. Wagner, E. M. Moraud, J. B. Mignardot, N. Buse, J. Gandar, Q. Barraud, D. Xing, E. Rey, S. Duis, Y. Jianzhong, W. K. Ko, Q. Li, P. Detemple, T. Denison, S. Micera, E. Bezard, J. Bloch and G. Courtine (2016). "A brain-spine interface alleviating gait deficits after spinal cord injury in primates." Nature **539**(7628): 284-288.

Carmel, J. B., L. J. Berrol, M. Brus-Ramer and J. H. Martin (2010). "Chronic electrical stimulation of the intact corticospinal system after unilateral injury restores skilled locomotor control and promotes spinal axon outgrowth." J Neurosci **30**(32): 10918-10926.

Carmel, J. B. and J. H. Martin (2014). "Motor cortex electrical stimulation augments sprouting of the corticospinal tract and promotes recovery of motor function." Frontiers in Integrative Neuroscience **8**.

Casale, E. J., A. R. Light and A. Rustioni (1988). "Direct projection of the corticospinal tract to the superficial laminae of the spinal cord in the rat." J Comp Neurol **278**(2): 275-286.

Chen, Y. J., S. A. Nabavizadeh, A. Vossough, S. Kumar, L. A. Loevner and S. Mohan (2016). "Wallerian Degeneration Beyond the Corticospinal Tracts: Conventional and Advanced MRI Findings." J Neuroimaging.

Darian-Smith, C. (2009). "Synaptic plasticity, neurogenesis, and functional recovery after spinal cord injury." Neuroscientist **15**(2): 149-165.

Drew, T., W. Jiang, B. Kably and S. Lavoie (1996). "Role of the motor cortex in the control of visually triggered gait modifications." Can J Physiol Pharmacol **74**(4): 426-442.

Drew, T., W. Jiang and W. Widajewicz (2002). "Contributions of the motor cortex to the control of the hindlimbs during locomotion in the cat." Brain Res Rev **40**(1-3): 178-191.

Fehlings, M. G. and C. H. Tator (1995). "The Relationships among the Severity of Spinal-Cord Injury, Residual Neurological Function, Axon Counts, and Counts of Retrogradely Labeled Neurons after Experimental Spinal-Cord Injury." Experimental Neurology **132**(2): 220-228.

Filli, L., A. K. Engmann, B. Zorner, O. Weinmann, T. Moraitis, M. Gullo, H. Kasper, R. Schneider and M. E. Schwab (2014). "Bridging the gap: a reticulo-propriospinal detour bypassing an incomplete spinal cord injury." J Neurosci **34**(40): 13399-13410.

Fink, K. L. and W. B. Cafferty (2016). "Reorganization of Intact Descending Motor Circuits to Replace Lost Connections After Injury." Neurotherapeutics **13**(2): 370-381.

Fouad, K., A. Krajacic and W. Tetzlaff (2011). "Spinal cord injury and plasticity: opportunities and challenges." Brain Res Bull **84**(4-5): 337-342.

Fouad, K., V. Pedersen, M. E. Schwab and C. Brosamle (2001). "Cervical sprouting of corticospinal fibers after thoracic spinal cord injury accompanies shifts in evoked motor responses." Curr Biol **11**(22): 1766-1770.

Fouad, K. and A. Tse (2008). "Adaptive changes in the injured spinal cord and their role in promoting functional recovery." Neurol Res **30**(1): 17-27.

Frigon, A. (2017). "The neural control of interlimb coordination during mammalian locomotion." J Neurophysiol **117**(6): 2224-2241.

Gad, P. N., J. Choe, K. G. Shah, A. Tooker, V. Tolosa, S. Pannu, G. Garcia-Alias, H. Zhong, Y. Gerasimenko, R. R. Roy and V. R. Edgerton (2013). Using in vivo spinally-evoked potentials to assess functional connectivity along the spinal axis. 6th Annual International IEEE EMBS Conference on Neural Engineering. San Diego, California.

Garcia-Alias, G., K. Truong, P. K. Shah, R. R. Roy and V. R. Edgerton (2015). "Plasticity of subcortical pathways promote recovery of skilled hand function in rats after corticospinal and rubrospinal tract injuries." Exp Neurol **266**: 112-119.

Guggenmos, D. J., M. Azin, S. Barbay, J. D. Mahnken, C. Dunham, P. Mohseni and R. J. Nudo (2013). "Restoration of function after brain damage using a neural prosthesis." PNAS **110**(52): 21177-21182.

Guth, L., Z. Zhang and O. Steward (1999). "The unique histopathological responses of the injured spinal cord. Implications for neuroprotective therapy." Ann N Y Acad Sci **890**: 366-384.

Harkema, S., Y. Gerasimenko, J. Hodes, J. Burdick, C. Angeli, Y. Chen, C. Ferreira, A. Willhite, E. Rejc, R. G. Grossman and V. R. Edgerton (2011). "Effect of epidural stimulation of the lumbosacral spinal cord on voluntary movement, standing, and assisted stepping after motor complete paraplegia: a case study." The Lancet **377**(9781): 1938-1947.

Hayes, N. L. and A. Rustioni (1981). "Descending Projections from Brainstem and Sensorimotor Cortex to Spinal Englargments in the Cat." Experimental Brain Research **41**: 89-107.

Hebb, D. O. (1949). The Organization of Behavior. Wiley, New York.

Hill, C. E., M. S. Beattie and J. C. Bresnahan (2001). "Degeneration and sprouting of identified descending supraspinal axons after contusive spinal cord injury in the rat." Exp Neurol **171**(1): 153-169.

Hilton, B. J., E. Anenberg, T. C. Harrison, J. D. Boyd, T. H. Murphy and W. Tetzlaff (2016). "Re-Establishment of Cortical Motor Output Maps and Spontaneous Functional Recovery via Spared Dorsolaterally Projecting Corticospinal Neurons after Dorsal Column Spinal Cord Injury in Adult Mice." J Neurosci **36**(14): 4080-4092.

Hongo, T., E. Jankovska and A. Lundberg (1969). "The rubrospinal tract. I. Effects on alpha-motoneurons innervating hindlimb muscles in cats." Exp. Brain Res. **7**: 344-364.

Ichiyama, R. M., Y. P. Gerasimenko, H. Zhong, R. R. Roy and V. R. Edgerton (2005). "Hindlimb stepping movements in complete spinal rats induced by epidural spinal cord stimulation." Neurosci Lett **383**(3): 339-344.

Jackson, A., J. Mavoori and E. E. Fetz (2006). "Long-term motor cortex plasticity induced by an electronic neural implant." Nature **444**(7115): 56-60.

Jackson, A. and J. B. Zimmermann (2012). "Neural interface for brain and spinal cord - restoring motor function." Nat Rev Neurol **8**: 690-699.

Kanagal, S. G. and G. D. Muir (2009). "Task-dependent compensation after pyramidal tract and dorsolateral spinal lesions in rats." Exp Neurol **216**(1): 193-206.

Kasten, M. R., M. D. Sunshine, E. S. Secrist, P. J. Horner and C. T. Moritz (2013). "Therapeutic intraspinal microstimulation improves forelimb function after cervical contusion injury." J Neural Eng **10**(4): 044001.

Kiehn, O. (2006). "Locomotor Circuits in the Mammalian Spinal Cord." Annual Review of Neuroscience **29**(1): 279-306.

Krizsan-Agbas, D., M. K. Winter, L. S. Eggimann, J. Meriwether, N. E. Berman, P. G. Smith and K. E. McCarson (2014). "Gait Analysis at Multiple Speeds Reveals Differential Functional

and Structural Outcomes in Response to Graded Spinal Cord Injury." Journal of Neurotrauma **31**(9): 846-856.

Kuchler, M., K. Fouad, O. Weinmann, M. E. Schwab and O. Raineteau (2002). "Red nucleus projections to distinct motor neuron pools in the rat spinal cord." J Comp Neurol **448**(4): 349-359.

Lavrov, I., P. E. Musienko, V. A. Selionov, S. Zdunowski, R. R. Roy, V. R. Edgerton and Y. Gerasimenko (2015). "Activation of spinal locomotor circuits in the decerebrated cat by spinal epidural and/or intraspinal electrical stimulation." Brain Res **1600**: 84-92.

Lemon, R. N. (2008). "Descending pathways in motor control." Annu Rev Neurosci **31**: 195-218.

Levy, W. B. and O. Steward (1983). "Temporal contiguity requirements for long-term associative potentiation/depression in the hippocampus." Neuroscience **8**(4): 791-797.

Liang, F., V. Moret, M. Wiesendanger and E. M. Rouiller (1991). "Corticomotoneuronal Connections in the Rat - Evidence from Double-Labeling of Motoneurons and Corticospinal Axon Arborizations." Journal of Comparative Neurology **311**(3): 356-366.

Liang, H., T. Bacskai, C. Watson and G. Paxinos (2014). "Projections from the lateral vestibular nucleus to the spinal cord in the mouse." Brain Struct Funct **219**(3): 805-815.

Liang, H., G. Paxinos and C. Watson (2011). "Projections from the brain to the spinal cord in the mouse." Brain Struct Funct **215**(3-4): 159-186.

Loy, D. N., D. S. Magnuson, Y. P. Zhang, S. M. Onifer, M. D. Mills, Q. L. Cao, J. B. Darnall, L. C. Fajardo, D. A. Burke and S. R. Whittemore (2002). "Functional redundancy of ventral spinal locomotor pathways." J Neurosci **22**(1): 315-323.

Matsuyama, K., F. Mori, B. Kuze and S. Mori (1999). "Morphology of Single Pontine Reticulospinal Axons in the Lumbar enlargement of the Cat: A Stud Using the Anterograde Tracer PHA-L." The Journal of Comparative Neurology **410**: 413-430.

McPherson, J. G., R. R. Miller and S. I. Perlmutter (2015). "Targeted, activity-dependent spinal stimulation produces long-lasting motor recovery in chronic cervical spinal cord injury." Proc Natl Acad Sci U S A **112**(39): 12193-12198.

Metz, G. A., V. Dietz, M. E. Schwab and H. van de Meent (1998). "The effects of unilateral pyramidal tract section on hindlimb motor performance in the rat." Behav Brain Res **96**(1-2): 37-46.

Metz, G. A. and I. Q. Whishaw (2002). "Cortical and subcortical lesions impair skilled walking in the ladder rung walking test: a new task to evaluate fore- and hindlmb stepping, placing, and co-ordination." Journal of Neuroscience Methods **115**: 169-179.

Mitchell, E. J., S. McCallum, D. Dewar and D. J. Maxwell (2016). "Corticospinal and Reticulospinal Contacts on Cervical Commissural and Long Descending Propriospinal Neurons in the Adult Rat Spinal Cord; Evidence for Powerful Reticulospinal Connections." PLoS One **11**(3): e0152094.

Mondello, S. E., M. R. Kasten, P. J. Horner and C. T. Moritz (2014). "Therapeutic intraspinal stimulation to generate activity and promote long-term recovery." Front Neurosci **8**: 21.

Moritz, C. T., T. H. Lucas, S. I. Perlmutter and E. E. Fetz (2007). "Forelimb movements and muscle responses evoked by microstimulation of cervical spinal cord in sedated monkeys." J Neurophysiol **97**(1): 110-120.

Moritz, C. T., S. I. Perlmutter and E. E. Fetz (2008). "Direct control of paralysed muscles by cortical neurons." Nature **456**(7222): 639-642.

Muir, G. D. and I. Q. Whishaw (2000). "Red nucleus lesions impair overground locomotion in rats: a kinetic analysis." Eur J Neurosci **12**(3): 1113-1122.

Mushahwar, V. K., D. F. Collins and A. Prochazka (2000). "Spinal cord microstimulation generates functional limb movements in chronically implanted cats." Exp Neurol **163**(2): 422-429.

Mushahwar, V. K. and K. W. Horch (2000). "Selective Activation of Muscle Groups in the Feline Hindlimb Through Electrical Microstimulation of the Ventral Lumbo-Sacral Spinal Cord." IEEE Transactions on Rehabilitation Engineering **8**(10): 11-21.

Musienko, P., G. Courtine, J. E. Tibbs, V. Kilimnik, A. Savochin, A. Garfinkel, R. R. Roy, V. R. Edgerton and Y. Gerasimenko (2012). "Somatosensory control of balance during locomotion in decerebrated cat." J Neurophysiol **107**(8): 2072-2082.

Nathan, P. W. (1994). "Effects on Movement of Surgical Incisions into the Human Spinal-Cord." Brain **117**: 337-346.

National Spinal Cord Injury Statistical Center, B., Alabama (2019). Spinal Cord Injury Facts and Figures at a Glance.

Nishimura, Y., S. I. Perlmutter and E. E. Fetz (2013). "Restoration of upper limb movement via artificial corticospinal and musculospinal connections in a monkey with spinal cord injury." Front Neural Circuits **7**: 57.

Nudo, R. J. and R. B. Masterton (1988). "Descending pathways to the spinal cord: a comparative study of 22 mammals." J Comp Neurol **277**(1): 53-79.

Nudo, R. J. and R. B. Masterton (1990). "Descending pathways to the spinal cord, III: Sites of origin of the corticospinal tract." J Comp Neurol **296**(4): 559-583.

Olivares-Moreno, R., Y. Moreno-Lopez, L. Concha, G. Martinez-Lorenzana, M. Condes-Lara, M. Cordero-Erausquin and G. Rojas-Piloni (2017). "The rat corticospinal system is functionally and anatomically segregated." Brain Struct Funct **222**(9): 3945-3958.

Orlovsky, G. N. (1972). "Activity of Rubrospinal Neurons during Locomotion." Brain Research **46**(Nov13): 99-&.

Orlovsky, G. N. (1972). "The effect of different descending systems on flexor and extensor activity during locomotion." Brain Research **40**: 359-371.

Oudega, M. and M. A. Perez (2012). "Corticospinal reorganization after spinal cord injury." J Physiol **590**(16): 3647-3663.

Pompeiano, O. (1972). Spinovestibular Relations: Anatomical and Physiological Aspects**:** 263-296.

Raineteau, O. and M. E. Schwab (2001). "Plasticity of motor systems after incomplete spinal cord injury." Nat Rev Neurosci **2**(4): 263-273.

Saigal, R., C. Renzi and V. K. Mushahwar (2004). "Intraspinal Microstimulation Generates Functional Movements After Spinal-Cord Injury." IEEE Transactions on Neural Systems and Rehabilitation Engineering **12**(4): 430-440.

Schucht, P., O. Raineteau, M. E. Schwab and K. Fouad (2002). "Anatomical Correlates of Locomotor Recovery Following Dorsal and Ventral Lesions of the Rat Spinal Cord." Experimental Neurology **176**(1): 143-153.

Shamboul, K. M. (1980). "Lumbosacral predominance of vestibulospinal fibre projection in the rat." J Comp Neurol **192**(3): 519-530.

Sharpe, A. N. and A. Jackson (2014). "Upper-limb muscle responses to epidural, subdural and intrapsinal stimulation of the cervicel spinal cord." J Neural Eng. **11**(1).

Sunshine, M. D., F. S. Cho, D. R. Lockwood, A. S. Fechko, M. R. Kasten and C. T. Moritz (2013). "Cervical intraspinal microstimulation evokes robust forelimb movements before and after injury." J Neural Eng **10**(3): 036001.

Terashima, T. (1995). "Anatomy, development and lesion-induced plasticity of rodent corticospinal tract." Neurosci Res **22**(2): 139-161.

Tresch, M. C. and E. Bizzi (1999). "Responses to spinal microstimulation in the chronically spinalized rat and their relationship to spinal systems activated by low threshold cutaneous stimulation." Exp. Brain Res. **129**: 401-416.

Ueno, M., Y. Nakamura, J. Li, Z. Gu, J. Niehaus, M. Maezawa, S. A. Crone, M. Goulding, M. L. Baccei and Y. Yoshida (2018). "Corticospinal Circuits from the Sensory and Motor Cortices Differentially Regulate Skilled Movements through Distinct Spinal Interneurons." Cell Rep **23**(5): 1286-1300 e1287.

Waldron, H. A. and D. G. Gwyn (1969). "Descending nerve tracts in the spinal cord of the rat. I. Fibers from the midbrain." J Comp Neurol **137**(2): 143-153.

Webb, A. A. and G. D. Muir (2003). "Unilateral dorsal column and rubrospinal tract injuries affect overground locomotion in the unrestrained rat." Eur J Neurosci **18**(2): 412-422.

Weidner, N., A. Ner, N. Salimi and M. H. Tuszynski (2001). "Spontaneous corticospinal axonal plasticity and functional recovery after adult central nervous sytem injury." PNAS **98**(6): 3513-3518.

Whishaw, I. Q., S. M. Pellis, B. Gorny, B. Kolb and W. Tetzlaff (1993). "Proximal and Distal Impairments in Rat Forelimb Use in Reaching Follow Unilateral Pyramidal Tract Lesions." Behavioural Brain Research **56**(1): 59-76.

Wilson, V. J., R. Boyle, K. Fukushima, P. K. Rose, Y. Shinoda, S. Y. and Y. Uchino (1995). "Journal of Vestibular Research." 5 **147-170**.

Yang, H. W. and R. N. Lemon (2003). "An electron microscopic examination of the corticospinal projection to the cervical spinal cord in the rat: lack of evidence for cortico-motoneuronal synapses." Exp Brain Res **149**(4): 458-469.

Zemlan, F. P., M. M. Behbehani and R. M. Beckstead (1984). "Ascending and Descending Projections from Nucleus Reticularis Magnocellularis and Nucleus Reticularis Gigantocellularis - an Autoradiographic and Horseradish-Peroxidase Study in the Rat." Brain Research **292**(2): 207-220.

Zimmermann, J. B. and A. Jackson (2014). "Closed-loop control of spinal cord stimulation to restore hand function after paralysis." Front Neurosci **8**: 87.

Zimmermann, J. B., K. Seki and A. Jackson (2011). "Reanimating the arm and hand with intraspinal microstimulation." J Neural Eng **8**(5): 054001.

CHAPTER THREE: Effects of a Contusive Spinal Cord Injury on Spinal Motor Neuron Activity, Corticospinal Coupling, and Conduction Time in Rats

Abstract

The purpose of this study was to determine the effects of spinal cord injury (SCI) on spike activity evoked in the hindlimb spinal cord of the rat from cortical electrical stimulation. Adult, male, Sprague Dawley rats were randomly assigned to a Healthy or SCI group. SCI rats were given a 175 kDyn dorsal midline contusion injury at the level of the T8 vertebrae. At four weeks post-SCI, intracortical microstimulation (ICMS) was delivered at several sites in the hindlimb motor cortex of anesthetized rats, and evoked neural activity was recorded from corresponding sites throughout the dorsoventral depths of the spinal cord and electromyography (EMG) activity from hindlimb muscles. In healthy rats, post-ICMS spike histograms showed reliable, evoked spike activity during a short-latency epoch 10-12 ms after the initiation of the ICMS pulse train (short). Longer latency spikes occurred between ~20-60 ms, generally following a Gaussian distribution, rising above baseline at time L1, followed by a peak response, and then falling below baseline at time L2. EMG responses occurred between L1 and peak (25-27 ms). In SCI rats, short-latency responses were still present, long-latency responses were disrupted or eliminated, and EMG responses were never evoked. The retention of the short-latency responses indicates that spared descending spinal fibers, most likely via the cortico-reticulospinal pathway, can still depolarize spinal cord neurons after a dorsal midline contusion injury. This study provides novel insights into the role of alternate pathways for voluntary control of hindlimb movements after SCI that disrupts the corticospinal tract in the rat.

Significance Statement

Neuronal spike activity in the spinal cord after spinal cord injury has rarely been examined. We used intracortical microstimulation techniques in hindlimb motor cortex to examine evoked multi-unit spike activity in the hindlimb spinal cord and EMG activity in hindlimb muscles of anesthetized rats. Using linear microelectrode arrays, neuronal spikes were recorded from multiple laminae through the depths of the spinal cord grey matter. The results show that after a contusion injury that disrupts corticospinal fibers in the dorsal columns, short-latency evoked spikes can still be recorded from spinal cord neurons as a result of intracortical microstimulation. These results suggest that hindlimb motor cortex influences spinal cord motor neuron activity with short latencies via alternate descending spinal pathways.

Introduction

Understanding the timing of excitation of spinal cord motor neurons via descending pathways and how spinal excitability is altered by spinal cord injury (SCI) is critical for the long-range goal of functional restoration via rehabilitative interventions. While SCI animal models have predominantly focused on cortical control of forelimb muscles, we recently established a reliable model of contusion injury in the lower thoracic spinal cord of the laboratory rat to gain insight into the capacity of spared descending fibers to participate in functional recovery of hindlimb motor behavior (Krizsan-Agbas, Winter et al. 2014, Frost, Dunham et al. 2015, Borrell, Frost et al. 2017).

The primary pathway for voluntary movement of skeletal musculature in mammals is the corticospinal tract (CST) originating largely from neurons in the sensorimotor cortex and terminating mainly in the deep dorsal horn and intermediate grey matter (Casale, Light et al. 1988, Mitchell, McCallum et al. 2016). The CST is located primarily in the contralateral dorsomedial column, while 10—20% of the fibers descend in the ipsilateral ventromedial funiculus (Lemon 2008). In addition to the CST, the reticulospinal (RtST) and rubrospinal tracts (RbST) each play an important role in movement. The RtST originates from medullary and pontine nuclei, is located primarily in the ventral and ventrolateral funiculi (Waldron and Gwyn 1969, Mitchell, McCallum et al. 2016), and terminates primarily within the intermediate grey matter of lamina VII and VIII in the rat (Matsuyama, Mori et al. 1999, Mitchell, McCallum et al. 2016). The RbST originates from magnocellular neurons in the red nucleus of the midbrain, is located primarily in the contralateral dorsolateral funiculus (Brown 1974, Kuchler, Fouad et al. 2002), and terminates primarily in the intermediate grey matter of laminae V, VI, and VII in the rat (Brown 1974).

Previous neurophysiological studies have evaluated corticospinal connectivity before and after injury to the spinal cord using transcranial magnetic stimulation (TMS) (Kamida, Fujiki

et al. 1998, Chiba, Oshio et al. 2003, Nielsen, Perez et al. 2007, Petrosyan, Alessi et al. 2017), epicortical stimulation (Elger, Speckmann et al. 1977, Janzen, Speckmann et al. 1977, Ryder, Zappulla et al. 1991), and intracortical microstimulation (ICMS) (Bannister and Porter 1967, Bogatyreva and Shapovalov 1973, Stewart, Quirk et al. 1990, Babalian, Liang et al. 1993, Alstermark, Ogawa et al. 2004). Although TMS and surface stimulation are less invasive, they are spatially non-specific compared with intracortical stimulation. Due to this non-specificity in the volume of cortical tissue that is stimulated, and the multiple descending pathways giving rise to evoked responses, there are discrepancies in the published literature with regard to corticospinal conduction times (i.e., onset of activity evoked by cortical stimulation) and conduction velocities in the rat. Likewise, conduction times are often based on relatively gross, motor evoked potentials (MEPs), that cannot discriminate peaks in activation related to depolarization of sub-populations of motor neurons and interneurons in the spinal cord. Reports of MEP latencies range from 1 – 14 ms in the cervical enlargement (Bannister and Porter 1967, Stewart, Quirk et al. 1990, Babalian, Liang et al. 1993, Alstermark, Ogawa et al. 2004, Nielsen, Perez et al. 2007) and from 2 – 35 ms in the lumbar enlargement (Bogatyreva and Shapovalov 1973, Elger, Speckmann et al. 1977, Stewart, Quirk et al. 1990).

Although several studies have analyzed stimulus-evoked onset latencies via MEPs in the cervical spinal cord before and after SCI, changes in neuronal activity and the synaptic coupling between primary motor cortex and hindlimb spinal cord neurons have rarely been examined before and after SCI. In the present study, we used ICMS in anesthetized rats to depolarize neurons in Layer V of the hindlimb motor cortex. Using a linear microelectrode array, we recorded simultaneously from multiple dorsoventral depths in the hindlimb spinal cord grey matter and clustered the recorded spikes for analysis. The resulting data allowed us to describe in a more detailed, quantitative manner, the changes in CS coupling, conduction time, and

conduction velocity after a contusive thoracic SCI. More importantly, the results gave insight into the descending motor pathways that may still be functional after injury.

Materials and Methods

Experimental Design

To examine the effects of a contusive SCI on cortically-evoked spinal neuronal activity, ICMS was delivered in the hindlimb area of motor cortex (HLA) and ICMS-evoked spikes and EMG signals were simultaneously recorded from hindlimb spinal cord and hindlimb muscles, respectively, in healthy and SCI rats (Figure 3.1).

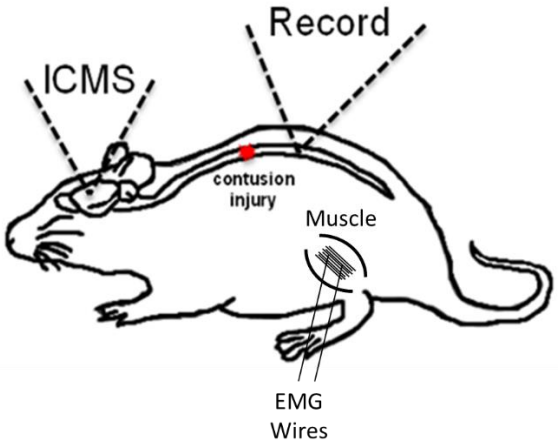

Figure 3.1. Overview of experimental design. ICMS was conducted in hindlimb area (HLA) of motor cortex in seven healthy and ten spinal cord injured (SCI) Sprague Dawley rats. ICMS-evoked spikes and EMG recordings were recorded simultaneously in the T13 vertebral segment (i.e., rostral lumbar enlargement) and four hindlimb muscles (EMG), respectively, for ~5 minutes during ICMS-evoked data acquisition periods.

Subjects

A total of 20 adult, male, Sprague Dawley rats were used in this study. Body weights ranged from 262 to 486 g (mean = 339.5 ± 55.2 g) and ages ranged from 59 to 308 days old (mean = 128 ± 74 days old). Rats were randomly assigned to one of two groups: Healthy group and SCI group. Three rats were removed from the study due to complications during surgical procedures, resulting in a total of seven healthy rats (n = 7) and ten SCI rats (n=10). Each group underwent the same acute electrophysiological analysis (Figure 3.1) described

below. This study was performed in accordance with all standards in the *Guide for the Care and Use of Laboratory Animals* (Institute for Laboratory Animal Research, National Research Council, Washington, DC: National Academy Press, 1996). The protocol was approved by the University of Kansas Medical Center Institutional Animal Care and Use Committee.

Spinal Cord Contusion Procedures

Spinal cord contusion procedures followed those described in previous experiments (Krizsan-Agbas, Winter et al. 2014). SCI surgeries were performed under ketamine hydrochloride (100 mg /kg IP)/xylene (5 mg /kg IP) anesthesia in aseptic conditions. Animals underwent a T8 laminectomy and 175 kDyn moderate impact contusion injury using an Infinite Horizon spinal cord impactor (Precision Systems and Instrumentation, LLC, Fairfax Station, VA). Displacement distance reported by the impactor software for each contusion was recorded at the time of surgery and was used as an initial quantitative marker for successful impact. At the conclusion of the surgery, 0.25% bupivacaine HCl was applied locally to the skin incision site. Buprenex (0.01 mg/kg, S.C.) was injected immediately after surgery and 1 day later. All animals were monitored daily until the end of the experiment. Before and after surgery, rats received a S.C. injection of 30,000 U of penicillin (Combi-Pen 48). Additionally, starting the first day after surgery, daily penicillin injections were given in 5 mL saline throughout the first week to prevent infections and dehydration. Bladders were expressed twice daily until animals recovered urinary reflexes. From the second week onward, animals were supplemented with vitamin C pellets (BioServ, Frenchtown, NJ) to avert urinary tract infection.

Behavioral Assessment Procedures

The Basso, Beattie, and Bresnahan (BBB) locomotor rating scale was used as a sensitive measure of locomotor ability after SCI (Basso, Beattie et al. 1995). Animals were habituated to the apparatus for 1-week preceding testing. BBB scoring was performed 1—3

days before SCI and at 7, 14, 21, and 28 days post-impact. Briefly, rats ran along a straight alley with a darkened goal box at the end for observational purposes. Scores were recorded for the left and right sides of each animal. Healthy rats were assessed pre-SCI to verify that they had no pre-existing motor deficits (i.e., displayed a BBB score of 21).

Surgical and Electrophysiological Procedures

Electrophysiological procedures were performed at 4 weeks post-SCI. After an initial stable anesthetic state was established using isoflurane anesthesia, the scalp and back were shaved. Then isoflurane was withdrawn, and an initial dose of ketamine hydrochloride (100 mg /kg; IP)/xylazine (5 mg /kg; IP) was administered. The anesthetic state was maintained throughout the remaining surgical and electrophysiological procedures with subsequent doses of ketamine (10 mg; IP or IM) and monitored via pinch and corneal reflexes. Additional doses of ketamine were administered if the rat reacted to a pinch of the forepaw/hindpaw, blinked after lightly touching the cornea, or exhibited increased respiration rate.

EMG electrode implantation.

EMG electrodes were implanted in four hindlimb muscles: the lateral gastrocnemius (LG), tibialis anterior (TG), vastus lateralis (VL), and biceps femoris (BF) (Borrell, Frost et al. 2017). Briefly, each EMG electrode consisted of a pair of insulated multi-stranded stainless-steel wires exposed approximately 1 mm, with the implanted end of the wire folded back on itself ('hook' electrode). Implantation locations were determined by surface palpation of the skin and underlying musculature. Once the hindlimbs were shaved, EMG electrodes were inserted into the belly of each muscle with the aid of a 22-gauge hypodermic needle. For each EMG electrode pair, wires were positioned approximately 5 mm apart in each muscle. The external portion of the wires were secured to the skin with surgical glue (3M Vetbond Tissue Adhesive, St. Paul, MN) and adhesive tape. An additional ground lead was placed into the base of the tail.

To verify that the EMG electrodes were in the belly of the target muscle, a stimulus isolator (BAK Electronics, Inc., Umatilla, FL) was used to deliver a biphasic (cathodic-leading) square-wave current pulse to the muscle through the implanted EMG electrodes. In addition, the impedance between the EMG electrodes was tested via an electrode impedance tester (BAK Electronics, Inc., Umatilla, FL). The EMG electrodes were determined to be inserted properly and in the desired muscle if: (a) the electrode impedance was approximately 7-8 kΩ; (b) direct current delivery to the muscle resulted in contraction of the desired muscle, and (c) the movement threshold was ≤ 5mA.

Intracortical microstimulation.

The rats were placed in a Kopf small-animal stereotaxic frame (David Kopf Instruments®, Tujunga, CA) and the incisor bar was adjusted until the heights of lambda and bregma were equal (flat skull position). The cisterna magna was punctured at the base of the skull to reduce edema during mapping. A craniectomy was performed over the hindlimb motor cortex. The general location of the craniectomy was based on previous motor mapping studies in the rat (Frost, Iliakova et al. 2013, Frost, Dunham et al. 2015). The dura over the cranial opening was incised and the opening was filled with warm, medical grade, sterile, silicone oil (50% Medical Silicone Fluid 12,500, 50% MDM Silicone Fluid 1000, Applied Silicone Corp., Santa Paula, CA) to prevent desiccation during the experiment.

A magnified digital color photograph of the exposed cortex was taken through a surgical microscope (Figure 3.2A and 3.2B). The image was transferred to a graphics program (Canvas 3.5) where a 200 µm grid was superimposed, by calibration with a millimeter ruler, to indicate intended sites for microelectrode penetration. The 0.0 mm rostrocaudal and mediolateral reference point was defined by the location of bregma.

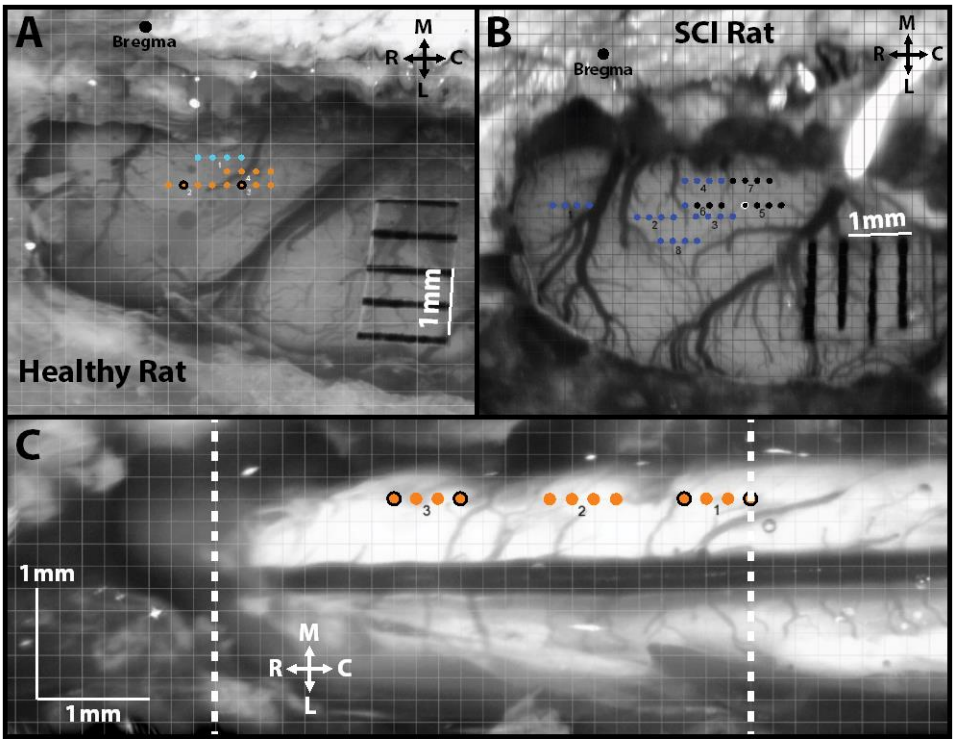

Figure 3.2. Overview of ICMS and intraspinal microstimulation (ISMS) mapping procedures. A) Cranial opening of a healthy rat over hindlimb motor cortex with superimposed grid for ICMS mapping. The black dot represents Bregma; each orange dot represents a site where ICMS evoked a hindlimb movement. Each light blue dot represents a site where ICMS evoked a trunk movement. **B)** Cranial opening of a SCI rat over hindlimb motor cortex with superimposed grid for ICMS mapping. The large black dot represents Bregma; each small black dot represents a site where ICMS did not evoke a movement. Each blue dot represents a site where ICMS evoked a forelimb movement. **C)** Spinal cord opening of a healthy rat over hindlimb spinal cord with superimposed grid for ISMS mapping. The two dashed white lines indicate the location under the T13 vertebrae. Each orange dot represents an ISMS-evoked hindlimb movement. **A, B, C)** Orange dots with black outline and black dot with white outline indicate sites with similarly evoked movements that were paired for analysis. Each square box is 200 x 200 µm. R = Rostral, C = Caudal, M = Medial, and L = Lateral.

ICMS was conducted in the hindlimb area (HLA) of the primary motor cortex using an activated single-shank, 8-site Neuronexus probe (Neuronexus, Ann Arbor, MI) optimized for microstimulation, following standard procedures (Frost, Iliakova et al. 2013, Frost, Dunham et al. 2015). ICMS was delivered at regularly spaced sites on the superimposed 200 µm grid at a depth of ~1.7 mm below the cortical surface (i.e., in Layer V) from the ventral-most site on the probe. Electrode depth was controlled using a Kopf hydraulic microdrive (Kopf Instruments, Tujunga, CA). To determine ICMS-evoked movements, stimuli consisted of thirteen, 200 µs biphasic cathodal pulses delivered at 300 Hz repeated at 1/sec from an electrically isolated,

charge-balanced (capacitively coupled) stimulation circuit. Each activated stimulation site had an impedance in the range of ~40 – 60 kΩ with a surface area of 1250 μm^2. The maximum compliance voltage of the system was 24 V.

ICMS-evoked movements. Movement that was evoked at the lowest ICMS current intensity (i.e., movement threshold) was recorded for each stimulation site. A movement was recorded only when a consistent joint displacement was observed and was described hierarchically, first by joint or whole leg movement. If the movement was restricted to a specific joint, it was then categorized as a hip, knee, ankle, or digit movement with a further category of flexion, extension, inversion, eversion, abduction, or adduction motion of the joint. ICMS current intensity did not exceed 100 µA to minimize current spread. If a movement was not evoked, it was labeled as "no response".

ICMS-evoked EMG. Using custom software (Matlab; The Mathworks, Inc., Natick, MA), stimulus-triggered averages (StTAs) of rectified EMG of all recorded leg muscle EMGs were analyzed to determine muscle activation (Hudson, Griffin et al. 2015, Borrell, Frost et al. 2017). For each of the implanted muscles, EMG data were recorded for at least 10 ICMS stimulus trains at movement threshold (or 80 µA in SCI rats) to obtain StTAs and averaged over a set time window of 220 ms. Since ICMS-evoked hindlimb movements could not be evoked in SCI rats, the amplitude of the stimulus trains was set at the average of movement thresholds seen in the healthy rats. StTAs were aligned to the time of the first stimulus pulse (i.e., 0 ms) and included data from -20.2 to +199.9 ms relative to the time of the first stimulus. A muscle was considered active when the average rectified EMG reached a peak ≥ 2.25 SD above baseline values in the interval from -20.2 to 0 ms and had a total duration of ≥ 3 ms. The stimulus artifact was minimal to absent in EMG recordings with no muscle activation. If an artifact was observed, the amplitude of the artifact was minimal compared to the amplitude of the evoked EMG; however, the averaging of the StTAs of EMG recordings largely eliminated the stimulus

artifact. As a result, the stimulus artifact was determined to have minimal to no effect on the recordings. EMG potentials were high- and low-pass filtered (30 Hz-2.5 kHz), amplified 200-1,000 fold, digitized at 5 kHz, rectified and recorded on an RX-8 multi-channel processor (Tucker-Davis Technology, Alachua, FL).

Intraspinal microstimulation mapping.

Following ICMS mapping, a midline incision was made over the spinal column, and a laminectomy was performed on the T13-L1 vertebrae exposing the L2-S1 segments of the spinal cord. Previously derived 3-dimensional ISMS-evoked topographic maps were used to guide the location of the spinal opening to obtain stimulation sites in the hindlimb spinal cord (Padmanabhan and Singh 1979, Borrell, Frost et al. 2017). The dura mater was removed using fine forceps and small scissors to allow electrode penetration. The spinal column was stabilized with a custom rodent spinal fixation frame (Keck Center for Collaborative Neuroscience Rutgers, The State University of New Jersey, USA) attached to the dorsal processes of vertebrae T12 and L2.

For the intraspinal microstimulation (ISMS) maps a digital photograph of the hindlimb spinal cord (i.e., T13-L1 vertebrae) was transferred to a graphics program (Canvas 3.5) where a 200 µm grid was superimposed to indicate intended sites for microelectrode penetration (Figure 3.2C). Stimulation sites were ~0.8 mm lateral of the central blood vessel (i.e., midline) at a depth ~2.27 mm below the surface of the spinal cord (i.e., in the ventral horn). Each stimulus consisted of three, 200 µs biphasic cathodal pulses delivered at 300 Hz repeated at 1/sec.

ISMS-evoked movements. Movements that were evoked at the lowest intensity of ISMS stimulation (i.e., movement threshold) were recorded for each stimulation site as described previously. Functionally similar movement sites in HLA and the ventral horn of the hindlimb spinal cord, derived from the ICMS and ISMS maps, respectively, were paired for

further neurophysiological assessment (e.g., ICMS and ISMS sites both resulting in hip flexion were paired together).

ISMS-evoked EMG. Recording and processing of EMG data paralleled those described above for ICMS-evoked EMG, except that the ISMS train consisted of only three pulses, further minimizing the effects of the stimulus artifact on the recorded data.

Extracellular spike recording in spinal cord (Healthy and SCI rats).

Microelectrode array placement. Electrode placement in the hindlimb cortex (stimulating electrode) and spinal cord (recording electrode) was derived from the ICMS- and ISMS-movement maps (Figure 3.2). Electrodes were placed in sites where movements about the hip were evoked in both the cortex and spinal cord (orange dots in Figures 3.2A and 3.2C). Since hindlimb responses cannot be evoked from hindlimb motor cortex in SCI rats (Frost, Dunham et al. 2015), the electrode was placed in a non-responsive site (black dot in Figure 3.2B) that was directly caudal to the forelimb motor cortex (blue dots in Figure 3.2B). The same stimulating electrode used during ICMS mapping was placed in the HLA and a recording microelectrode probe simultaneously placed in the hindlimb movement-matched spinal cord site. The recording microelectrode was a single-shank, 16-channel Michigan-style linear microelectrode probe (Neuronexus, Ann Arbor, MI), optimized for extracellular spike recording (Figure 3.3). Each of the 16 electrode sites had a site area of 703 μm^2, separation of 100 µm, shank thickness of 15 µm in diameter, and impedance of ~0.3 MΩ. The tip of the electrode was lowered to a depth of ~2270 µm below the spinal cord surface. For analysis of spike responses by depth, the 16 recording channels were divided into 4 sectors based on depth below the surface of the spinal cord: Dorsal Sector (720—1020 mm; dorsal horn), Upper Intermediate Sector (1120—1420 mm; intermediate layer), Lower Intermediate Sector (1520—1820 mm; intermediate layer), and Ventral Sector (1920—2220 mm; ventral horn). ICMS was used to test corticospinal coupling by delivering a test stimulus in HLA, and ICMS-evoked spikes were

simultaneously recorded from the 16 microelectrode channels in the spinal cord and EMG from the hindlimb muscles. For the corticospinal coupling procedure, the ICMS stimulus consisted of three, 200 µs biphasic cathodal pulses delivered at 300 Hz repeated at 1/sec at movement threshold. Restricting ICMS to three stimulation pulses prevented the influence of movement artifacts in the recorded data. Also, the minimal pulse train minimized the effects of artifacts on our ability to discriminate spikes. A maximum current of 100 µA was set for sites in which no movement was evoked. Simultaneous stimulation and recording sessions were conducted ~5 min at each ICMS test site.

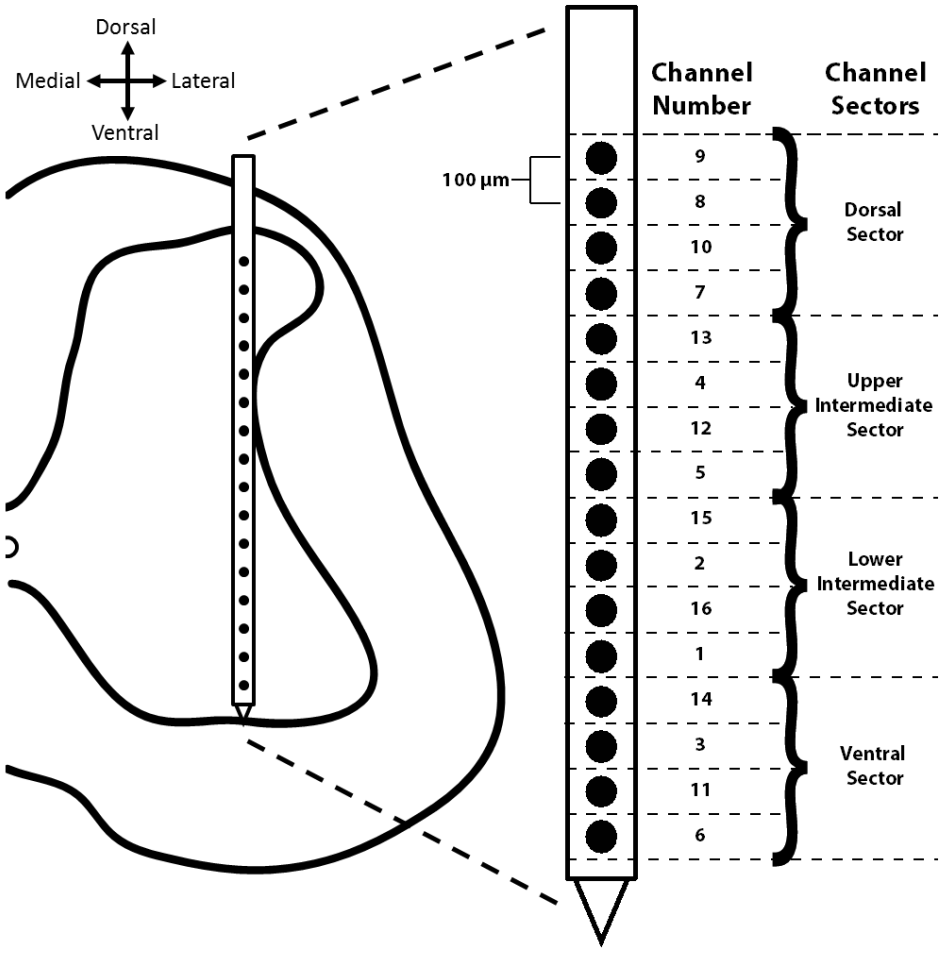

Figure 3.3. Cross sectional diagram of hindlimb spinal cord with placement of the recording probe during ICMS. ICMS-evoked extracellular spikes were recorded with a 16-channel Neuronexus recording probe inserted into the hindlimb spinal cord under T13 vertebrae ~0.8 mm from midline to a depth of ~2.27 mm below the surface of the spinal cord spanning virtually the entire dorsoventral extent of the spinal cord grey matter from the dorsal horn to the ventral horn. The schematic diagram of the recording shank indicates the channel numbers of the recording sites and corresponding dorsoventral sectors.

Spike recording and analysis. ICMS-evoked spike activity was recorded from each of the 16 active recording channels for ~5 min for each ICMS site using neurophysiological recording and analysis equipment (Tucker Davis Technologies, Alachua, FL). Neural spikes were discriminated using principle component analysis (Lewicki 1998). ICMS-evoked spike activity was sorted and averaged into 1 ms bins over the ~5 min recording bout (i.e., averaged over ~300 ICMS trains). Activity is represented in post-stimulus spike histograms for 200 ms around the onset of each ICMS stimulus (ICMS began at 0 ms; histogram extended -100 ms before and +100 ms after onset ICMS), using custom software (Matlab; The Mathworks, Inc., Natick, MA). Spike activity could not be discriminated over the first ~7 ms due to the stimulus artifact from the three stimulus pulses.

Firing rate (FR) calculation. To quantitatively analyze these data and compare healthy and SCI groups, the ICMS-evoked firing rate (FR) (i.e., total number of recorded spikes per 1ms bin/total time of recording) was calculated within each time bin of the post-stimulus spike histograms using custom software (Matlab; The Mathworks, Inc., Natick, MA). The FR was only considered for analysis if the FR for the respective time bin was greater than 2x standard deviation (horizontal, dashed, red line; Figure 3.6) above average baseline (horizontal, solid, red line; Figure 3.6) FR. Baseline FR was derived by averaging the FR of each time bin 10 ms before the onset of ICMS (i.e., from -10 to 0 ms in the post-stimulus spike histogram).

Probability of activation. The Probability of Activation (POA) is the likelihood that spikes are evoked during each ICMS stimulus event. The POA of ICMS-evoked spikes occurring during each test stimulus of ICMS was calculated for each 5-min recording. POA = number of recorded ICMS-evoked spiking incidences/total number of ICMS-test stimuli. The POA was calculated for each recording channel across all healthy and SCI rats at each specified latency and compared between each rat group and dorsoventral sector. The mean and standard error were calculated by averaging the POA of each channel within each respective dorsoventral sector.

Euthanasia

At the end of each experiment, animals were euthanized with an intraperitoneal injection of beuthanasia (100 mg /kg), the rat was transcardially perfused with fixative and the spinal cord examined.

Statistical Analyses

Statistical analyses were performed using JMP 11 software (SAS Institute Inc., Cary, NC). Dorsoventral sector spiking differences were evaluated by an initial one-way repeated measures analysis of variance (ANOVA). When a significance of $p < 0.05$ was obtained, the data were further analyzed using a student's t-test to compare means of each dorsoventral sector between healthy and SCI rats. Data are presented as average ± standard error of the mean unless otherwise stated.

Results

BBB Scores

Each of the healthy rats scored 21 on the BBB scale (normal) while the SCI rats displayed an average BBB score of 14.7 ± 0.8 (mean ± SD) at 4 weeks post-SCI. This BBB score indicates that the SCI rats had consistent weight-supported plantar steps, no or occasional toe clearance (i.e., scraping of the digits on the ground) during forward limb advancement, consistent forelimb-hindlimb coordination, and predominant paw position during locomotion that was always rotated externally just before it lifted off at the end of stance and either externally rotated or parallel to the body at initial contact with the surface

SCI Verification

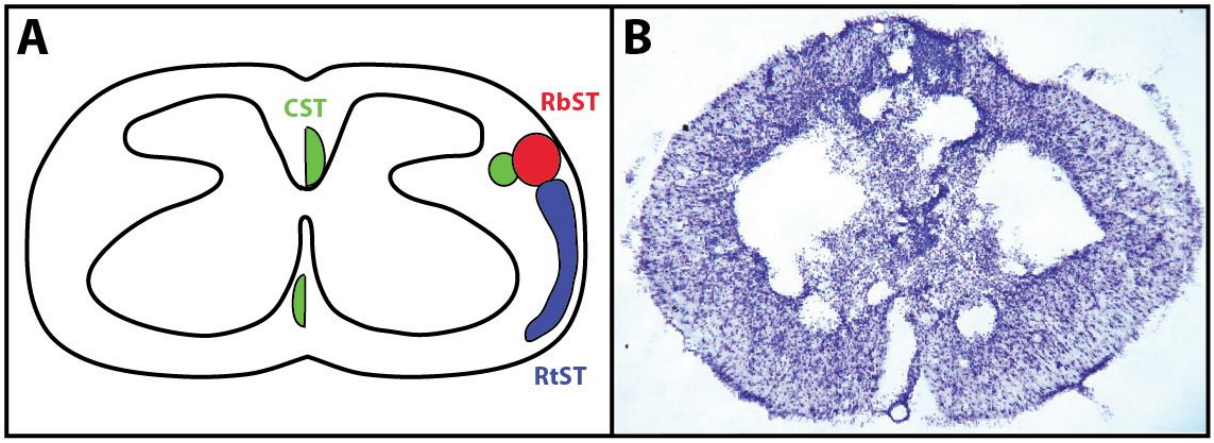

Figure 3.4. Verification of spinal cord injury under T8 vertebrae. A) Location of descending corticospinal tract (CST; green), rubrospinal tract (RbST; red), and reticulospinal tract (RtST; blue) (Lemon 2008, Fink and Cafferty 2016). B) Representative image of spinal cord injury epicenter stained with cresyl violet 4 weeks after injury.

All SCI rats received a 175 kDyn impact at the level of the T8 vertebrae. The average displacement value of the impactor was 1041.80 ± 111.11 µm (mean ± SD) from the surface of the spinal cord. At the conclusion of the study, SCI rats were perfused, and the spinal cords were removed for histological verification of the lesion. An exemplar coronal histological section

through the center of the injury is shown in Figure 3.4. After SCI, the spinal grey matter at the epicenter was severely damaged. The ventromedial (location of the ventral CST and RtST) and dorsolateral (location of the RbST and dorsolateral CST) spinal cord white matter tracts generally remained intact while the dorsal column white matter tracts (location of the dorsomedial CST in rodents) was severely damaged (Figure 3.4B).

Neurophysiological Results

Neurophysiological stimulation and recording sessions were conducted in seven healthy rats (56 sessions) and ten SCI-injured rats (10 sessions; 4 weeks post-SCI) using 16 channel linear microelectrode arrays spanning the dorsoventral extent of the spinal cord grey matter. In healthy rats, ICMS-evoked activity was examined at multiple sites in separate data collection periods. Due to the inability to evoke hindlimb movements via ICMS after SCI, only one cortical site was used per SCI rat. Each cortical stimulation site in SCI rats was selected based on the location of ICMS-evoked hip movement sites from ICMS maps in healthy rats. In healthy rats, hip movement sites are consistently located caudal to the forelimb representation and caudolateral to the trunk representation (Frost, Dunham et al. 2015). Both forelimb and trunk movements can still be evoked after SCI.

ICMS-evoked movements.

In healthy rats, evoked movements from ICMS in hindlimb motor cortex were observed as described in previous studies (Borrell, Frost et al. 2017). Evoked responses consisted of hip flexion (n = 23 sites), lateral leg rotation (n = 5 sites), knee flexion (n = 8 sites), ankle flexion (n = 9 sites), digit extension (n = 6 sites), and no response (n = 5 sites). In SCI rats, no ICMS-evoked hindlimb movements were elicited. The average ICMS movement threshold current intensity was 80.66 ± 31.78 μA (mean ± SD) in healthy rats. Based on the average ICMS movement threshold seen in healthy rats, a constant ICMS current amplitude of 80 μA was used

in SCI rats. No significant differences in ICMS threshold currents were found among the different movement categories ($p > 0.05$). Thus, data from the different hindlimb movement categories were pooled in subsequent analyses of ICMS-evoked activity in the spinal cord.

ICMS- and ISMS-evoked EMG onset latencies in healthy rats.

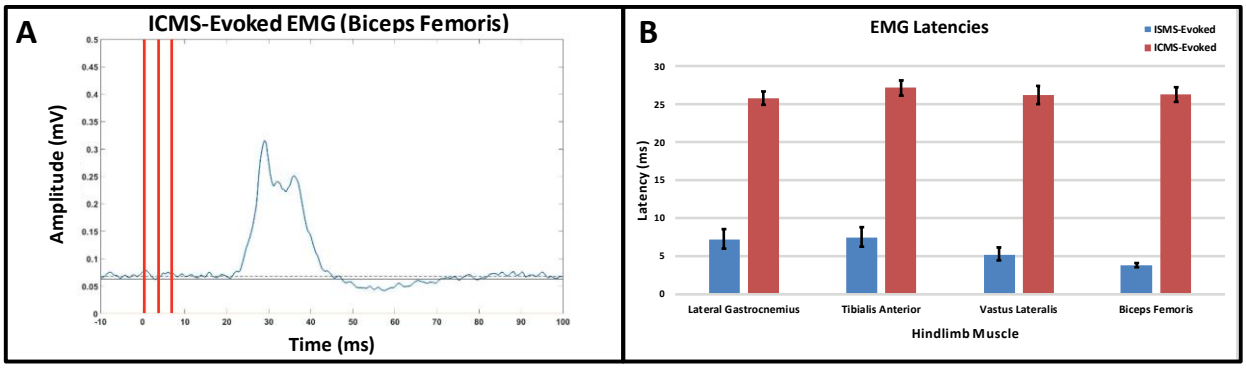

Figure 3.5. ICMS- and ISMS-evoked EMG recordings from the hindlimb muscles in healthy rats. ICMS was conducted in layer V of the hindlimb area (HLA) of the motor cortex and ISMS was conducted in the ventral horn of the hindlimb spinal cord (vertebrae T13-L1) while recordings were simultaneously conducted in four hindlimb muscles: Lateral Gastrocnemius, Tibialis Anterior, Vastus Lateralis, and Biceps Femoris. ICMS and ISMS were conducted separately, not simultaneously. **A)** Representative ICMS-evoked EMG recording from the Biceps Femoris of a healthy rat**.** Stimulus-triggered averaging (StTA) was used to analyze the EMG recordings. Latency was measured as the first instance a muscle was active after onset stimulation at 2.25 standard deviations above baseline average. Vertical red lines are the superimposed stimulus artifacts from the 3-pulse stimulation train. **B)** Mean ICMS- and ISMS-evoked EMG latencies for each hindlimb muscle of the healthy rats. Error bars indicate standard error of the mean.

In healthy rats, ICMS- and ISMS-evoked EMG potentials were recorded from four hindlimb muscles: Biceps Femoris (BF) Vastus Lateralis (VA), Tibialis Anterior (TA), and Lateral Gastrocnemius (LG). Onset latencies were determined from stimulus-triggered averages (StTAs) of each ICMS and ISMS recording (Figure 3.5A). ICMS-evoked EMG onset latencies (i.e., 2.25 standard deviations above baseline) from healthy rats (Figure 3.5B) were as follows (mean ± standard error): BF = 26.30 ± 1.00 ms, VL = 26.27 ± 1.23 ms, TA = 27.21 ± 1.03 ms, and LG = 25.82 ± 0.94 ms. ISMS-evoked EMG latencies (mean ± standard error) in healthy rats are shown in Figure 3.5B: Lateral Gastrocnemius (7.21 ± 1.28 ms), Tibialis Anterior (7.44 ± 1.27 ms), Vastus Lateralis (5.21 ± 0.84 ms), and Biceps Femoris (3.79 ± 0.24 ms). Post hoc comparisons (student's t-test) showed no significant differences in mean EMG latencies when

comparing ICMS-evoked muscles and when comparing ISMS-evoked muscles. After SCI, ICMS-evoked EMG activity could not be elicited. To avoid confounding the primary outcome in this study (ICMS-evoked spikes in spinal cord neurons), ISMS experiments were not performed in SCI rats. Further ISMS would have required additional penetrations of the spinal cord which could have caused additional trauma that could have disrupted the circuitry and projections that were involved during the 5-minute ICMS recordings.

ICMS-evoked spike activity in spinal cord neurons.

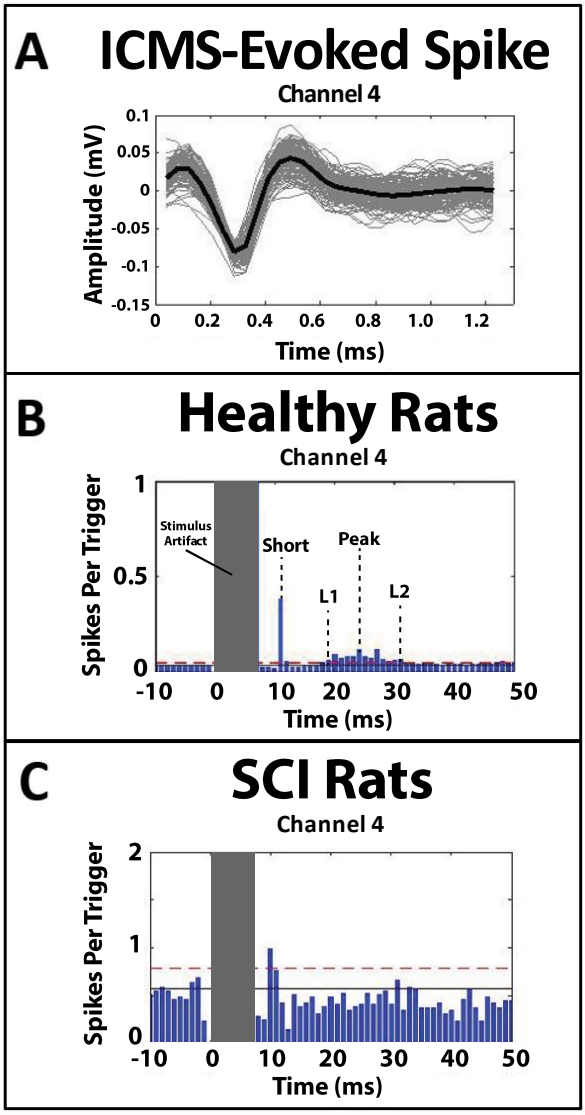

Figure 3.6. ICMS-evoked activity in the spinal cord. Sample ICMS-evoked action potentials (i.e., spikes) recorded from hindlimb spinal cord and post-stimulus spike histogram analysis from the summation of all rats in recording channel 4 (i.e., depth of 1220 µm). Data were normalized to the largest spiking bin. **A)** ICMS-evoked spikes recorded from one channel in an intermediate layer of hindlimb spinal cord. Solid black spike is the average of all recorded spikes from channel 4, and grey spikes are all spikes of similar spiking profiles recorded from channel 4. **B)** Post-stimulus spike histogram of spikes recorded from channel 4 from all healthy rats. Solid horizontal line is baseline average. Red dashed horizontal line is 2 standard deviations (SDs) above baseline average. Onset of ICMS stimulation is at 0 ms. Spinal cord spiking activity was seen at two different latencies, which were separated into short- and long-latency times. "Short" is the short-latency time at ~10 ms. L1 is onset time when long latency evoked spiking activity reaches above 2 SDs above baseline average, Peak is the peak of long latency evoked spiking activity, and L2 is offset time before long latency spiking activity dips below 2 SDs above baseline average. The stimulus artifact occurred from 0-7 ms. **C)** Post-stimulus spike histogram of spikes recorded from channel 4 of all SCI rats. Short latency spikes consistently occurred in all dorsoventral sectors. The solid horizontal line is the baseline average. Red dashed horizontal line is 2 standard deviations (SDs) above baseline average. The long latency responses were greatly diminished in all dorsoventral sectors after SCI.

Overview of spike latencies. ICMS-evoked spikes in the spinal cord (Figure 3.6A) were recorded extracellularly, sorted, and displayed in post-stimulus time histograms. Healthy rats typically displayed two populations in the post-stimulus histograms, differing in onset latency: 1) short latency and 2) long latency. Short latency spikes typically occurred between 10-12 ms post-ICMS (Figure 3.6B). Long latency spikes were distributed over a broader Gaussian distribution (~20-60 ms) after the short latency responses. Long latency spikes were divided into “long-latency response 1” (L1; i.e., onset of Gaussian distribution; rising above 2x standard deviation of average baseline activity), "peak latency” (i.e., peak of Gaussian distribution), and “long-latency response 2” (L2; i.e., offset of Gaussian distribution; falling below 2x standard deviation of average baseline activity) (Figure 3.6B). L2 latencies were not consistent and displayed high variability (mean ± standard deviation; Dorsal Sector = 61.73 ± 26.90 ms, Upper Intermediate Sector = 66.86 ± 27.17 ms, Lower Intermediate Sector = 63.87 ± 23.89 ms, and Ventral Sector = 63.95 ± 24.01 ms). Thus, L2 latencies were not considered for further analysis.

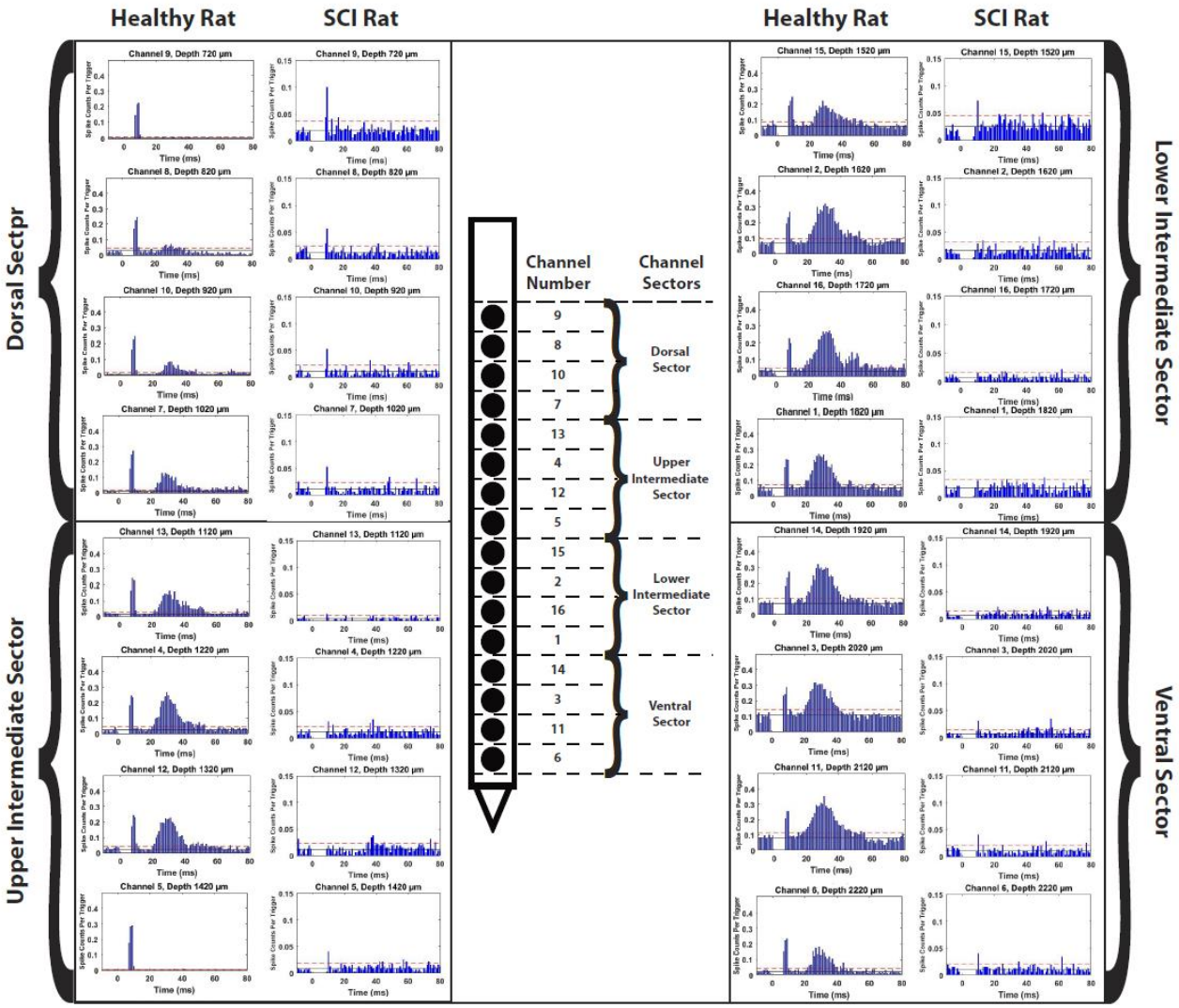

Figure 3.7. Representative recordings from one healthy and one SCI rat from multiple recording channels (i.e., dorsoventral depths) divided into dorsoventral sectors based on depth.

Post-ICMS spike histograms at different dorsoventral depths. For each rat in both healthy and SCI groups, ICMS-evoked spikes were sorted and examined in post-stimulus spike histograms organized by channel (dorsoventral depth). Not all recorded latencies (Short, L1, Peak, and L2) were observed in all channels (Figure 3.7), nor in each rat; particularly in the SCI rats, nor was this absence of observed latencies specific to a particular dorsoventral depth. In the seven healthy rats, evoked spikes occurred at the Short latency in six rats (86%). In the ten SCI rats, evoked spikes occurred at the Short latency in nine rats (90%). Representative recordings from a single ICMS/ISMS site pair in one healthy and one SCI rat are shown in Figure 3.7. In the healthy rat in this example, two channels did not display any long-latency responses. The SCI rat in this example showed diminished evoked activity compared with the healthy rat; however, in nine channels ICMS-evoked activity occurred at the Short latency.

Table 3.1. The Probability of Activation (POA) of ICMS-evoked spikes at each specified latency. The POA was calculated for each group for each dorsoventral sector. A green up-arrow indicates a significant increase in POA after SCI while a red down-arrow indicates a significant decrease in POA after SCI. ***** = Significant difference ($p < 0.05$) when compared to healthy rats of the same dorsoventral sector and specified latency.

Dorsoventral Sector	Rat Group	Probability of Activation (Mean ± SE)					
		Short		L1		Peak	
Dorsal	Healthy	0.22 ± 0.03	↑	0.72 ± 0.03	=	0.78 ± 0.03	=
	SCI	0.48 ± 0.03*		0.73 ± 0.05		0.70 ± 0.04	
Upper Intermediate	Healthy	0.27 ± 0.02	↑	0.90 ± 0.02	=	0.93 ± 0.02	↓
	SCI	0.50 ± 0.04*		0.85 ± 0.05		0.78 ± 0.09*	
Lower Intermediate	Healthy	0.18 ± 0.02	↑	0.64 ± 0.09	↑	0.66 ± 0.08	=
	SCI	0.35 ± 0.09*		0.80 ± 0.04*		0.75 ± 0.03	
Ventral	Healthy	0.19 ± 0.02	↑	0.54 ± 0.07	↑	0.56 ± 0.05	↑
	SCI	0.43 ± 0.03*		0.80 ± 0.06*		0.83 ± 0.03*	

Probability of activation (POA). The POA for Healthy and SCI rats was calculated for each dorsoventral sector and listed in Table 3.1. At the Short latency, the POA significantly increased ($p < 0.05$) in all dorsoventral sectors after SCI. At the L1 latency, the POA significantly increased in the Lower Intermediate ($p = 0.0138$) and Ventral ($p = 0.0001$) Sectors

after SCI. At the Peak latency, the POA significantly decreased in the Upper Intermediate (p = 0.0187) Sector and significantly increased in the Ventral (p < 0.0001) Sector after SCI.

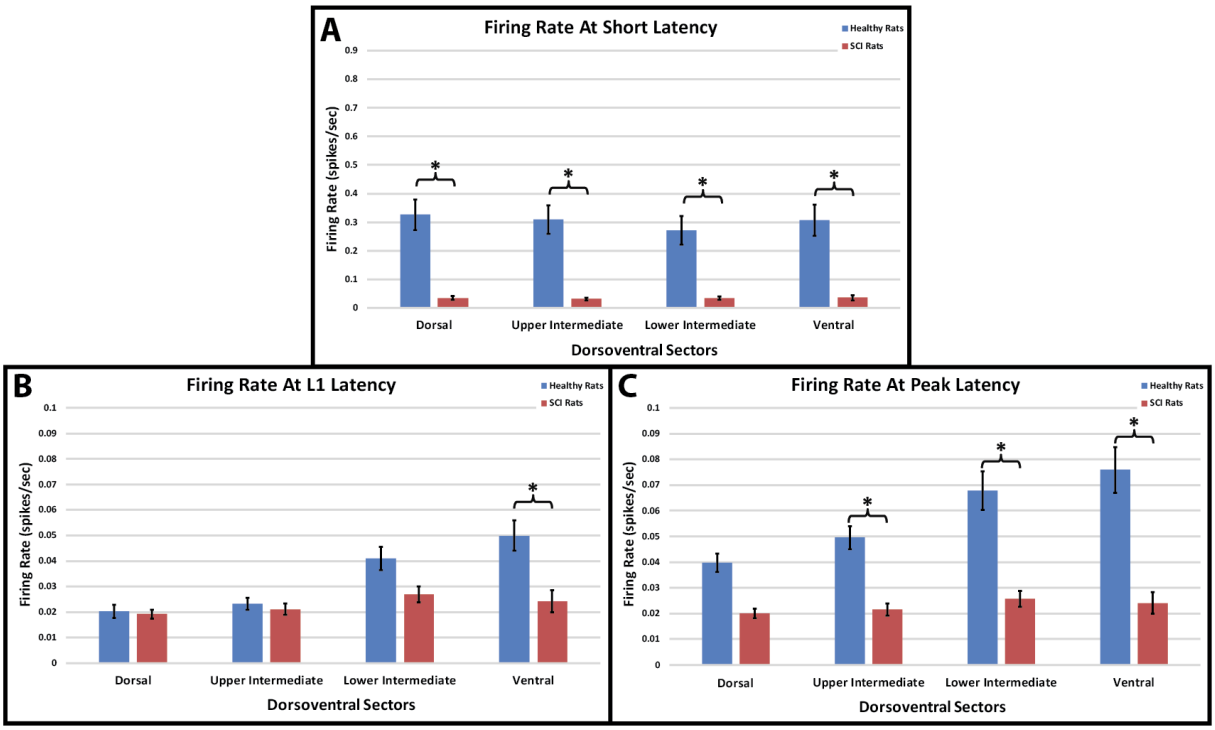

Figure 3.8. Average firing rates of ICMS-evoked spikes at specified latencies in dorsoventral sectors based on depth below the surface of the spinal cord. The 16 recording channels were divided into 4 sectors based on depth below the surface of the spinal cord. Average firing rates of ICMS-evoked spikes (mean ± standard error): at **A)** Short, **B)** L1, and **C)** Peak latencies. ***** = Significant difference between healthy and SCI rats in the same dorsoventral sector (p < 0.05).

Firing rate. The average firing rate of ICMS-evoked spikes was calculated for Healthy and SCI rats and is displayed in Figure 3.8. When comparing Healthy and SCI rats, the average firing rate of ICMS-evoked spikes at Short, L1, and Peak latencies generally decreased. The average firing rate of ICMS-evoked spikes at Short latencies was significantly lower (p < 0.05) in all dorsoventral sectors (Dorsal Sector, p = 0.006; Upper Intermediate Sector, p = 0.0007; Lower Intermediate Sector, p = 0.0151; Ventral Sector, p = 0.0027) after SCI. The average firing rate of ICMS-evoked spikes at L1 latencies was significantly lower (p < 0.05) in only the Ventral Sector (p = 0.0027) after SCI. The average firing rate of ICMS-evoked spikes at peak long latencies was significantly lower (p < 0.05) in all of the dorsoventral sectors

except for the Dorsal Sector (Upper Intermediate Sector, $p = 0.0348$; Lower Intermediate Sector, $p = 0.0024$; Ventral Sector, $p = 0.0001$) after SCI.

Spike amplitude. The peak-to-peak amplitude of ICMS-evoked spikes recorded in the hindlimb spinal cord of healthy and SCI rats are shown in Table 3.2. When comparing spike amplitudes between dorsoventral sectors in healthy rats, the average ICMS-evoked spike amplitude was significantly higher in the Ventral Sector than in the Dorsal ($p = 0.0021$), Upper Intermediate ($p = < 0.0001$), and Lower Intermediate ($p < 0.05$) Sectors. In addition, the average ICMS-evoked spike amplitude was significantly higher in the Lower Intermediate Sector than in the Upper Intermediate Sector ($p < 0.05$). When comparing the average ICMS-evoked spike amplitudes of each dorsoventral sector between Healthy and SCI rats, the average ICMS-evoked spike amplitude was significantly lower in the Dorsal ($p = 0.0026$), Lower Intermediate ($p = 0.0106$), and Ventral ($p < 0.0001$) Sectors.

Table 3.2. ICMS-evoked spike amplitude in healthy and SCI rats. Spike amplitude was calculated from peak-to-peak of the spike profile. The average (mean ± std) spike amplitude was calculated for each dorsoventral sector. * = significantly lower ($p < 0.05$) when compared to healthy rats of the same dorsoventral sector.

ICMS-Evoked Spike Amplitude (mV)				
Rat Groups	**Dorsoventral Sectors**			
	Dorsal	**Upper Intermediate**	**Lower Intermediate**	**Ventral**
Healthy Rats	0.12 ± 0.11	0.11 ± 0.09	0.13 ± 0.14	0.15 ± 0.15
SCI Rats	0.07 ± 0.06*	0.09 ± 0.06	0.09 ± 0.04*	0.08 ± 0.04*

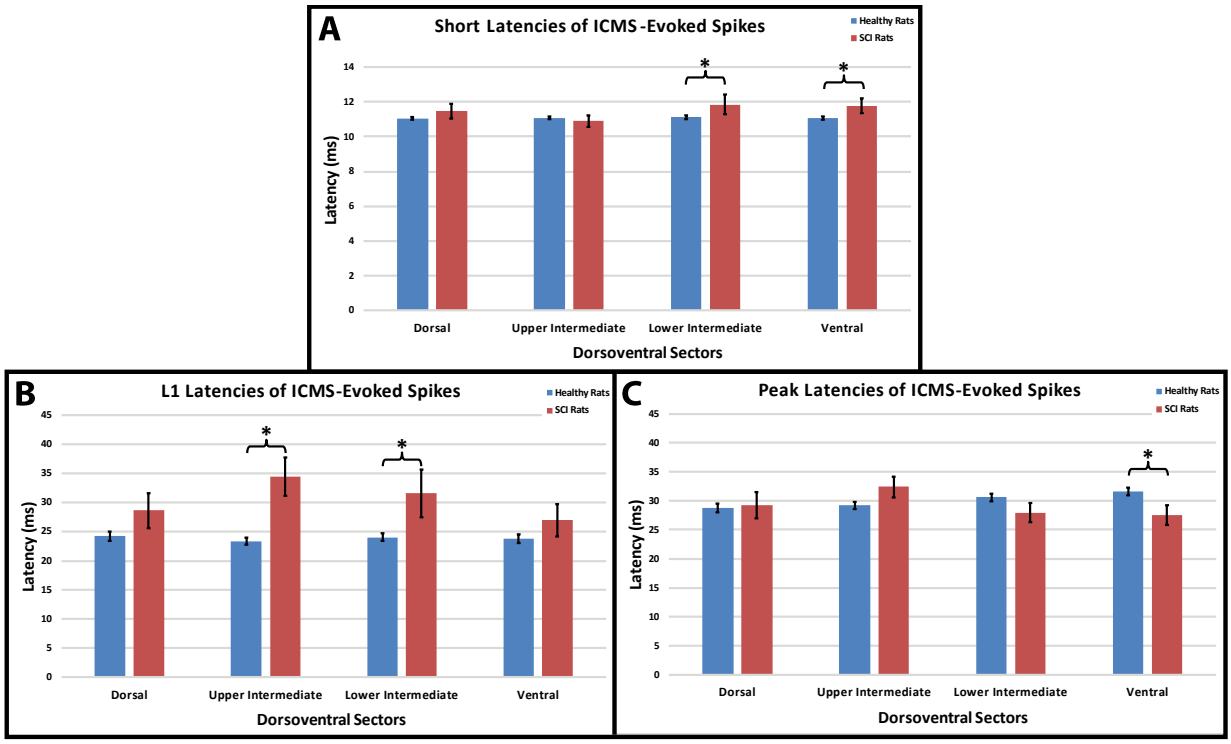

Figure 3.9. Average latencies of ICMS-evoked spikes by dorsoventral depth. The 16 recording channels were divided into 4 sectors based on depth below the surface of the spinal cord. Average latencies of ICMS-evoked spikes (mean ± standard error): at **A)** Short, **B)** L1, and **C)**, Peak latencies. ***** = Significant difference between healthy and SCI rats in the same dorsoventral sector ($p < 0.05$).

Spike latencies at different dorsolateral depths. The spike latencies of ICMS-evoked spikes recorded in the hindlimb spinal cord of healthy and SCI rats are shown in Figure 3.9. When comparing the average ICMS-evoked spike latencies of each dorsoventral sector between Healthy and SCI rats, short latencies (Figure 3.9A) were significantly longer ($p < 0.05$) in SCI rats in the Lower Intermediate ($p = 0.0245$) and Ventral ($p = 0.0207$) Sectors. L1 latencies (Figure 3.9B) were significantly longer ($p < 0.05$) in SCI rats in the Upper ($p < 0.0001$) and Lower Intermediate ($p = 0.0006$) Sectors. Peak long latencies (Figure 3.9C) were significantly shorter ($p < 0.05$) in SCI rats in the Ventral Sector ($p = 0.016$).

Correspondence of recording sites to anatomical locations of Rexed laminae. To better understand the ICMS-evoked spike latencies recorded at various dorsoventral depths of the hindlimb spinal cord of the rat, the depth of each channel was compared to the anatomical

locations of Rexed laminae in the lumbar spinal cord. Previous topographical studies by Gilerovich *et al* (Gilerovich, Moshonkina et al. 2008) indicate the rostral sector of vertebrae T13 of the Sprague Dawley rat is located at spinal cord segmental level L2-L3. From our previous derived topographic map of the hindlimb spinal cord using ISMS (Borrell, Frost et al. 2017), we know that at ~0.8 mm from midline and at a depth of ~2.27 mm below the surface of the spinal cord, all channels were in the grey matter of the hindlimb spinal cord. Using the laminar cytoarchitectonic organization presented by Molander *et al,*(Molander, Xu et al. 1984) we can conclude that we were recording in or near all laminae except for laminae VI (seen only in L3-S1 segments of the rat) and laminae X (found medially around the central canal) (Figure 3.10).

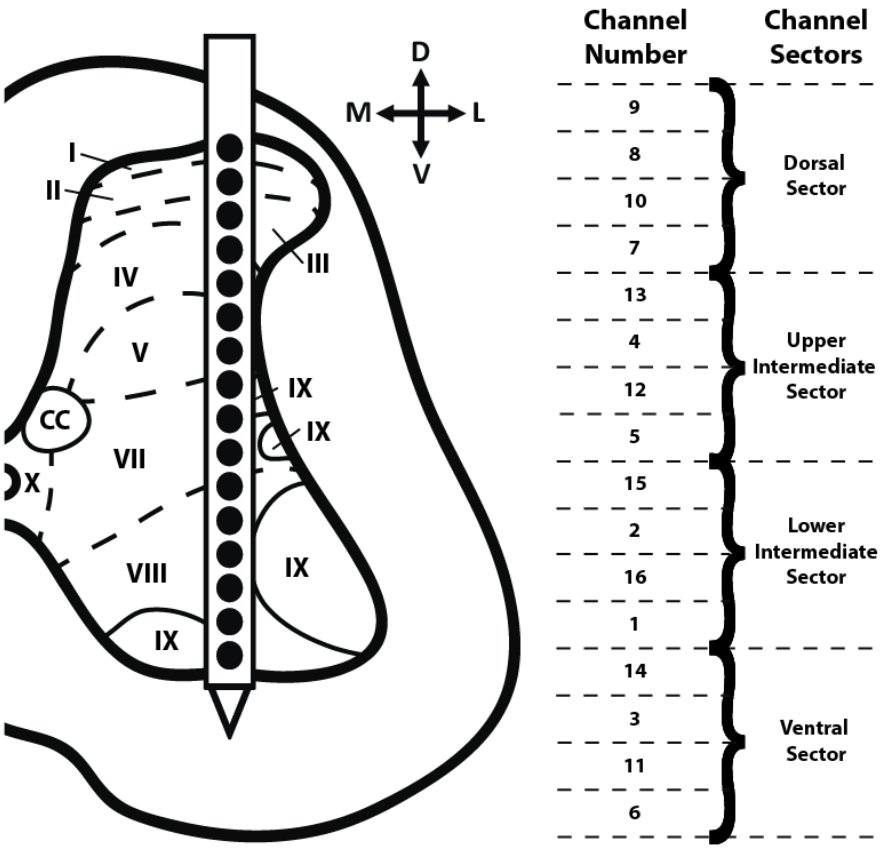

Figure 3.10. Cross sector of hindlimb spinal cord with the anatomical locations of Rexed laminae at T13 relative to each recording channel.

More specifically, channels 9, 8, 10, and 7, defined as the Dorsal Sector, were in the dorsal horn which corresponds to laminae I, II, III, and possibly IV. Channels 13, 4, 12, and 5 were in the lower dorsal to upper intermediate areas, thus defined as the Upper Intermediate Sector, which correspond to laminae IV, V, and possibly VII. Channels 15, 2, 16 and 1 were in the intermediate space, defined as the Lower Intermediate Sector, which corresponds to laminae VII and VIII. Channels 14, 3, 11, and 6 were in the ventral horn, thus defined as the Ventral Sector, which corresponds to laminae VIII and IX. With the possibility of laminae IX being located in the lateral intermediate grey matter and extending into the ventral horn, there is a possibility of the Lower Intermediate and Ventral Sectors recording ICMS-evoked spikes in these sectors of nuclei as well (Molander, Xu et al. 1984).

Discussion

The goal of this study was to determine the effects of a contusive SCI on spinal motor neuron activity, corticospinal coupling, and conduction time in rats at various dorsoventral depths of the hindlimb spinal cord. In healthy rats, ICMS-evoked activity in spinal cord neurons exhibited a distinct population of short-latency spikes reliably evoked at 10-12 ms at all dorsoventral depths of the spinal cord. Four weeks after a contusion injury, severely damaging the CST in the dorsal columns, the short latency spikes were still present. Here we discuss the likely pathways underlying these short-latency responses and implications for understanding of how spared descending fibers participate in motor control after SCI.

Functional Recovery after SCI in Rats

It has been shown in rats that synaptic coupling may be dysregulated after SCI, leading to hyperreflexia and spasticity (Yates, Garrison et al. 2011). Immediately after SCI in humans, the spinal cord enters a state of spinal shock, a loss of sensation accompanied by motor paralysis, followed by a gradual recovery of reflexes (Ditunno, Little et al. 2004). This is evident in this rat model of contusive SCI, where there is a loss of hindlimb motor function for roughly three days after injury, with reflexes and some voluntary use of hindlimbs returning over time. It has been reported that the duration and severity of spinal shock lasts up to two weeks in the rat (Bennett, Gorassini et al. 1999). Recovery of voluntary function plateaus at four weeks post-injury, but after a thoracic contusion deficits in control of hindlimb movements remain, as shown in this and a previous study (Krizsan-Agbas, Winter et al. 2014).

ICMS-Evoked Neuronal Spikes in the Spinal Cord of Healthy Rats

Following ICMS in motor cortex, spikes were recorded reliably at all dorsoventral depths of the grey matter. ICMS-driven spikes theoretically occur via one of three major routes: corticospinal tract (CST; either monosynaptic or disynaptic via spinal cord interneurons), cortico-

rubro-spinal pathway, and cortico-reticulo-spinal pathway. Based on antidromic activation studies, CST axons to the thoracic cord of rats have a maximum conduction velocity of ~19 m/s (average = 11 m/s) (Mediratta and Nicoll 1983). Since the distance between the CST soma and the T13-L1 microelectrodes is ~20 cm, and assuming a synaptic delay of 0.75 ms (Katz and Miledi 1965), one would predict that the earliest spikes resulting from CST activation could occur at about 11 ms. However, based on the average conduction velocity (11 m/s), the CST-based spike distribution would peak at ~19 ms. Assuming a disynaptic connection (Alstermark, Ogawa et al. 2004), the earliest CST-based spikes would occur at ~12 ms and the peak at ~20 ms. Based on these assumptions, it is unlikely that the CST contributed substantially to the short-latency spike population in the present data. However, the long-latency spikes may be, at least in part, a result of disynaptic and polysynaptic CST connections and demonstrated by higher firing rates in intermediate and ventral laminae of the spinal cord grey matter. EMG latencies were observed beginning at 26-27 ms. Long-latency spikes recorded after the EMG response onset are likely intermixed with spike responses from Ia afferents subsequent to muscle contraction.

ICMS-evoked spikes also could have resulted from indirect activation via the cortico-rubrospinal and cortico-reticulospinal pathways. Rubrospinal tract (RbST) fibers have a similar conduction velocity to those of the CST (Al-Izki, Kirkwood et al. 2008), so cortico-rubrospinal activity would at least partially overlap that of the corticospinal activity (with an additional synaptic delay) and could contribute to the long-latency response. Since the corticospinal and rubrospinal pathways are coupled with the evoked EMG activity, the CST and RbST may have a more direct influence on voluntary motor function, such as overground locomotion (DiGiovanna, Dominici et al. 2016). But again, the longer latency responses are more difficult to interpret due to recurrent activation via Ia afferents.

Finally, while few studies have examined the conduction velocity of the reticulospinal tract (RtST) in rats, it appears that RtST conduction velocities in rats are broadly distributed, but generally much faster than the CST or RbST in rats (Fox 1970), and are similar to other species (Takakusaki, Chiba et al. 2016). Conduction velocities of RtST neurons range from 16-80 m/s with a mean conduction velocity of 37 m/s (Fox 1970). Thus, the earliest cortico-reticulospinal-based spikes could have occurred at T13-L1 at 4-5 ms. If spikes occurred at this time point, they could not be discriminated due to overlap with the stimulus artifact. Based on the mean conduction velocity, spikes would occur at about 8 ms. But due to the wide range of conduction velocities expected in the RtST, it is likely that the short-latency responses at 10-12 ms were primarily due to cortico-reticulospinal fiber activation. This pathway is assumed to have disynaptic or polysynaptic connections either directly onto long-propriospinal neurons or commissural interneurons located in the grey matter (Mitchell, McCallum et al. 2016). In the present study, firing rates were similar throughout the dorsoventral layers.

ICMS-Evoked Neuronal Spikes in the Spinal Cord of SCI Rats

A moderate contusion applied to the dorsal midline of the thoracic spinal cord (modeling a clinical injury in humans) destroys the central core of the spinal cord at the lesion epicenter, ablating the spinal grey matter and sparing a limited amount of circumferential descending motor pathways (Basso, Beattie et al. 1996, Lemon 2008, Fink and Cafferty 2016). Specifically, the dorsomedial funiculi are severely damaged, while the dorsolateral, ventral, and ventromedial funiculi remain largely intact.

Most notably, short-latency spikes were still present despite severe damage to the CST. This is most likely due to the maintenance of the cortico-reticulospinal tract. Although the firing rate was diminished, the probability of activation (POA) for short-latency spikes was increased in SCI rats in all dorsoventral laminae, roughly doubling in dorsal, upper intermediate and ventral laminae, and nearly tripling in the lower intermediate laminae. This suggests that in

healthy rats the dorsomedial CST exerts an inhibitory influence on spinal cord neurons, and that after SCI, ICMS-evoked spike activity via other descending pathways is released from inhibition. This remaining short-latency spike activity provides a putative substrate for the effects of spared descending spinal fibers to influence spinal cord function after injury.

Additionally, after injury, the mean conduction time of the short-latency spikes was the same in the dorsal and upper intermediate laminae but slightly longer in the lower intermediate and ventral laminae ($p < 0.05$). This is strong evidence that the spared cortico-reticulospinal fibers terminating in the dorsal and upper intermediate layers remained unaltered after injury. Furthermore, forelimb-hindlimb and left-right coordination is controlled via long descending propriospinal pathways (Frigon 2017), which receive a larger number of terminals from reticulospinal neurons as compared to corticospinal neurons, suggesting that left-right activity is strongly controlled by the RtST (Mitchell, McCallum et al. 2016). Furthermore, at 4 weeks post-SCI, rats recovered coordination as noted by their BBB scores, suggesting that RtST remained intact.

After SCI, the long-latency (L1 and peak) spikes were still present, but firing rate was significantly diminished in intermediate (peak) and ventral (L1 and peak) laminae. The latency of the L1 response was longer in the intermediate laminae while the peak response was longer in the ventral laminae. But, the POA was increased in the lower intermediate (L1) and ventral laminae (L1 and peak) and decreased in the upper intermediate laminae (peak). The unaltered spiking activity and POA in the dorsal laminae suggests that the CST and RbST have a relatively minor influence on the dorsal laminae, at least in the lumbar spinal cord, and that any influence of the RtST on the dorsal laminae remains unchanged.

In rats, the injured CST has been shown to sprout at cervical locations in response to a bilateral transection of the thoracic spinal cord, adding novel connections onto long propriospinal neurons that may transmit signals to denervated neurons below the injury (Fouad,

Pedersen et al. 2001, Bareyre, Kerschensteiner et al. 2004). The delayed conduction times and increased POA could be evidence of corticospinal fibers sprouting onto long propriospinal neurons that bridge the lesion, which in turn could have a greater influence on spinal cord neurons below the lesion in intermediate and ventral laminae (Bareyre, Kerschensteiner et al. 2004). However, the conduction times of the peak long-latency response was significantly shorter in the ventral laminae. It is possible that the disruption of CST fibers resulted in disinhibited reticulospinal influence on spinal cord neurons in the ventral laminae. Furthermore, plasticity of other pathways could play a role in these changes, such as the dorsolateral (Hilton, Anenberg et al. 2016) and ipsilateral ventral (Bareyre, Kerschensteiner et al. 2004) CST.

Conclusion

The effects of a contusive SCI on spinal motor neuron activity, corticospinal coupling, and conduction time in rats were presented and described. ICMS-evoked spiking activity decreased after SCI; however, the presence of ICMS-evoked spikes at short latencies (10-12 ms) after SCI indicates that cortico-reticulospinal fibers, with their faster conduction velocities, remain intact after a moderate contusive injury, and CST damage may release their effects from inhibition. These data inform the further development of latency specific stimulation therapies and neuromodulation techniques in the lumbar spinal cord for recovery after SCI.

Acknowledgements

This work was supported by the Paralyzed Veterans of America Research Foundation #3068, The Ronald D. Deffenbaugh Family Foundation, NIH/NINDS R01 NS030853, T32 Neurological and Rehabilitation Sciences Training Program, and NIH/NINDS F31 NS105442.

References

Al-Izki, S., P. A. Kirkwood, R. N. Lemon and M. Enriquez Denton (2008). "Electrophysiological actions of the rubrospinal tract in the anaesthetised rat." Exp Neurol **212**(1): 118-131.

Alstermark, B., J. Ogawa and T. Isa (2004). "Lack of monosynaptic corticomotoneuronal EPSPs in rats: disynaptic EPSPs mediated via reticulospinal neurons and polysynaptic EPSPs via segmental interneurons." J Neurophysiol **91**(4): 1832-1839.

Babalian, A., F. Liang and E. M. Rouiller (1993). "Cortical influences on cerivical motoneurons in the rat: recordings of synaptic responses from motoneurons and compound action potential from corticospinal axons." Neuroscience Research **16**: 301-310.

Bannister, C. M. and R. Porter (1967). "Effects of limited direct stimulation of the medullary pyramidal tract on spinal motoneurons in the rat." Exp Neurol **17**(3): 265-275.

Bareyre, F. M., M. Kerschensteiner, O. Raineteau, T. C. Mettenleiter, O. Weinmann and M. E. Schwab (2004). "The injured spinal cord spontaneously forms a new intraspinal circuit in adult rats." Nat Neurosci **7**(3): 269-277.

Basso, D. M., M. S. Beattie and J. C. Bresnahan (1995). "A sensitive and reliable locomotor rating scale for open field testing in rats." J Neurotrauma **12**(1): 1-21.

Basso, D. M., M. S. Beattie and J. C. Bresnahan (1996). "Graded histological and locomotor outcomes after spinal cord contusion using the NYU weight-drop device versus transection." Experimental Neurology **139**(2): 244-256.

Bennett, D. J., M. Gorassini, K. Fouad, L. Sanelli, Y. Han and J. Cheng (1999). "Spasticity in rats with sacral spinal cord injury." J Neurotrauma **16**(1): 69-84.

Bogatyreva, E. S. and A. I. Shapovalov (1973). "Synaptic Processes Evoked by Intracortical Microstimulation in Lumbar Motoneurons of Rats." Neirofiziologiya (USSR) **5**: 174-180.

Borrell, J. A., S. B. Frost, J. Peterson and R. J. Nudo (2017). "A 3D map of the hindlimb motor representation in the lumbar spinal cord in Sprague Dawley rats." J Neural Eng **14**(1): 016007.

Brown, L. T. (1974). "Rubrospinal projections in the rat." J Comp Neurol **154**(2): 169-187.

Casale, E. J., A. R. Light and A. Rustioni (1988). "Direct projection of the corticospinal tract to the superficial laminae of the spinal cord in the rat." J Comp Neurol **278**(2): 275-286.

Chiba, A., K. Oshio and M. Inase (2003). "Magnetically evoked EMGs in rats." Neurol Res **25**(1): 87-91.

DiGiovanna, J., N. Dominici, L. Friedli, J. Rigosa, S. Duis, J. Kreider, J. Beauparlant, R. van den Brand, M. Schieppati, S. Micera and G. Courtine (2016). "Engagement of the Rat Hindlimb Motor Cortex across Natural Locomotor Behaviors." J Neurosci **36**(40): 10440-10455.

Ditunno, J. F., J. W. Little, A. Tessler and A. S. Burns (2004). "Spinal shock revisited: a four-phase model." Spinal Cord **42**(7): 383-395.

Elger, C. E., E. J. Speckmann, H. Caspers and R. W. Janzen (1977). "Cortico-spinal connections in the rat. I. Monosynaptic and polysynaptic responses of cervical motoneurons to epicortical stimulation." Exp Brain Res **28**(3-4): 385-404.

Fink, K. L. and W. B. Cafferty (2016). "Reorganization of Intact Descending Motor Circuits to Replace Lost Connections After Injury." Neurotherapeutics **13**(2): 370-381.

Fouad, K., V. Pedersen, M. E. Schwab and C. Brosamle (2001). "Cervical sprouting of corticospinal fibers after thoracic spinal cord injury accompanies shifts in evoked motor responses." Curr Biol **11**(22): 1766-1770.

Fox, J. E. (1970). "Reticulospinal neurones in the rat." Brain Res **23**(1): 35-40.

Frigon, A. (2017). "The neural control of interlimb coordination during mammalian locomotion." J Neurophysiol **117**(6): 2224-2241.

Frost, S. B., C. L. Dunham, S. Barbay, D. Krizsan-Agbas, M. K. Winter, D. J. Guggenmos and R. J. Nudo (2015). "Output Properties of the Cortical Hindlimb Motor Area in Spinal Cord-Injured Rats." J Neurotrauma **32**(21): 1666-1673.

Frost, S. B., M. Iliakova, C. Dunham, S. Barbay, P. Arnold and R. J. Nudo (2013). "Reliability in the location of hindlimb motor representations in Fischer-344 rats: laboratory investigation." J Neurosurg Spine **19**(2): 248-255.

Gilerovich, E. G., T. R. Moshonkina, E. A. Fedorova, T. T. Shishoko, N. V. Pavlova, Y. P. Geraasimenko and V. A. Otellin (2008). "Morphofunctional Characteristics of the Lumbar Enlargement of the Spinal Cords in Rats." Neuroscience and Behavioral Physiology **38**(8): 855-860.

Hilton, B. J., E. Anenberg, T. C. Harrison, J. D. Boyd, T. H. Murphy and W. Tetzlaff (2016). "Re-Establishment of Cortical Motor Output Maps and Spontaneous Functional Recovery via Spared Dorsolaterally Projecting Corticospinal Neurons after Dorsal Column Spinal Cord Injury in Adult Mice." J Neurosci **36**(14): 4080-4092.

Hudson, H. M., D. M. Griffin, A. Belhaj-Saif and P. D. Cheney (2015). "Properties of primary motor cortex output to hindlimb muscles in the macaque monkey." J Neurophysiol **113**(3): 937-949.

Janzen, R. W., E. J. Speckmann, H. Caspers and C. E. Elger (1977). "Cortico-spinal connections in the rat. II. Oligosynaptic and polysynaptic responses of lumbar motoneurons to epicortical stimulation." Exp Brain Res **28**(3-4): 405-420.

Kamida, T., M. Fujiki, S. Hori and M. Isono (1998). "Conduction pathways of motor evoked potentials following transcranial magnetic stimulation: A rodent study using a "figure-8" coil." Muscle & Nerve **21**(6): 722-731.

Katz, B. and R. Miledi (1965). "The Measurement of Synaptic Delay, and the Time Course of Acetylcholine Release at the Neuromuscular Junction." Proceedings of the Royal Society of London Series B-Biological Sciences **161**(985): 483-495.

Krizsan-Agbas, D., M. K. Winter, L. S. Eggimann, J. Meriwether, N. E. Berman, P. G. Smith and K. E. McCarson (2014). "Gait Analysis at Multiple Speeds Reveals Differential Functional and Structural Outcomes in Response to Graded Spinal Cord Injury." Journal of Neurotrauma **31**(9): 846-856.

Kuchler, M., K. Fouad, O. Weinmann, M. E. Schwab and O. Raineteau (2002). "Red nucleus projections to distinct motor neuron pools in the rat spinal cord." J Comp Neurol **448**(4): 349-359.

Lemon, R. N. (2008). "Descending pathways in motor control." Annu Rev Neurosci **31**: 195-218.

Lewicki, M. S. (1998). "A review of methods for spike sorting: the detection and classification of neural action potentials." Network **9**(4): R53-78.

Matsuyama, K., F. Mori, B. Kuze and S. Mori (1999). "Morphology of Single Pontine Reticulospinal Axons in the Lumbar enlargement of the Cat: A Stud Using the Anterograde Tracer PHA-L." The Journal of Comparative Neurology **410**: 413-430.

Mediratta, N. K. and J. A. Nicoll (1983). "Conduction velocities of corticospinal axons in the rat studied by recording cortical antidromic responses." J Physiol **336**: 545-561.

Mitchell, E. J., S. McCallum, D. Dewar and D. J. Maxwell (2016). "Corticospinal and Reticulospinal Contacts on Cervical Commissural and Long Descending Propriospinal Neurons in the Adult Rat Spinal Cord; Evidence for Powerful Reticulospinal Connections." PLoS One **11**(3): e0152094.

Molander, C., Q. Xu and G. Grant (1984). "The cytoarchitectonic organization of the spinal cord in the rat. I. The lower thoracic and lumbosacral cord." J Comp Neurol **230**(1): 133-141.

Nielsen, J. B., M. A. Perez, M. Oudega, M. Enriquez-Denton and J. M. Aimonetti (2007). "Evaluation of transcranial magnetic stimulation for investigating transmission in descending motor tracts in the rat." Eur J Neurosci **25**(3): 805-814.

Padmanabhan, R. and S. Singh (1979). "Observations on the topographical relations of spinal nerve roots in the rat." Acta Anat (Basel) **105**(3): 378-380.

Petrosyan, H. A., V. Alessi, S. A. Sisto, M. Kaufman and V. L. Arvanian (2017). "Transcranial magnetic stimulation (TMS) responses elicited in hindlimb muscles as an assessment of synaptic plasticity in spino-muscular circuitry after chronic spinal cord injury." Neurosci Lett **642**: 37-42.

Ryder, J., R. Zappulla and J. Nieves (1991). "Motor evoked potentials elicited from pyramidal stimulation and recorded from the spinal cord in the rat." Neurosurgery **28**(4): 550-558.

Stewart, M., G. J. Quirk and V. E. Amassian (1990). "Corticospinal responses to electrical stimulation of motor cortex in the rat." Brain Res **508**(2): 341-344.

Takakusaki, K., R. Chiba, T. Nozu and T. Okumura (2016). "Brainstem control of locomotion and muscle tone with special reference to the role of the mesopontine tegmentum and medullary reticulospinal systems." J Neural Transm (Vienna) **123**(7): 695-729.

Waldron, H. A. and D. G. Gwyn (1969). "Descending nerve tracts in the spinal cord of the rat. I. Fibers from the midbrain." J Comp Neurol **137**(2): 143-153.

Yates, C., K. Garrison, N. B. Reese, A. Charlesworth and E. Garcia-Rill (2011). "Chapter 11--novel mechanism for hyperreflexia and spasticity." Prog Brain Res **188**: 167-180.

CHAPTER FOUR: Use of Activity Dependent Stimulation to Increase Synaptic Efficacy in Remaining Pathways in an Acute, Anesthetized Rat Model of Spinal Cord Injury

Abstract

The purpose of this study was to determine a spike-stimulus delay for increasing synaptic efficacy in descending motor pathways using an activity dependent stimulation (ADS) paradigm in an acute, anesthetized rat model of spinal cord injury (SCI). Experiments were carried out in adult, male, Sprague Dawley rats with T8 contusion injury. Under ketamine/xylazine anesthesia, fine wire electromyographic (EMG) electrodes were implanted into 4 muscles of right hindlimb. After exposure of the left hindlimb motor cortex (HLA), laminectomy of the T13-L1 vertebrae, and removal of the dura matter, intracortical (ICMS) and intraspinal microstimulation (ISMS) were used to determine the location of evoked hip movements. One pair of sites evoking hip movements were chosen for each experimental procedure. For ADS conditioning, a single shank, 16-channel, Neuronexus recording microelectrode was used to detect neuronal spikes in HLA that were used to trigger ISMS in the spinal cord (SC) grey matter. SCI rats were randomly selected for one of four different parameters of cortical spike-triggered ISMS stimulus delays (10 ms or 25 ms time delay) and number of stimulus pulses used (1 pulse or 3 pulse square-wave stimulation). ADS sessions were conducted in three 1-hour conditioning bouts for a total of 3 hours. Synaptic efficacy was measured by number of ICMS-evoked spikes in the matched site in the lumbar SC in one 5-minute pre-ADS period and three 5-minute test periods following each 1-hour ADS conditioning bout. During the testing periods, recording and stimulating microelectrodes were switched and ICMS was applied to the HLA while evoked-spikes were simultaneously recorded from the hindlimb SC. Evoked spikes were recorded, sorted, and displayed in post-stimulus spike histograms in 1-ms bins. Post-stimulus spike histograms and EMG recordings were characterized using stimulus triggered averaging techniques. The results showed that after 3 hours of ADS conditioning using a 10 ms time delay and one stimulation pulse, ICMS-evoked spiking activity was significantly increased in the ventral horn at 10 ms post-onset ICMS. ADS

conditioning using a 25 ms time delay and one or three stimulation pulses resulted in significant increases in ICMS-evoked spiking activity in the dorsal/intermediate layers of the spinal gray matter at 10 ms post-onset ICMS after 2 hours of ADS and continued to increase after 3 hours of ADS conditioning. EMG responses were never evoked with ICMS pre-or post-ADS. These results show that bouts of ADS conditioning can increase synaptic efficacy in descending motor pathways, as measured by cortically evoked activity in the spinal cord, after SCI.

Introduction

Closed-loop, activity dependent stimulation (ADS) paradigms record and digitize extracellular neural activity from one location, discriminate individual action potentials in real time, and deliver small amounts of electrical current to another population of neurons. By activating two synaptically connected neurons, a change in the strength of synapses between them may occur. This type of plasticity led to Donald Hebb's famous implementation of the rule that when cell A reliably contributes to spiking of postsynaptic cell B, the functional strength of the synapse from A to B increases (Hebb 1949). It was later added to Hebb's idea that there is also a weakening of ineffective synapses (Stent 1973). Currently, it is recognized that associative synaptic strengthening and weakening are implemented at synapses by long-term potentiation (LTP) and depression (LTD). The main requirement when to initiate LTP or LTD at most synapses was found to be temporal correlation between presynaptic spiking and postsynaptic depolarization, with strong depolarization leading to LTP, and weaker, more sustained depolarization leading to LTD (Lisman 1989). In addition, a few *in vitro* studies have noted an effect due to spike order, with LTP occurring when presynaptic inputs occurred first or were synchronous with postsynaptic spikes, and LTD occurring when presynaptic input followed postsynaptic spikes (Levy and Steward 1983, Debanne, Gahwiler et al. 1994, Debanne, Gahwiler et al. 1997, Fung, Law et al. 2016). Gerstner et al. (Gerstner, Kempter et al. 1996) predicted precise timing- and order-dependent plasticity, while Markram et. al. (Markram, Lubke et al. 1997) showed that the sign and magnitude of LTP and LTD depended on the order and timing of pre- and postsynaptic spikes on the 10 ms time scale. Bi and Poo (Bi and Poo 1999) further characterized this dependence temporally by showing that a 10-50 ms time delay increased spiking probability.

It is now believed that the use of ADS to replicate the natural timing of pre- and post-synaptic events may contribute to strengthening the synaptic efficacy of spared fibers/pathways

after injury and may enhance functional recovery. This replication of the natural timing of pre- and post-synaptic events has been shown to potentiate, or condition, specific neuronal pathways (Jackson, Mavoori et al. 2006). It has been demonstrated in a traumatic brain injury model that conditioning of a corticocortical pathway can enhance synaptic efficacy between the cortical regions of interest and result in rapid behavioral recovery (Guggenmos, Azin et al. 2013). Additionally, in rats with a cervical contusion of the spinal cord, McPherson *et. al.* synchronized ISMS below the injury with the arrival of functionally related volitional motor commands signaled by muscle activity in the impaired forelimb, which resulted in improved behavioral performance in a forelimb reach and grasp task (McPherson, Miller et al. 2015). In non-human primates with a unilateral transection, Capogrosso *et. al.* triggered epidural stimulation below the injury with recorded neural activity from the hindlimb motor cortex, which restored weight-bearing locomotion of the paralyzed leg on a treadmill and overground (Capogrosso, Milekovic et al. 2016).

Currently, no data are available to direct the optimal stimulus timing for conditioning using spike-triggered ISMS in a contusion SCI rat model specific to voluntary hindlimb motor function. In a previous study, we determined the conduction times of intracortical microstimulation (ICMS) evoked action potentials in the hindlimb spinal cord (i.e., pathway from hindlimb motor cortex to hindlimb spinal cord) in healthy and SCI rats (Frost, Borrell et al. 2018). In healthy rats, the latencies of the ICMS-evoked spikes occurred at a short latency response (10-12 ms) as well as at a longer latency response that mimicked a Gaussian distribution (from ~20-40 ms). ICMS-evoked muscle activity was determined at ~25-28 ms (i.e., between L1 and Peak latencies). In SCI rats, the only ICMS-evoked spiking activity to remain was at the Short latency (~10-12 ms).

The purpose of this study was to determine the optimal spike-stimulus delay for increasing synaptic efficacy in descending motor pathways using an ADS paradigm in an acute,

anesthetized rat model of SCI that mimics the contusion injury seen in the clinic. The hypothesis is that the synaptic efficacy of the descending corticospinal tract can be strengthened by using ADS to replicate the natural timing of pre- and post-synaptic events, that would result in an increase in cortically evoked-activity within the hindlimb spinal cord. From the results of our previous study (Frost, Borrell et al. 2018), time delays of 10 ms and 25 ms were chosen for ADS parameters. In order to focus on strengthening remaining fibers after injury, 10 ms was chosen because cortically-evoked spikes at that latency remained after the SCI contusion, and 25 ms was chosen to replicate the timing of hindlimb muscle activation. This study sought to demonstrate that ADS may be used as therapy to strengthen the synaptic efficacy of spared fibers/pathways after injury. It is the long-term goal that the application of ADS pairing hindlimb cortical activity with ISMS in hindlimb spinal cord, to strengthen synaptic efficacy and help restore control of lower limb muscles. Before this goal can be tested in a chronic application, optimal ADS stimulation parameters must first be derived.

Materials and Methods

Subjects

Forty adult, male, Sprague Dawley rats with T8 moderate spinal cord contusion injury were randomly selected in this study. Body weights ranged from 356—486 g (407.9 ± 28.1 g) and ages ranged from 90—105 days old at the time of the experiment. Ten rats were removed from the study due to adverse surgical complications. ADS parameter groups tested two stimulation variables: 1) The time delay between recorded action potential (i.e., spike) in hindlimb area (HLA) of the primary motor cortex and onset stimulation in ventral horn of lumbar spinal cord (e.g., 10 ms or 25 ms time delay) and 2) the number of biphasic stimulation pulses (e.g., either 1 pulse or 3 pulses). Rats were randomly divided into four groups: 10 ms time delay with 1 stimulation pulse (10ms_1P; n = 7) group, 10 ms time delay with 3 pulses (10ms_3P; n = 5) group, 25 ms time delay with 1 pulse (25ms_1P; n = 7) group, and 25 ms time delay with 3 pulses (25ms_3P; n = 5) group. All procedures were performed in accordance with all standards in *Guide for the Care and Use of Laboratory Animals* (Institute for Laboratory Animal Research, National Research Council, Washington, DC: National Academy Press, 1996). The protocol was approved by the University of Kansas Medical Center Institutional Animal Care and Use Committee.

Experimental paradigm

Spike-stimulus conditioning (i.e., ADS) was conducted for a total of 3 hours, in three, 1-hour ADS conditioning bouts. Changes in synaptic efficacy were inferred during one Catch Trial before ADS (i.e., baseline recording) and three Catch Trials following each ADS bout for ~5 min (Figure 4.1).

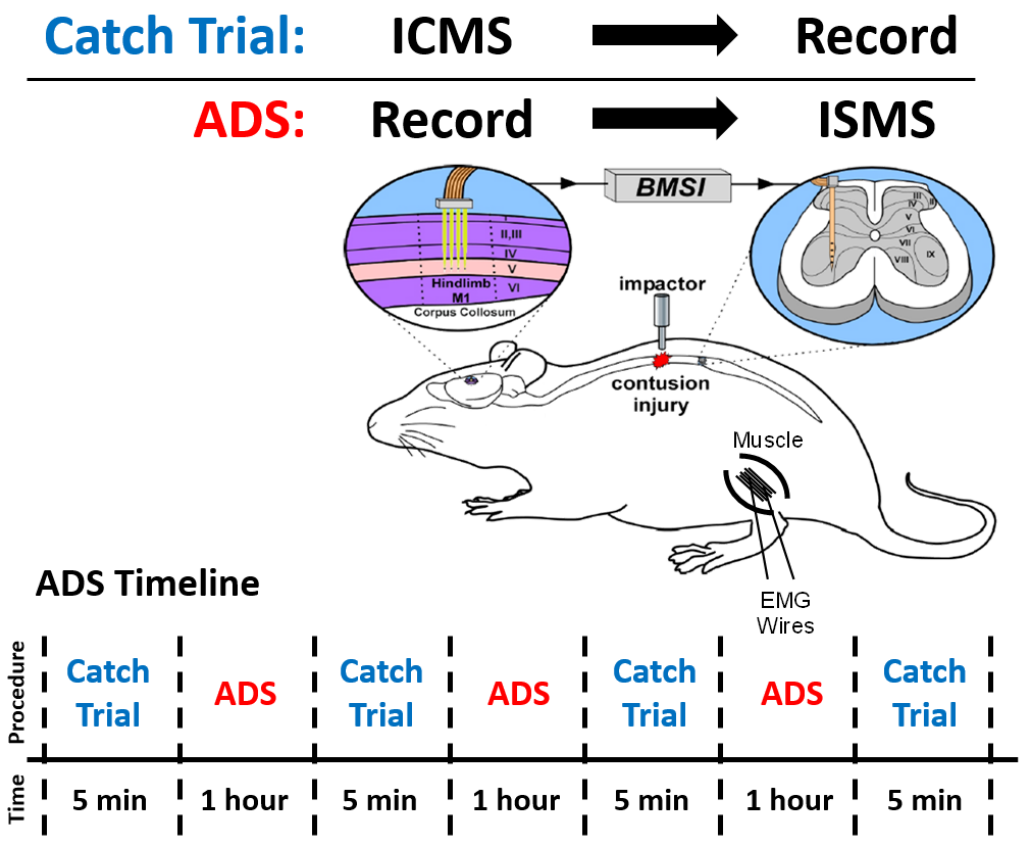

Figure 4.1. Overview of experimental design. Catch Trial: Intracortical microstimulation (ICMS) was applied to hindlimb motor cortex (HLA) while ICMS-evoked spikes were recorded from hindlimb spinal cord at movement matched sites. **ADS:** Spikes from HLA were recorded and used to trigger intraspinal microstimulation (ISMS) in the ventral horn of the hindlimb spinal cord via a brain-computer-spinal cord interface (BMSI). **ADS Timeline:** ADS was applied in one-hour sessions for three hours. Catch trials were recorded before and after each hour of ADS.

Two surgical procedures were performed during this study: spinal cord injury (i.e., contusion) and acute ADS procedure (Figure 4.1). After a stable anesthetic state was reached using isoflurane anesthesia, all procedures were performed with initial ketamine hydrochloride (100 mg kg^{-1}; IP)/xylene (5 mg kg^{-1}; IP) anesthesia. Anesthesia was maintained with subsequent doses of ketamine (0.1 mL; IP or IM) and monitored via pinch and corneal responses. Additional doses of ketamine were administered if the rat reacted to a pinch of the forepaw/hindpaw or blinked after lightly touching the cornea. Aseptic conditions were adhered for both procedures.

Spinal cord injury (SCI)

Animals underwent T8 laminectomy and moderate contusion injury using an Infinite Horizon spinal cord impactor (Precision Systems and Instrumentation, LLC, Fairfax Station, VA) with 175 kDyn impact. Displacement distance reported by the impactor software for each contusion was recorded at the time of surgery. At the conclusion of the surgery, 0.25% bupivacaine HCl was applied locally to the incision site. Buprenex (0.01 mg kg^{-1}; SC) was injected immediately after surgery and 1 day later. All animals were monitored daily until the end of the experiment. For the first two days post-surgery including the day of surgery, the rats received a daily SC injection of 30,000 U of penicillin (Combi-Pen 48) in 5 mL of saline to prevent infections and dehydration. Rats' bladders were expressed twice-daily until animals recovered urinary function. From the second week onward, animals were supplemented with vitamin C pellets (BioServ, Frenchtown, NJ) to avert urinary tract infection (Behrmann, Bresnahan et al. 1992).

BBB Scoring

Locomotor performance was assessed using the Basso, Beattie, and Bresnahan (BBB) scale (Basso, Beattie et al. 1995). BBB scoring was performed before SCI and once a week for up to 4 weeks post-SCI. Four weeks was chosen because BBB scores typically plateau by 4 weeks and behavior is relatively stable (Scheff, Rabchevsky et al. 2003, Krizsan-Agbas, Winter et al. 2014). A straight walkway was utilized for the testing. Rats were habituated to the apparatus for 1 week prior to BBB scoring. A BBB score of 13-15 at 4 weeks post-SCI was set as the inclusion criteria for this study; however, no rats were removed from this study due to this criterion.

EMG electrode implantation

The implantation and verification of fine-wire EMG electrodes into hindlimb muscles was conducted as previously described (Borrell, Frost et al. 2017). EMG electrodes were implanted in four hindlimb muscles: the lateral gastrocnemius (LG), tibialis anterior (TG), vastus lateralis (VL), and biceps femoris (BF). Each EMG electrode consisted of a pair of insulated multi-stranded stainless-steel wires exposed approximately 1 mm, with the exposed, implanted end of the wire folded back on itself ('hook' electrode). Implantation locations were determined by surface palpation of the skin and underlying musculature. Once the hindlimbs were shaved, EMG electrodes were inserted into the belly of each muscle with the aid of a 22-gauge hypodermic needle. For each EMG electrode pair, wires were positioned approximately 5 mm apart in each muscle. The external portion of the wires was secured to the skin with surgical glue (3M Vetbond Tissue Adhesive, St. Paul, MN) and adhesive tape. An additional ground lead was placed into the base of the tail.

To verify that the EMG electrodes were within the belly of the muscle, a stimulus isolator (BAK Electronics, Inc., Umatilla, FL) was used to deliver a biphasic (cathodic-leading) square-wave current pulse to the muscle through the implanted EMG electrodes. In addition, the impedance between the EMG electrodes was tested via an electrode impedance tester (BAK Electronics, Inc., Umatilla, FL). The EMG electrodes were determined to be inserted properly and within the desired muscle if: (a) the electrode impedance was approximately 7-8 kΩ; (b) direct current delivery to the muscle resulted in contraction of the desired muscle, and (c) the movement threshold was ≤ 5mA.

Intracortical microstimulation

The rats were placed in a Kopf small-animal stereotaxic frame (David Kopf Instruments®, Tujunga, CA) and the incisor bar was adjusted until the heights of lambda and

bregma were equal (flat skull position). The cisterna magna was punctured at the base of the skull to reduce edema during mapping. A craniectomy was performed over the motor cortex. The general location of the craniectomy was based on previous motor mapping studies in the rat (Frost, Iliakova et al. 2013, Frost, Dunham et al. 2015). The dura over the cranial opening was incised and the opening was filled with warm, medical grade, sterile, silicone oil (50% Medical Silicone Fluid 12,500, 50% MDM Silicone Fluid 1000, Applied Silicone Corp., Santa Paula, CA) to prevent desiccation during the experiment.

A magnified digital color photograph of the exposed cortex was taken through a surgical microscope. The image was transferred to Canvas 3.5 where a 200 μm grid was superimposed, by calibration with a millimeter ruler, to indicate intended sites for microelectrode penetration. The 0.0 mm rostrocaudal and mediolateral reference were defined as the location of bregma.

Intracortical microstimulation (ICMS) was conducted in the hindlimb area (HLA) of the primary motor cortex (M1) (Figure 4.2A). Stimuli were delivered to the ventral-most site on a 1-shank Neuronexus (Neuronexus, Ann Arbor, MI) probe positioned regularly spaced sites on the superimposed 200 μm grid. Each stimulation site had an impedance in the range of ~50-70 kΩ with a surface area of 1250 μm^2. The maximum compliance voltage of the system was 24 V. Electrode depth was controlled using a Kopf hydraulic microdrive (Kopf Instruments, Tujunga, CA) and reached ~1700 μm (i.e., Layer V of the cortex). The stimuli consisted of 13, 200 μs biphasic cathodal pulses delivered at 300 Hz repeated at 1/sec from an electrically isolated, charge-balanced (capacitively coupled) stimulation circuit.

Spinal cord exposure

Following initial anesthesia, ICMS mapping, and shaving of the back, a midline incision was made over the skin of the back, exposing the T12-L2 vertebrate. A laminectomy was

performed on the T13-L1 vertebrae exposing the L2-S1 segments of the spinal cord. The dura mater was removed using fine forceps and small scissors to allow electrode penetration. Animals were stabilized with a custom rodent spinal fixation frame (Keck Center for Collaborative Neuroscience Rutgers, The State University of New Jersey, USA) attached to the dorsal processes of vertebrae T12 and L2.

Intraspinal microstimulation mapping

Previously derived 3-dimensional ISMS-evoked topographic maps were used in the guidance of stimulation sites in the hindlimb spinal cord (Borrell, Frost et al. 2017). A similar 200 µm grid was used for the intraspinal microstimulation map of the hindlimb spinal (Figure 4.2B). Stimulation sites were ~0.8 mm lateral of the central blood vessel (i.e., midline) on the right side of the spinal cord and at a depth ~2.27 mm below the surface of the spinal cord (i.e., in the ventral horn). ISMS stimuli consisted of 3, 200 µs biphasic (cathodal leading) pulses delivered at 300 Hz repeated at 1/sec.

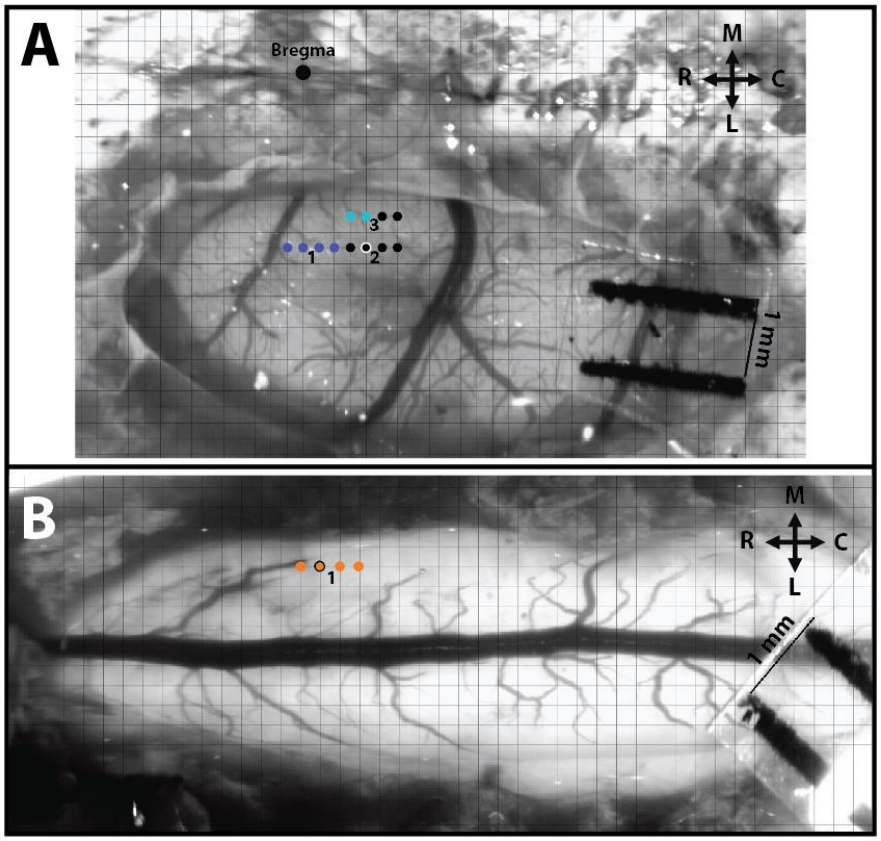

Figure 4.2. Intracortical and intraspinal microstimulation mapping and site pairing. A) Hindlimb motor cortex with superimposed grid for ICMS mapping. The bigger black dot represents Bregma, the dark blue dots represent stimulation sites that resulted in ICMS-evoked forelimb movements, the light blue dots represent evoked trunk movements, and the small black dots represent sites of no evoked movement. The small black dot with white outline is the site chosen to be paired with the site in the spinal cord. **B)** Hindlimb spinal cord with superimposed grid for ISMS mapping. Each orange dot represents a stimulation site that resulted in ISMS-evoked hindlimb movement. The orange dot with the black outline represents the site of an ISMS-evoked hip movement paired for ADS. R = Rostral, C = Caudal, M = Medial, and L = Lateral.

Intracortical and intraspinal evoked movement site matching

Functionally similar sites in HLA and the ventral horn of the hindlimb spinal cord, derived from the ICMS and ISMS maps, were paired for further neurophysiological assessment (e.g., ICMS and ISMS both evoking hip movements are paired together). In SCI rats, ICMS-evoked hindlimb movements cannot be elicited from HLA; however, ICMS-evoked forelimb and trunk movements can be elicited. In maps derived from healthy, uninjured rats, hip movements are consistently evoked immediately caudal to the forelimb area (blue dots in Figure 4.2A) and lateral to the trunk area (light blue dots in Figure 4.2A). After a small ICMS map was derived in

the SCI rats, a potential hip site (black dot with white outline in Figure 4.2A) was matched/paired with an ISMS-evoked hip site in the lumbar spinal cord (orange dot with black outline in Figure 4.2B).

ICMS-evoked activity recording (Catch Trial)

Using the paired sites of the HLA and hindlimb spinal cord, a stimulating electrode was inserted into the HLA and a recording microelectrode was simultaneously inserted in the hindlimb spinal cord site. The recording microelectrode was a single-shank, 16-channel Michigan-style linear microelectrode (Neuronexus, Ann Arbor, MI). Each of the 16 sites had an area of 703 μm^2, separation of 150 µm, thickness of 15 µm in diameter, and impedance of ~0.3 MΩ. The tip of the electrode was lowered to a depth of ~2270 µm below the spinal cord surface. ICMS was used to test corticospinal coupling by delivering a test stimulus in HLA, and ICMS-evoked spikes were recorded from the spinal cord and EMG from the hindlimb muscles. The ICMS stimulus consisted of 3, 200 µs biphasic cathodal pulses delivered at 300 Hz repeated at 1/sec at movement threshold. During each ICMS-evoked activity recording, neural and EMG activity were recorded and digitized for ~5 min from each of the 16 active recording sites and four fine-wire pairs, respectively, using neurophysiological recording and analysis equipment (Tucker Davis Technologies, Alachua, FL).

Activity-dependent-stimulation (ADS) paradigm

Using the paired hip sites, the recording electrode was inserted into the HLA site and the stimulating electrode was simultaneously inserted into the hindlimb spinal cord site. Using principle component analysis (Lewicki 1998), spikes were recorded and sorted in real-time from a single channel in HLA and used to trigger stimulation in the paired site in the hindlimb spinal cord. The triggered ISMS stimulus consisted of 1 or 3, 200 µs biphasic cathodal pulses delivered at 300 Hz repeated at 1/sec at 50% movement threshold. The stimulus intensity for

ADS was set at 50% of the ISMS threshold in each rat as to not evoke movement during ADS therapy and to eliminate the possibility of fatigue on the muscle. The timed delay between the recorded spike and subsequent stimuli was either 10 ms or 25 ms. ADS was applied in three 1-hour intervals.

Selection of ADS stimulation parameters

During this experiment, the stimulation variables of interest were time delay and the number of stimulation pulses. Ideally for ADS, a single biphasic square-wave stimulation pulse is desired to minimize disruption of natural locomotion; however, in an acute experiment 3 pulses are typically needed to observe reliable effects. For this reason, both 1 and 3 biphasic square-wave pulses were tested during this experiment since 1 pulse may not produce an effect in this acute experiment. Delays of 10 and 25 ms between recorded HLA spike and triggered stimulus pulse(s) were chosen based on natural response times observed in previous experiments (Frost, Borrell et al. 2018). Briefly, ICMS-evoked spiking activity in the hindlimb spinal cord was consistently observed with a 10 ms conduction latency, hence a 10 ms time delay was chosen. A 25 ms time delay was chosen because it matched the conduction latency of hindlimb EMG activity, which could be significant for functional motor recovery. Additionally, *in vitro* experiments indicate that time delays between 0 and 50 ms will induce an increase in activity instead of a suppression of activity (Bi and Poo 1999). A time delay of 10 and 25 ms fell within this range and were deemed suitable test parameters for this study.

Spike sorting from catch trials

Neural spikes were discriminated offline using OpenSorter software (Tucker Davis Technologies, Alachua, FL) using principle component analysis (Lewicki 1998). ICMS-evoked activity recorded during the catch trials from each channel in the hindlimb spinal cord were represented in post-stimulus spike histograms for 200 ms around the onset of each ICMS

stimuli (ICMS begins at 0 ms; histogram extends -100 ms before and +100 ms after onset ICMS) using custom software (Matlab; The Mathworks, Inc., Natick, MA). Spiking activity was averaged into 1 ms bins over the ~5 min recording (i.e., averaged over ~300 ICMS trains). Spike activity could not be discriminated over the first 7 ms due to the stimulus artifact that was present due to the three stimulus pulses used in this study.

For analysis of spiking responses during the catch trials, the 16 recording channels in the hindlimb spinal cord were divided into four dorsoventral sections based on depth below the surface of the spinal cord as described previously (Frost, Borrell et al. 2018). The dorsoventral sections (Figure 4.3) were: Dorsal Section (720—1020 mm; dorsal horn), Upper Intermediate Section (1120—1420 mm; intermediate layer), Lower Intermediate Section (1520—1820 mm; intermediate layer), and Ventral Section (1920—2220 mm; ventral horn).

Firing rate (FR) calculation

To quantitatively analyze these data, the ICMS-evoked firing rate (FR) (i.e., total number of recorded spikes per 1ms bin/total time of recording) was calculated for each time bin of the post-stimulus spike histograms using custom software (Matlab; The Mathworks, Inc., Natick, MA). The FR was only considered for analysis (i.e., considered active) if the FR for the respective time bin was greater than 2x standard deviation (horizontal, dashed, red line of Figure 4.7) above average baseline (horizontal, solid, red line of Figure 4.7) FR. Baseline FR was derived by averaging the FR of each time bin 10 ms before the onset of ICMS (i.e., from -10 to 0 ms in the post-stimulus spike histogram).

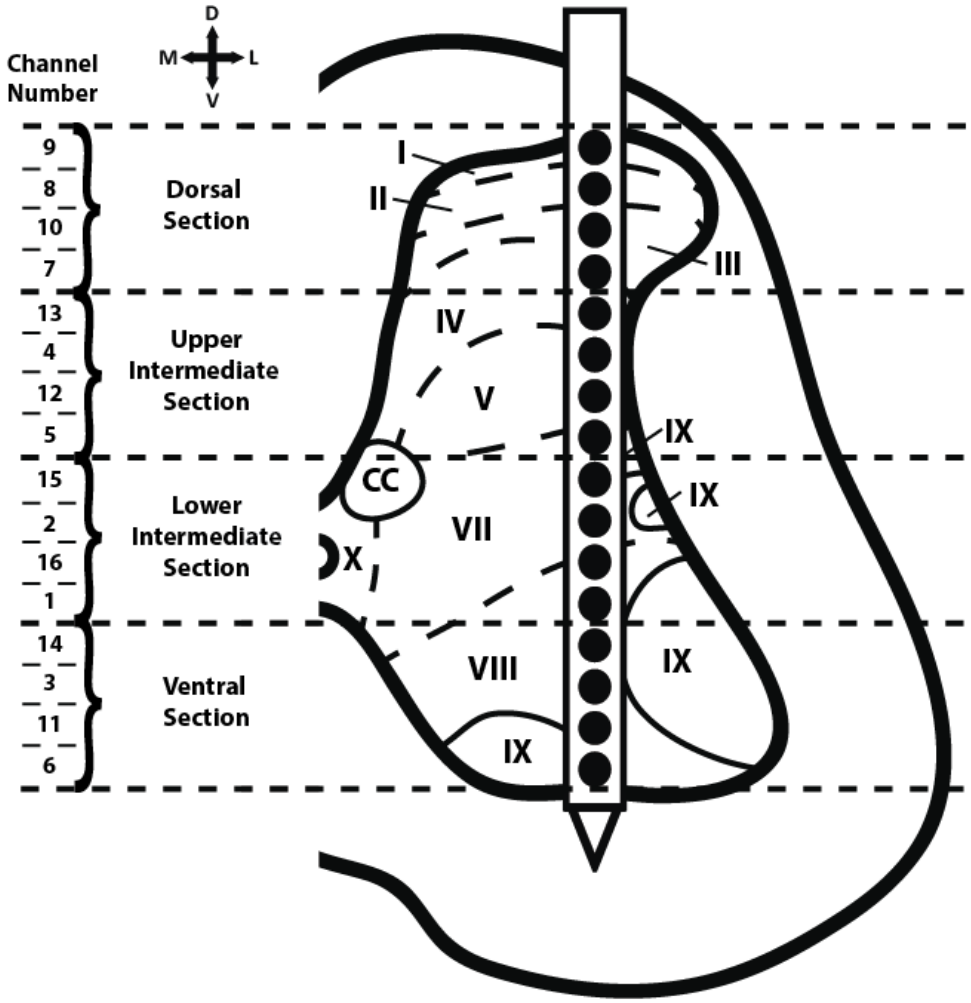

Figure 4.3. Cross sectional diagram of hindlimb spinal cord with placement of the recording electrode during the catch trials. The schematic diagram of the recording shank shows the channel numbers of the recording sites and the sections in which the channels were divided into sections based on depth.

Stimulus-triggered average (StTA) of EMG

Using custom software (Matlab; The Mathworks, Inc., Natick, MA), StTAs of rectified EMG of all recorded leg muscle EMGS were constructed to determine muscle activation (Hudson, Griffin et al. 2015, Borrell, Frost et al. 2017). For each of the implanted muscles, EMG data were recorded for at least 10 stimulus trains at movement threshold to obtain StTAs and averaged over a set time window of 220 ms. StTAs were aligned to the time of the first stimulus (i.e., 0 ms) and included data from -20.2 to +199.9 ms relative to the time of the first stimulus. A

muscle was considered active when the average rectified EMG reached a peak ≥ 2.25 SD above baseline values in the interval from -20.2 to 0 ms and had a total duration of ≥ 3 ms. The stimulus artifact was minimal to absent in EMG recordings with no muscle activation. If an artifact was observed, the amplitude of the artifact was minimal compared to the amplitude of the evoked movement; however, the averaging of the StTAs of EMG recordings largely eliminated the stimulus artifact. As a result, the stimulus artifact was determined to have minimal to no effect on the recordings. ISMS- and ICMS-evoked EMG potentials were high- and low-pass filtered (30 Hz-2.5 kHz), amplified 200-1000 fold, digitized at 5 kHz, rectified and recorded on an RX-8 multi-channel processor (Tucker-Davis Technology, Alachua, FL).

Statistical analysis

Statistical analyses were performed using JMP 11 software (SAS Institute Inc., Cary, NC). Dorsoventral section differences were evaluated by a 2x2 repeated measures analysis of variance (ANOVA). When a significance of $p < 0.05$ was obtained, a post hoc student's t-test was used to conduct within-group comparisons of all dorsoventral sections. Data are presented as average ± standard error of the mean unless otherwise stated.

Histology

At the end of each experiment, animals were euthanized with an intraperitoneal injection of sodium pentobarbital (Beuthanasia-D; 100 mg kg^{-1}) and transcardially perfused with 4% paraformaldehyde in 0.1 M PBS. The spinal cord was sectioned at 30 µm on a cryostat in the coronal plane. Histology was performed on selected sections with cresyl violet stain for Nissl bodies and silver stain for nerve fibers/structures.

Results

BBB Scores & Histology

Comparison of each week of BBB scores between groups is shown in Table 4.1. There was no statistical difference between BBB scores across groups for any week ($p > 0.05$). At 4-weeks post-SCI SCI rats stepped with consistent coordination, but had deficits in paw placement, toe clearance, and trunk stability. There was no statistical difference in the displacement of the impactor at the time of SCI between groups (Table 4.1; $p > 0.05$). A representative image of the injury epicenter is shown in Figure 4.4.

Table 4.1. Mean BBB score before and once a week for four weeks post-SCI and displacement of impactor at time of SCI for each rat group and all rats combined. There was no statistical difference between BBB scores for each week between groups ($p > 0.05$) as well as displacement recordings between groups ($p > 0.05$).

Group	BBB Scores (Mean ± SD)					Displacement at SCI (μm)
	Baseline	Week 1	Week 2	Week 3	Week 4	
Overall	21.0 ± 0.0	11.1 ± 2.5	12.9 ± 2.7	13.8 ± 2.4	14.3 ± 1.5	1000.4 ± 123.8
10ms_3P	21.0 ± 0.0	10.8 ± 1.3	12.0 ± 1.4	13.0 ± 1.6	13.4 ± 0.9	1057.8 ± 94.5
25ms_3P	21.0 ± 0.0	11.0 ± 3.4	13.2 ± 4.4	14.0 ± 3.5	14.8 ± 1.5	937.8 ± 251.2
10ms_1P	21.0 ± 0.0	10.1 ± 2.3	11.9 ± 2.5	13.7 ± 2.4	14.1 ± 1.7	997.3 ± 47.7
25ms_1P	21.0 ± 0.0	12.4 ± 2.4	14.3 ± 1.6	14.4 ± 2.1	14.9 ± 1.7	1007.3 ± 49.1

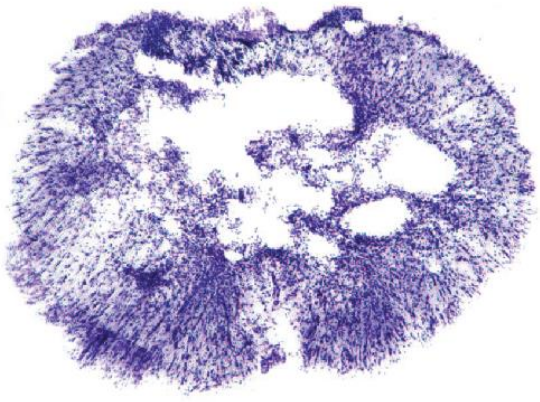

Figure 4.4. Representative image of spinal cord injury epicenter 4 weeks after injury stained with a cresyl violet acetate solution.

HLA Recorded Spikes

The profiles of cortical HLA recorded spikes remained relatively consistent over the 3-hours of ADS (Figure 4.5, Left). There were minor increases in average spike frequencies in the 10ms_1P and 25ms_3P groups; however, there were decreases in average spike frequencies in the 10ms_3P and 25ms_1P groups. Nonetheless, there were no significant changes in the spiking frequency of HLA recorded spikes in any of the ADS groups after 3 hours of ADS (Figure 4.5, Right).

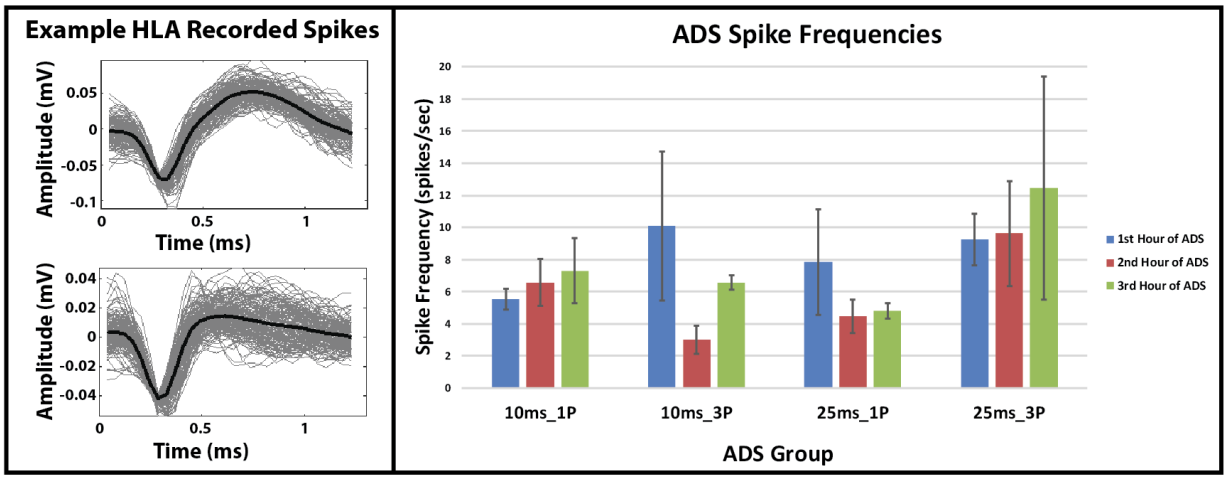

Figure 4.5. Hindlimb motor cortex (HLA) recorded spikes during ADS. Left) Example spike profiles recorded from layer V of hindlimb motor cortex of two different rats. These spikes were used to trigger ISMS pulses in the hindlimb spinal cord during ADS. **Right)** Average spike frequencies of recorded spikes during ADS for each group over each hour of ADS. Averages were taken from 5-minutes recordings at the end of each hour of ADS.

Stimulus Thresholds

ISMS-evoked movement threshold was measured during ISMS mapping and recorded as the lowest current needed to evoke a consistent, repetitive joint displacement. The average ISMS threshold was 9.00 ± 5.90 µA. There was no statistical difference in ISMS thresholds between groups (Table 4.2; $p > 0.05$). The average stimulus intensity used for ADS was 4.50 ± 2.95 µA, regardless of group. There was no statistical difference in ADS intensity used between groups (Table 4.2; $p > 0.05$). ICMS movement threshold was recorded during ICMS mapping.

Since movement could not be evoked during ICMS mapping in SCI rats used in this study, a constant intensity of 100 µA was used for ICMS during the 5-minute catch trials. The average stimulus thresholds used for each group are reported in Table 4.2.

Table 4.2. Mean and standard deviations at four weeks post-SCI during the ADS procedure. ISMS threshold was recorded during ISMS mapping at movement threshold. ADS intensity was 50% of ISMS threshold. ICMS intensity was set at a constant 100 µA and used during the 5-minute catch trials.

Group	ISMS Threshold (µA)	ADS Intensity (µA)	ICMS Intensity (µA)
10ms_1P	7.14 ± 2.27	3.57 ± 1.13	100.00 ± 0.00
25ms_1P	8.86 ± 5.98	4.43 ± 2.99	100.00 ± 0.00
10ms_3P	10.80 ± 8.79	5.40 ± 4.39	100.00 ± 0.00
25ms_3P	10.00 ± 7.07	5.00 ± 3.54	100.00 ± 0.00

EMG Activity

ICMS-evoked EMG activity was never observed before or after each hour of ADS (i.e., no EMG activity was evoked during the catch trials). During ADS, EMG recordings were inconsistent for each ADS group. Of the few active EMG recordings during ADS, a few scenarios were of note over the three hours of ADS: 1) EMG activity was consistent for each hindlimb muscle and EMG amplitude increased over 3 hours of ADS (Figure 4.6; n = 6 instances), 2) EMG activity was present during the 1st hour of ADS and was eliminated after the 2nd or 3rd hour of ADS (n = 3 instances), 3) EMG activity was never present over the 3 hours of ADS (n = 10 instances), and 4) EMG activity increased during the 2nd hour of ADS but was eliminated after the 3rd hour of ADS (n = 1 instance). These scenarios were not specific to one ADS group which resulted in a low n-value of active EMG recordings for each group. Due to a low n-value per group, a statistical analysis could not be conducted, and the instances reported above were not separated based on group.

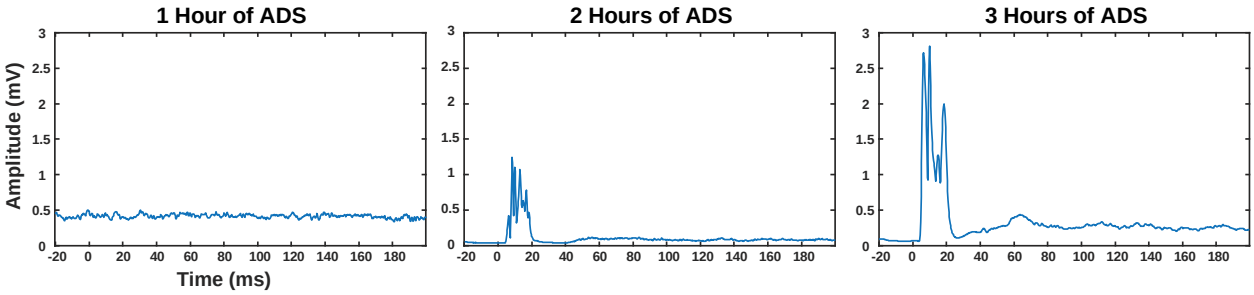

Figure 4.6. Example of ISMS-evoked EMG activity during the last 5 minutes of each 1-hour ADS session from one rat. In this example from the 25ms_3P group, EMG activity was recorded from the Tibialis Anterior, and EMG amplitude increased after 3 hours of ADS.

Post-stimulus spike histograms

To quantify the post-stimulus spike histograms, the ICMS-evoked spiking activity at each known latency, derived in previous experiments (Frost, Borrell et al. 2018), were recorded for each channel and divided into four dorsoventral sections based on depth below the surface of the spinal cord. Briefly, the number of evoked spikes were quantified from the following latency bins: Short latency (10-12 ms post-onset ICMS), L1 latency (onset of Gaussian distribution), and Peak latency (peak of Gaussian distribution). After 3 hours of ADS, post-stimulus spike histograms from the 10ms_1P group (Figure 4.7) show qualitatively that ICMS-evoked spiking activity increases at a latency of ~10 ms from onset of ICMS (i.e. 0 ms).

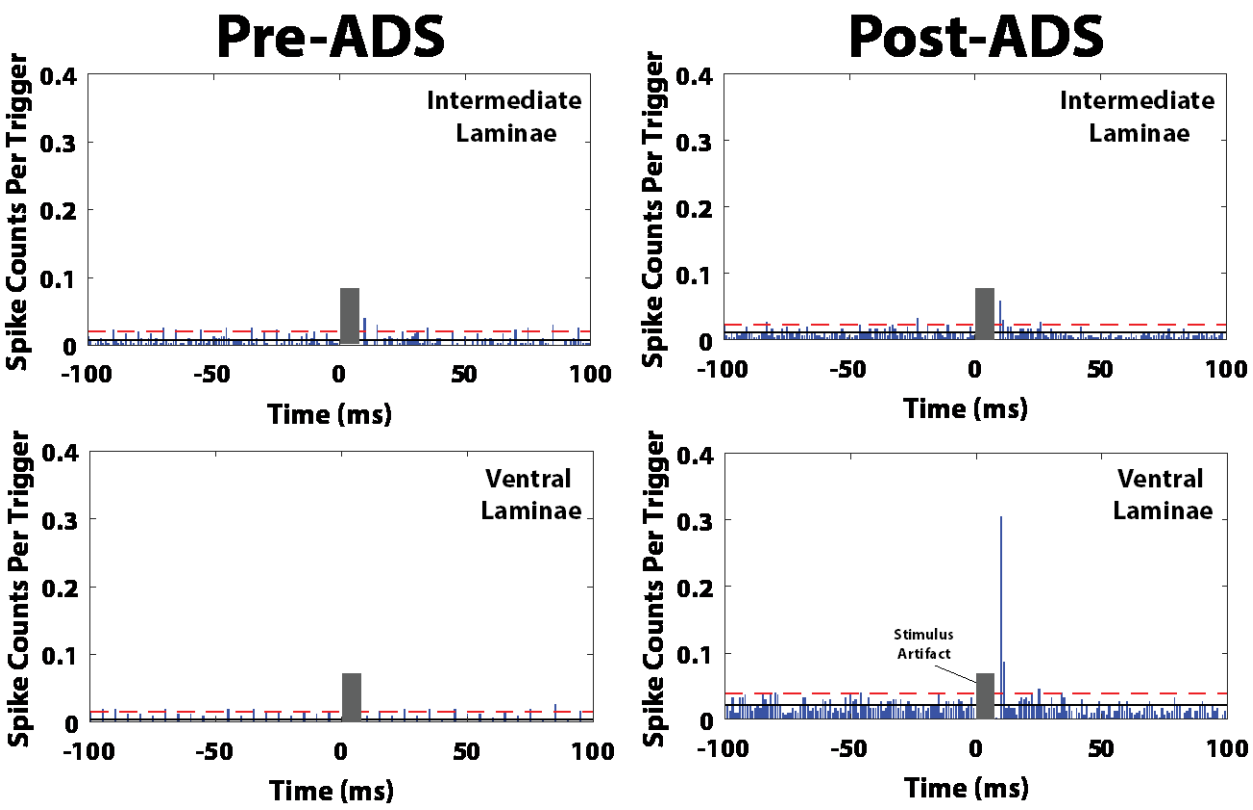

Figure 4.7. Post-stimulus spike histograms of combined data from all rats in the 10ms_1P group before and after 3 hours of ADS. An increase in the number of ICMS-evoked spikes can qualitatively be seen in the recording channel in the ventral laminae (lower right panel) in the 10 ms bin. Solid black line is baseline average. Red dashed line is 2x standard deviations above the baseline average. A spiking bin was considered active and used for quantification if it reached above the red dashed line.

Firing Rate at Short Latency

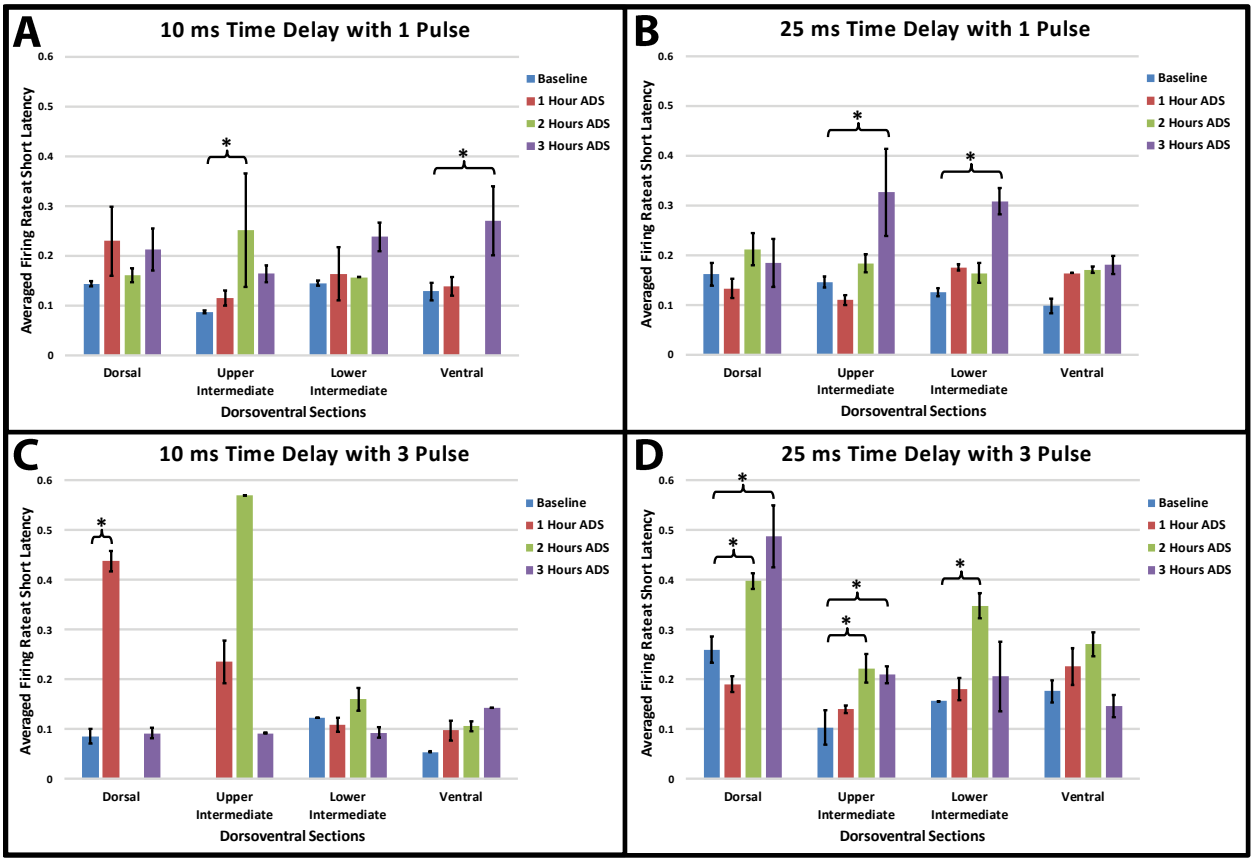

Figure 4.8. Averaged firing rate at Short Latency separated into dorsoventral sections for A) 10ms_1P ADS group, B) 25ms_1P ADS group, C) 10ms_3P ADS group, and D) 25ms_3P ADS group. ***** = Significant increase of firing rate when compared to baseline recordings ($p < 0.05$).

At the Short latency, the firing rate tended to increase after a few hours of ADS. In the 10ms_1P group (Figure 4.8A), there was a significant increase in firing rate after 2 hours of ADS in the Upper Intermediate layers ($p = 0.009$) but not after 3 hours of ADS. There was a significant increase of firing rate after 3 hours of ADS in the Ventral layers ($p = 0.007$) of the lumbar spinal cord. There was no significant change in firing rate after 3 hours of ADS in the Dorsal ($p = 0.2164$) and Lower Intermediate ($p = 0.1900$) layers. In the 25ms_1P group (Figure 4.8B), there was a significant increase in firing rate after 3 hours of ADS in the Upper ($p = 0.0003$) and Lower Intermediate ($p = 0.0006$) layers of the lumbar spinal cord. There was no significant change in firing rate after 3 hours of ADS in the Dorsal ($p = 0.6402$) and Ventral ($p =$

0.1406) layers. In the 10ms_3P group (Figure 4.8C), there was a significant increase in firing rate after 1 hour of ADS in the Dorsal ($p < 0.0001$) layers but decreased after 2 hours of ADS. There was no significant change of firing rate after 3 hours of ADS in the Upper Intermediate, Lower Intermediate, and Ventral layers. Within the 25ms_3P group (Figure 4.8D), there was a significant increase in firing rate after 2 hours of ADS in the Dorsal ($p = 0.0046$), Upper Intermediate ($p = 0.0245$), and Lower Intermediate ($p = 0.0128$) layers of the lumbar spinal cord. This increase of activity remained significantly increased from baseline firing rate after 3 hours of ADS in the Dorsal ($p < 0.0001$) and Upper Intermediate ($p = 0.0439$) layers but decreased in the Lower Intermediate layers. There was no significant change of firing rate after 3 hours of ADS in the Ventral ($p = 0.5641$) layers.

Firing Rate at L1 Latency

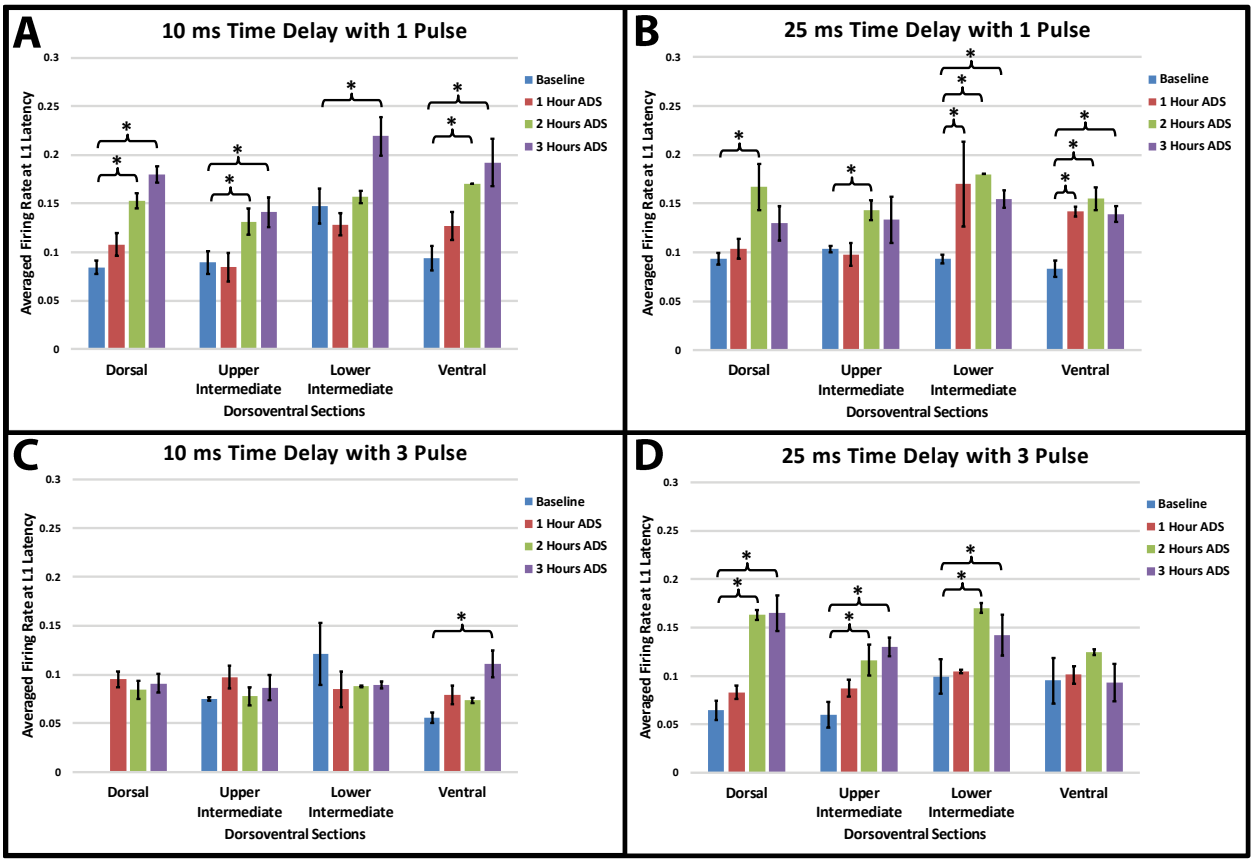

Figure 4.9. Averaged ICMS-evoked firing rate at L1 Latency separated into dorsoventral sections for A) 10ms_1P ADS group, B) 25ms_1P ADS group, C) 10ms_3P ADS group, and D) 25ms_3P ADS group. * = Significant increase of firing rate when compared to baseline recordings ($p < 0.05$).

At the L1 latency, the firing rate tended to increase after a few hours of ADS. Within the 10ms_1P group (Figure 4.9A), there was a significant increase of firing rate after 2 hours of ADS in the Dorsal (p = 0.0001), Upper Intermediate (p = 0.0261), and Ventral (p = 0.0057) layers and remained significantly increased (p < 0.05) after 3 hours of ADS. In addition, there was a significant increase of firing rate after 3 hours of ADS in the Lower Intermediate (p = 0.0002) layers of the lumbar spinal cord. Within the 25ms_1P group (Figure 4.9B), there was a significant increase of firing rate after 1 hour of ADS in the Lower Intermediate (p = 0.0004) and Ventral (p = 0.0066) layers and remained significantly increased (p < 0.05) after 2 and 3 hours of ADS. In addition, there was a significant increase of firing rate after 2 hours of ADS but decreased (p > 0.05) after 3 hours in the Dorsal (p = 0.0007) and Upper Intermediate (p = 0.0337) layers of the lumbar spinal cord. Within the 10ms_3P group (Figure 4.9C), there was a significant increase of firing rate after 3 hours of ADS in the Ventral (p = 0.0018) layers of the lumbar spinal cord. There was no significant change of firing rate after 3 hours of ADS in the Dorsal, Upper Intermediate, and Lower Intermediate layers. Within the 25ms_3P group (Figure 4.9D), there was a significant increase of firing rate after 2 hours of ADS in the Dorsal (p < 0.0001), Upper Intermediate (p = 0.0013), and Lower Intermediate (p = 0.0002) layers and remained significantly increased (p < 0.05) after 3 hours of ADS. There was no significant change of firing rate after 3 hours of ADS in the Ventral layers.

Firing Rate at Peak Latency

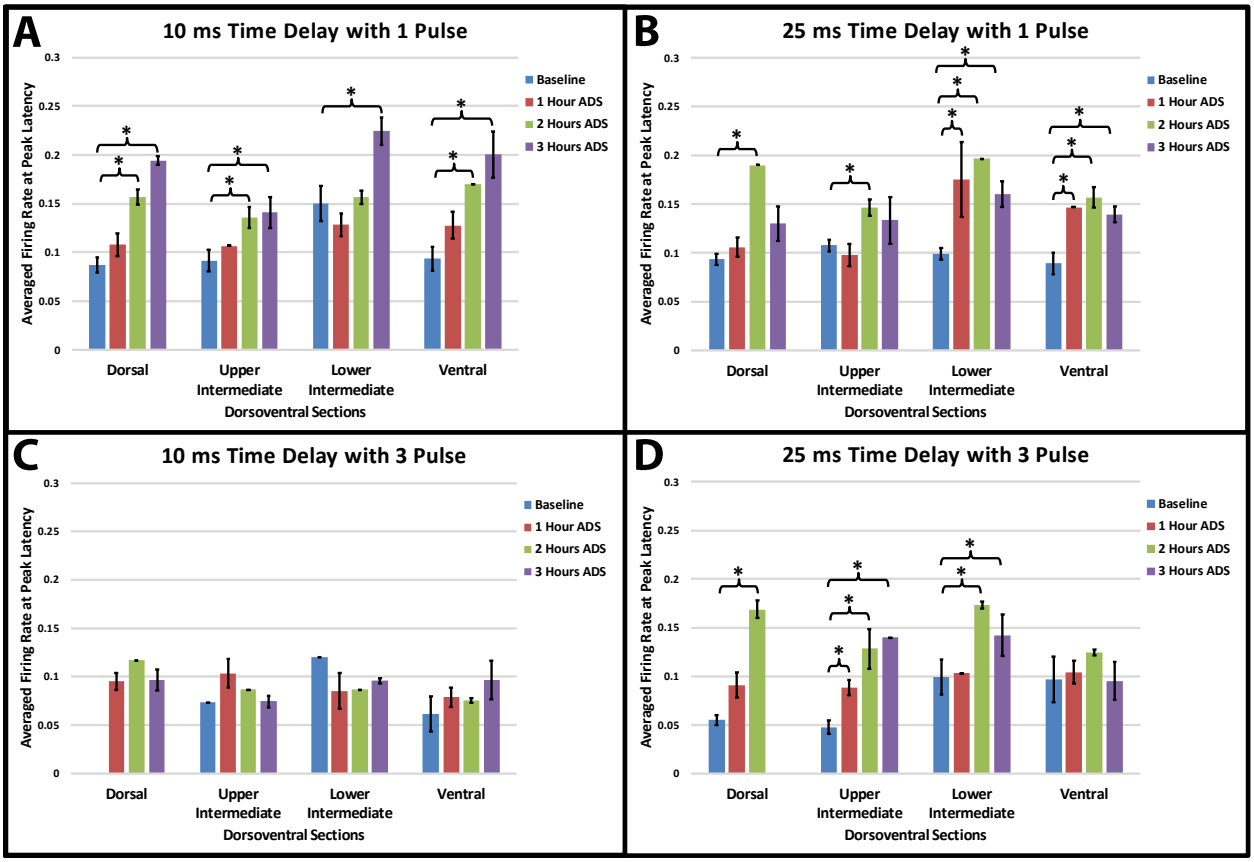

Figure 4.10. Averaged ICMS-evoked firing rate at Peak Latency separated into dorsoventral sections for A) 10ms_1P ADS group, B) 25ms_1P ADS group, C) 10ms_3P ADS group, and D) 25ms_3P ADS group. * = Significant increase of firing rate when compared to baseline recordings ($p < 0.05$).

At the Peak latency, the firing rate tended to increase after a few hours of ADS. Within the 10ms_1P group (Figure 4.10A), there was a significant increase of firing rate after 2 hours of ADS in the Dorsal ($p = 0.0001$), Upper Intermediate ($p = 0.0218$), and Ventral ($p = 0.0064$) layers of the lumbar spinal cord and remained significantly increased after 3 hours of ADS. In addition, there was a significant increase of firing rate after 3 hours of ADS in the Lower Intermediate ($p = 0.0001$) layers of the lumbar spinal cord. Within the 25ms_1P group (Figure 4.10B), there was a significant increase of firing rate after 1 hour of ADS in the Lower Intermediate ($p = 0.001$) and Ventral ($p = 0.0396$) layers of the lumbar spinal cord and remained significantly increased after 2 and 3 hours of ADS. In addition, there was a significant increase

of firing rate after 2 hours of ADS in the Dorsal (p = 0.0007) and Upper Intermediate (p = 0.0401) layers but decreased after 3 hours of ADS. Within the 10ms_3P group (Figure 4.10C), there was no significant increase of firing rate after 3 hours of ADS in any layers (p > 0.05) of the lumbar spinal cord. Within the 25ms_3P group (Figure 4.10D), there was a significant increase of firing rate after 1 hour of ADS in the Upper Intermediate (p = 0.0337) layers of the lumbar spinal cord and remained significantly increased after 2 and 3 hours of ADS. In addition, there was a significant increase of firing rate after 2 hours of ADS in the Dorsal (p < 0.0001) and Lower Intermediate (p = 0.0001) layers; however, the firing rate remained significantly increased in the Lower Intermediate (p = 0.0243) layers and decreased in the Dorsal layers after 3 hours of ADS. There was no significant change of firing rate at peak latency after 3 hours of ADS in the Ventral layers.

ICMS-Evoked Spike Amplitudes

The ICMS-evoked spike amplitudes displayed in Table 4.3 generally decreased at all latencies in most dorsoventral sections. For the 10ms_1P group, ICMS-evoked spike amplitudes significantly decreased (p < 0.05) after one hour of ADS and continued for three hours after ADS in all dorsoventral sections at the Short latency (Table 4.3.1), L1 latency (Table 4.3.2), and Peak latency (Table 4.3.3). For the 25ms_1P group, ICMS-evoked spike amplitudes significantly decreased (p < 0.05) after three hours of ADS only in the Upper Intermediate Section at the L1 latency (Table 4.3.2) and Peak latency (Table 4.3.3). For the 10ms_3P group, ICMS-evoked spike amplitudes significantly decreased (p < 0.05) after one hour of ADS and continued for three hours after ADS in all dorsoventral sections at the Peak latency (Table 4.3.3). In addition, ICMS-evoked spike amplitudes significantly decreased (p < 0.05) after two hours of ADS and continued after three hours of ADS in the Lower Intermediate Section at the L1 Latency (Table 4.3.2). ICMS-evoked spike amplitudes significantly decreased (p < 0.05) after three hours of ADS in the Dorsal Section at the L1 latency (Table 4.3.2). For the 25ms_3P

group, ICMS-evoked spike amplitudes significantly decreased ($p < 0.05$) after three hours of ADS in the Doral, Upper Intermediate, and Lower Intermediate Section at the L1 latency (Table 4.3.2). In addition, ICMS-evoked spike amplitudes significantly decreased ($p < 0.05$) after three hours of ADS in the Dorsal Section at the S2 latency (Table 4.3.1) and Peak latency (Table 4.3.3) and in the Upper Intermediate Section at the Peak latency (Table 4.3.3).

Table 4.3. ICMS-evoked spike amplitudes (mean ± SE) for each ADS group at all latencies in each dorsoventral section before and after each hour of ADS. Grey box and ***** = Significant difference from baseline recordings in the same dorsoventral section and ADS rat group ($p < 0.05$).

Table 4.3.1: ICMS-Evoked Spike Amplitudes (μV) at S2 Latency

Rat Group	Dorsoventral Sections	ADS Time			
		Baseline	1 Hour ADS	2 Hours ADS	3 Hours ADS
10ms_1P	Dorsal	65.1 ± 14.2	**35.7 ± 3.8***	**32.2 ± 2.0***	**35.5 ± 2.5***
	Upper Int.	78.4 ± 12.7	**53.2 ± 6.0***	**44.0 ± 2.9***	**39.9 ± 2.4***
	Lower Int.	106.2 ± 14.8	**54.7 ± 3.1***	**49.4 ± 2.1***	**56.7 ± 3.4***
	Ventral	83.9 ± 14.5	**56.5 ± 4.7***	**59.3 ± 4.3***	**56.2 ± 4.4***
25ms_1P	Dorsal	40.7 ± 3.7	35.0 ± 2.1	33.9 ± 1.6	37.8 ± 3.1
	Upper Int.	53.9 ± 5.3	44.8 ± 3.2	43.9 ± 2.7	39.0 ± 1.7
	Lower Int.	68.0 ± 5.1	60.5 ± 5.2	58.8 ± 4.5	59.3 ± 6.4
	Ventral	59.3 ± 2.9	63.8 ± 9.7	50.5 ± 3.3	48.4 ± 2.2
10ms_3P	Dorsal	45.3 ± 11.0	41.2 ± 4.1	37.5 ± 4.5	21.7 ± 1.3
	Upper Int.	63.7 ± 17.1	50.7 ± 5.8	**42.3 ± 3.4***	38.8 ± 5.4
	Lower Int.	69.3 ± 10.6	60.2 ± 4.8	52.3 ± 6.1	**33.5 ± 5.1**
	Ventral	57.7 ± 10.9	49.6 ± 3.7	49.9 ± 3.7	45.6 ± 7.9
25ms_3P	Dorsal	64.8 ± 9.0	49.1 ± 3.3	46.3 ± 4.4	**37.3 ± 3.4***
	Upper Int.	69.3 ± 7.2	49.4 ± 4.8	53.5 ± 3.9	47.0 ± 4.1
	Lower Int.	69.6 ± 11.3	55.8 ± 3.5	**50.2 ± 2.4***	53.4 ± 4.3
	Ventral	56.5 ± 3.9	65.5 ± 3.5	59.5 ± 5.5	50.0 ± 3.5

Table 4.3.2: ICMS-Evoked Spike Amplitudes (μV) at L1 Latency

Rat Group	Dorsoventral Sections	ADS Time			
		Baseline	1 Hour ADS	2 Hours ADS	3 Hours ADS
10ms_1P	Dorsal	74.6 ± 18.3	**36.2 ± 3.6***	**36.6 ± 2.8***	**36.1 ± 2.3***
	Upper Int.	82.4 ± 13.5	**50.4 ± 5.6***	**44.9 ± 5.4***	**44.1 ± 3.1***
	Lower Int.	109.6 ± 13.1	**54.1 ± 3.0***	**49.3 ± 1.9***	**55.9 ± 3.7***
	Ventral	78.6 ± 11.9	**55.1 ± 5.0***	**56.7 ± 4.5***	**56.2 ± 2.1***
25ms_1P	Dorsal	41.1 ± 3.4	37.0 ± 2.6	35.8 ± 1.8	39.4 ± 3.5
	Upper Int.	55.0 ± 4.1	45.6 ± 2.9	44.5 ± 2.4	**36.6 ± 1.4***
	Lower Int.	66.9 ± 4.4	59.7 ± 4.8	64.1 ± 4.2	58.5 ± 6.6
	Ventral	56.9 ± 4.4	59.7 ± 4.8	64.1 ± 4.2	58.5 ± 6.6
10ms_3P	Dorsal	51.7 ± 15.4	44.0 ± 5.8	36.0 ± 4.5	**31.9 ± 4.9***
	Upper Int.	58.2 ± 10.0	55.1 ± 6.2	40.8 ± 3.6	39.6 ± 4.4
	Lower Int.	74.4 ± 11.2	62.1 ± 5.7	**44.5 ± 3.9***	**33.0 ± 3.8***
	Ventral	61.1 ± 11.3	47.8 ± 3.2	45.8 ± 3.2	50.5 ± 5.4
25ms_3P	Dorsal	58.5 ± 6.9	48.6 ± 3.0	48.4 ± 4.3	**37.0 ± 3.1***
	Upper Int.	65.2 ± 7.3	54.8 ± 5.2	51.4 ± 3.6	**41.5 ± 4.2***
	Lower Int.	68.3 ± 11.9	57.6 ± 3.8	55.3 ± 2.6	**43.8 ± 2.9***
	Ventral	59.7 ± 4.2	63.1 ± 2.9	62.0 ± 4.9	54.7 ± 4.3

Table 4.3.3: ICMS-Evoked Spike Amplitudes (μV) at Peak Latency

Rat Group	Dorsoventral Sections	ADS Time			
		Baseline	1 Hour ADS	2 Hours ADS	3 Hours ADS
10ms_1P	Dorsal	70.2 ± 16.2	**36.3 ± 3.4***	**35.7 ± 2.8***	**35.0 ± 2.1***
	Upper Int.	82.8 ± 13.2	**47.6 ± 3.9***	**45.0 ± 5.4***	**41.6 ± 1.8***
	Lower Int.	110.1 ± 12.7	**52.4 ± 2.9***	**49.5 ± 1.9***	**54.9 ± 3.3***
	Ventral	80.4 ± 12.0	**53.2 ± 4.0***	**55.7 ± 3.9***	**55.6 ± 4.2***
25ms_1P	Dorsal	41.2 ± 3.3	36.8 ± 2.5	36.3 ± 1.9	40.0 ± 3.3
	Upper Int.	55.1 ± 4.2	44.6 ± 2.8	46.0 ± 2.6	**38.5 ± 1.3***
	Lower Int.	66.6 ± 4.3	59.7 ± 4.8	59.4 ± 3.8	58.7 ± 5.7
	Ventral	56.3 ± 2.9	65.7 ± 9.5	48.8 ± 3.4	51.9 ± 2.0
10ms_3P	Dorsal	80.9 ± 18.0	**46.6 ± 4.8***	**35.7 ± 4.3***	**31.7 ± 4.6***
	Upper Int.	78.4 ± 13.8	**54.6 ± 4.5***	**39.9 ± 3.1***	**39.7 ± 4.4***
	Lower Int.	86.2 ± 13.1	**63.3 ± 4.7***	**46.5 ± 4.2***	**35.0 ± 3.5***
	Ventral	88.3 ± 15.6	**52.8 ± 3.3***	**48.2 ± 3.2***	**50.7 ± 5.5***
25ms_3P	Dorsal	58.5 ± 7.0	47.2 ± 2.9	47.2 ± 4.1	**35.9 ± 2.9***
	Upper Int.	68.3 ± 8.0	52.5 ± 4.5	53.9 ± 3.5	**42.7 ± 3.1***
	Lower Int.	69.1 ± 11.6	57.3 ± 3.8	55.4 ± 2.7	50.4 ± 5.3
	Ventral	57.8 ± 3.0	62.7 ± 3.1	60.1 ± 5.1	53.4 ± 3.3

Discussion

The primary goal of this study was to determine a spike-stimulus delay for increasing efficacy in descending motor pathways using an activity dependent stimulation (ADS) paradigm in an acute, anesthetized rat model of SCI. This study describes a novel intervention to facilitate and guide activity-dependent neural plasticity to increase efficacy in cortical descending motor pathways to the hindlimb spinal cord. By pairing sites of similarly evoked movements in the hindlimb motor cortex and hindlimb spinal cord and synchronizing the delivery of ISMS with natural neural activity, we can increase the efficacy of neural circuits, as evidenced by an increase in cortically-evoked spinal cord responses, after injury. Importantly, efficacy in descending motor pathways can be increased in different dorsoventral sections of the hindlimb spinal cord by using different time delays and a different number of ISMS, biphasic pulses during ADS therapy (i.e., using different ADS parameters). Here we discuss the likely motor pathways affected by ADS and the functional impact these plastic effects could have in motor control.

Time Delays during ADS are Consistent with STDP-Based Strengthening

In spike timing-dependent plasticity (STDP), the timing between recorded action potentials and triggered stimulation (i.e., ADS) has been shown to determine the polarity and magnitude (i.e., potentiation or depression) of any change in post-synaptic potentials (Markram, Lubke et al. 1997, Bi and Poo 1998, Fung, Law et al. 2016). McPherson *et al.* demonstrated that ADS can induce neural plasticity, with a time delay of ~10 ms, that improves behavioral recovery after SCI by synchronizing ISMS below the injury with the arrival of functional related volitional motor commands signaled by muscle activity in the impaired forelimb (McPherson, Miller et al. 2015). The time delays used during ADS in this study fell within the range of causal latencies (i.e., ~25 ms or less), where robust enhancement of synaptic strength was determined in *in vitro* (Feldman 2012) and *in vivo* (Nishimura, Perlmutter et al. 2013) studies.

Short-Latency Neuronal Spikes after Acute ADS

Different ADS parameters increased the firing rate of short-latency neurons located in different dorsoventral layers of the spinal cord after an acute application of ADS. After a moderate spinal cord contusion, we have shown in a previous experiment that short-latency spikes can still be evoked and were most likely from cortico-reticulospinal pathways (Frost, Borrell et al. 2018). Anatomically, it has been shown that the reticulospinal tract terminates mainly within the intermediate grey matter of lamina VII and VIII in the hindlimb spinal cord of the rat (Matsuyama, Mori et al. 1999, Mitchell, McCallum et al. 2016), which corresponds to the Lower Intermediate and Ventral Sections of the spinal cord described in this study. Based on this anatomical literature, the 10ms_1P, 25ms_1P, and 25ms_3P groups could have increased the efficacy of these cortico-reticulospinal fibers. More specifically, the 25ms_1P and the 25ms_3P groups may have less of an effect on the reticulospinal fibers that terminate in the Ventral Section. Conversely, the 10ms_1P group appears to only effect the reticulospinal fibers that terminate in the Ventral Section.

After injury, it has been shown that a greater recovery of locomotion is due to spared reticulospinal fibers instead of spared corticospinal fibers; thus, the reticulospinal tract appears to have an important role in the initiation and control of open-field locomotion (Schucht, Raineteau et al. 2002). Anatomically, a large number of reticulospinal neurons terminate onto long descending propriospinal pathways, which control the coordination between forelimb-hindlimb and left-right limbs (Frigon 2017), suggesting that the reticulospinal pathway is strongly involved in coordination during locomotion (Mitchell, McCallum et al. 2016). With the inclusion criteria of 13-15 BBB score, the SCI rats in this study had recovered coordination by the start time of ADS therapy which suggests that long descending propriospinal pathways are still intact after injury. Spared reticulospinal fibers have been shown to sprout below the SCI; this suggests that spared reticulospinal fibers might be involved in the recovery of locomotion

following incomplete SCI (Ballermann and Fouad 2006). The increased firing rate of short-latency neurons seen in this study suggests strengthening of the cortico-reticulo-spinal pathway.

Long-Latency Neuronal Spikes & EMG Activity after Acute ADS

In a previous experiment, it was shown that the ICMS-evoked long-latency activity in a healthy, uninjured rat was represented in a Gaussian distribution beginning ~20ms after onset ICMS (i.e., L1 latency), included the onset of EMG activity at ~25ms, and peaked (i.e., Peak latency) around ~30ms (Frost, Borrell et al. 2018). After injury, this Gaussian distribution was disrupted, and any remaining spiking activity was constricted to one or two spiking bins at these latencies (i.e., the Gaussian distribution was severely restricted to ~1-2ms bins). This was similarly seen in this study, where comparable increases in the firing rate of the long-latency (i.e., L1 and Peak latency) neuronal spikes are from the same or adjacent spiking bins. It was concluded in the previous experiment that the evoked spikes with L1 and Peak latencies were most likely from neurons pertaining to the corticospinal tract due to the known conduction velocity of this tract.

The question of motor functionality of the descending motor pathways can be tied to the ability to activate motor neurons which in turn evoke hindlimb muscle activity. If it is possible to evoke hindlimb movement via ICMS in the hindlimb motor cortex, then it can be assumed that the activated descending motor pathways are functionally significant. In this study, hindlimb movements could not be evoked via ICMS before and after 3 hours of ADS which indicates that the plasticity seen after 3 hours of ADS is not functionally significant at that time.

Contrary to the observed short-latency neuronal spikes, the increased firing rate of the long-latency neuronal spikes occurred after 2 hours of ADS, with some instances occurring after 1 hour of ADS, and remained increased after 3 hours of ADS. The increase of firing rate occurred earlier, within all dorsoventral sections, and in all rat groups except for the 10ms_3P

group. This result could be indicative of STDP-based strengthening. In all rat groups, the time delays used during ADS were shorter or matched the natural conduction time of the L1 latency response seen in healthy rats. Thus, the similar increases in firing rate of long-latency spikes seen in each rat group suggests time delays that are shorter or matching the natural conduction time can modulate these pathways. However, it is still uncertain if there are any remaining corticospinal fibers after spinal cord contusion in this study. Anatomically, it has been shown that the corticospinal tract terminates mainly in the deep dorsal horn and intermediate grey matter in the hindlimb spinal cord of the rat with some terminal patterns observed in all dorsoventral sectors (Casale, Light et al. 1988, Akintunde and Buxton 1992, Mitchell, McCallum et al. 2016). The electrophysiological results reported here could be further proof that corticospinal fibers remain after this injury and are strengthened after an acute application of ADS.

Nonetheless, a more chronic application of ADS may be needed for the plasticity to result in functional motor recovery. Furthermore, in the present study, 3 biphasic stimulation pulses were used during ICMS catch trials whereas 13 biphasic stimulation pulses are most commonly used during hindlimb motor mapping procedures (Frost, Iliakova et al. 2013, Frost, Dunham et al. 2015). As a result, the low number of stimulation pulses used in this study may not have been enough to activate the motor neurons in the hindlimb spinal cord (i.e., the current and stimulation pulse combination used was below movement threshold).

Impact of Acute Plasticity on Recovery

The increased firing rate of neuronal spikes in as early as 3 hours after therapy is a novel and highly significant finding that is also clinically relevant. The application of ADS may drive future electrical stimulation-based therapies. To date, these electrical stimulation-based therapies are contingent on the maintained delivery of stimulation. Future studies will have to determine the functional significance of this plasticity, the effect on functional motor recovery in

the chronic condition, and the potential for behavioral improvement compared to less-invasive electrical stimulation-based therapies.

Effects of Acute ADS on Hindlimb Motor Cortex

In each ADS group, small changes in the spiking frequency of HLA recorded spikes occurred after each hour of ADS; however, there were no significant changes in each ADS group. In previous studies with a similar SCI but located at T10 vertebral segment, it was reported that the spiking frequency in HLA was 3.68 ± 0.32 spikes/sec under anesthesia and was slightly higher than the spiking frequency in HLA of healthy/uninjured rats (Frost, Dunham et al. 2015). The spiking frequencies reported in the present study do agree with the firing rates reported earlier under the same anesthetic conditions. With minor changes (but not significant) in firing rate after an acute administration of ADS, it can be assumed that plasticity does not occur in HLA within at least within 3-hours of ADS. However, a chronic administration of ADS would need to be conducted in order to determine if any plasticity occurs in HLA due to ADS.

Possible Suppressive Effect after Acute ADS

The overall decrease of ICMS-evoked spike amplitudes in all ADS rat groups was unexpected. Markram, *et. al.*, reported that excitatory post-synaptic potentials (EPSPs) can be up- or down-regulated depending on the precise timing of EPSPs with respect to postsynaptic action potentials (i.e., delay/conduction time of neurons between areas of interest) (Markram, Lubke et al. 1997). Bi and Poo also point to long-term potentiation or long-term depression due to timing of post-synaptic spiking and presynaptic activation (Bi and Poo 1999). There is a difference in the recording methods in this study from those of Markram, *et. al.*, and Bi and Poo. In this study, extracellular recordings were conducted while intracellular recordings were conducted in the other studies. Nonetheless, the decrease in ICMS-spiking amplitude after 3 hours of ADS could be assumed to be a result of the following: 1) There is a weakening of ineffective synapses; 2) The distance between recording site on the electrode and evoked-

neuron changed between recordings (i.e., removal and reinsertion of the electrode changed the distance); 3) The damage to the spinal cord due to the removal and reinsertion of the electrode caused the decrease in ICMS-evoked spike amplitude. Overall, it can be assumed that the decrease of ICMS-evoked spike amplitude was a combination of the proposed reasons. This observed decrease in ICMS-evoked spike amplitudes, in addition to the increase of firing rate of short- and long-latency neuronal spikes may suggest that some descending pathways are suppressed while others are strengthened after 3 hours of ADS; however, a simple change in the distance between recording site and evoked neuron during each catch trial cannot be ruled out.

Consistency of Injury Model

An inclusion criterion based on behavioral deficits due to the SCI contusion was used to ensure that injury was constant between groups. The SCI rats for each group had to have a BBB score within the range of 13 to 15 to be included in the study. At 4-weeks post-moderate SCI, animals step with consistent coordination but have deficits in paw placement (i.e., externally rotated hindlimb paws), toe clearance, and trunk stability and is described as a BBB score of 13, 14, or 15 (Basso, Beattie et al. 1995). Krizsan-Agbas *et al.* have reported that BBB scores at 4 weeks post-injury are highly correlated with spinal cord displacements from the impactor during injury, and the calculated myelin loss in epicenter areas of the injury are significantly correlated with spinal cord displacement values at the time of injury (Krizsan-Agbas, Winter et al. 2014). The displacement values and the resulting behavioral deficits (i.e., BBB scores) reported in Table 4.1 of this experiment are consistent with those reported by other researchers using the same contusion device with the same force on impact (Scheff, Rabchevsky et al. 2003, Cao, Zhang et al. 2005, Krizsan-Agbas, Winter et al. 2014). In addition, the resulting BBB scores, displacement values, and behavioral deficits are expected based on the level of injury used in this study. The representative image of the resulting

moderate (175 kDyn) contusion agrees with other studies using the same impact force (Krizsan-Agbas, Winter et al. 2014) or moderate contusion (Basso, Beattie et al. 1995, Basso, Beattie et al. 1996).

Limitations of Study

The main limitation to this study was the necessity to remove and reinsert the electrodes between the 1-hour ADS sessions and the 5-minute catch trials. During ADS, the recording electrode was inserted in the hindlimb motor cortex while the stimulating electrode was inserted in the hindlimb spinal cord. The electrodes were then switched during the catch trials (i.e., the stimulating electrode was inserted in the hindlimb motor cortex and the recording electrode was inserted in the hindlimb spinal cord). When removing and reinserting the electrodes, there was a possibility that the electrodes were not reinserted into the exact position as before. In addition, there could be neuronal damage with each reinsertion of the electrode. The ICMS and ISMS mapping did reduce the amount of variation in site location between each ADS session and catch trial. The use of two micromanipulators (one for each electrode) also aided with the consistency of electrode insertion and placement on a micron scale. The consistency in recorded HLA spiking profiles over the ADS sessions also indicates that the recording electrode inserted in HLA was consistently in the same site each time; however, the change in spike amplitudes of the evoked spikes in the spinal cord may suggest a slight shift of the recording electrode between bouts of ADS. In order for an electrode to stimulate and/or record, it needs to be hooked up (i.e., tethered) to a particular headstage. A switchable headstage that can automatically switch between recording and stimulation would allow for the electrodes to remain in their original sites; however, this type of switchable headstage has yet to be properly developed to our knowledge. An advancement in electrode design and technology would eliminate these limitations.

Conclusion

The significant increase in firing rate of short-latency spikes after 3 hours of ADS indicates a strengthening of the remaining cortico-reticulospinal fibers, while the significant increase in firing rate of long-latency spikes indicates that corticospinal fibers may still exist and are being strengthened as well. It is unlikely that any axonal sprouting is occurring in this short amount of time. This plasticity after an acute administration of ADS is promising for future neurorehabilitation and neuromodulatory studies involving moderate spinal cord injuries and adds translational value to similar injuries seen in clinical settings. It is notable that different ADS parameters did cause increased firing rate, but at different dorsoventral depths. The increased firing rate in different dorsoventral sections could indicate different types of plasticities; however, any functional aspects of these increased firing rates were not determined in this study. Chronic administration of ADS in a SCI rat model may determine any ADS-mediated enhanced recovery of motor function.

Acknowledgments

This work was supported by the Paralyzed Veterans of America Research Foundation #3068, The Ronald D. Deffenbaugh Family Foundation, NIH/NINDS R01 NS030853, T32 Neurological and Rehabilitation Sciences Training Program, and NIH/NINDS F31 NS105442.

References

Akintunde, A. and D. F. Buxton (1992). "Differential sites of origin and collateralization of corticospinal neurons in the rat: a multiple fluorescent retrograde tracer study." Brain Res **575**(1): 86-92.

Ballermann, M. and K. Fouad (2006). "Spontaneous locomotor recovery in spinal cord injured rats is accompanied by anatomical plasticity of reticulospinal fibers." Eur J Neurosci **23**(8): 1988-1996.

Basso, D. M., M. S. Beattie and J. C. Bresnahan (1995). "A sensitive and reliable locomotor rating scale for open field testing in rats." J Neurotrauma **12**(1): 1-21.

Basso, D. M., M. S. Beattie and J. C. Bresnahan (1996). "Graded histological and locomotor outcomes after spinal cord contusion using the NYU weight-drop device versus transection." Experimental Neurology **139**(2): 244-256.

Behrmann, D. L., J. C. Bresnahan, M. S. Beattie and B. R. Shah (1992). "Spinal Cord Injury Produced by Consistent Mechanical Displacement of the Cord in Rats: Behavioral and Histological Analysis." Journal Of Neurotrauma **9**(3).

Bi, G. and M. Poo (1998). "Synaptic Modifications in Culutured Hippocampal Neurons: Dependence on Spike Timing, Synaptic Strength, and Postsynaptic Cell Type." The Journal of Neuroscience **18**(24): 10464-10472.

Bi, G. and M. Poo (1999). "Distributed synaptic modification in neural networks induced by patterned stimulation." Nature **401**(6755): 792-796.

Borrell, J. A., S. B. Frost, J. Peterson and R. J. Nudo (2017). "A 3D map of the hindlimb motor representation in the lumbar spinal cord in Sprague Dawley rats." J Neural Eng **14**(1): 016007.

Cao, Q., Y. P. Zhang, C. Iannotti, W. H. DeVries, X. M. Xu, C. B. Shields and S. R. Whittemore (2005). "Functional and electrophysiological changes after graded traumatic spinal cord injury in adult rat." Exp Neurol **191 Suppl 1**: S3-S16.

Capogrosso, M., T. Milekovic, D. Borton, F. Wagner, E. M. Moraud, J. B. Mignardot, N. Buse, J. Gandar, Q. Barraud, D. Xing, E. Rey, S. Duis, Y. Jianzhong, W. K. Ko, Q. Li, P. Detemple, T. Denison, S. Micera, E. Bezard, J. Bloch and G. Courtine (2016). "A brain-spine interface alleviating gait deficits after spinal cord injury in primates." Nature **539**(7628): 284-288.

Casale, E. J., A. R. Light and A. Rustioni (1988). "Direct projection of the corticospinal tract to the superficial laminae of the spinal cord in the rat." J Comp Neurol **278**(2): 275-286.

Debanne, D., B. H. Gahwiler and S. M. Thompson (1994). "Asynchronous pre- and postsynaptic activity induces associative long-term depression in area CA1 of the rat hippocampus in vitro." Proc Natl Acad Sci U S A **91**(3): 1148-1152.

Debanne, D., B. H. Gahwiler and S. M. Thompson (1997). "Bidirectional associative plasticity of unitary CA3-CA1 EPSPs in the rat hippocampus in vitro." J Neurophysiol **77**(5): 2851-2855.

Feldman, D. E. (2012). "The spike-timing dependence of plasticity." Neuron **75**(4): 556-571.

Frigon, A. (2017). "The neural control of interlimb coordination during mammalian locomotion." J Neurophysiol **117**(6): 2224-2241.

Frost, S. B., J. A. Borrell, D. Krizsan-Agbas and R. J. Nudo (2018). Effects of contusive spinal cord injury on spinal motor neuron activity, corticospinal coupling, and conduction time in rats. Society for Neuroscience. San Diego, Abstract.

Frost, S. B., C. L. Dunham, S. Barbay, D. Krizsan-Agbas, M. K. Winter, D. J. Guggenmos and R. J. Nudo (2015). "Output Properties of the Cortical Hindlimb Motor Area in Spinal Cord-Injured Rats." J Neurotrauma **32**(21): 1666-1673.

Frost, S. B., M. Iliakova, C. Dunham, S. Barbay, P. Arnold and R. J. Nudo (2013). "Reliability in the location of hindlimb motor representations in Fischer-344 rats: laboratory investigation." J Neurosurg Spine **19**(2): 248-255.

Fung, T. K., C. S. Law and L. S. Leung (2016). "Associative spike timing-dependent potentiation of the basal dendritic excitatory synapses in the hippocampus in vivo." J Neurophysiol **115**(6): 3264-3274.

Gerstner, W., R. Kempter, J. L. van Hemmen and H. Wagner (1996). "A neuronal learning rule for sub-millisecond temporal coding." Nature **383**(6595): 76-81.

Guggenmos, D. J., M. Azin, S. Barbay, J. D. Mahnken, C. Dunham, P. Mohseni and R. J. Nudo (2013). "Restoration of function after brain damage using a neural prosthesis." PNAS **110**(52): 21177-21182.

Hebb, D. O. (1949). The Organization of Behavior. Wiley, New York.

Hudson, H. M., D. M. Griffin, A. Belhaj-Saif and P. D. Cheney (2015). "Properties of primary motor cortex output to hindlimb muscles in the macaque monkey." J Neurophysiol **113**(3): 937-949.

Jackson, A., J. Mavoori and E. E. Fetz (2006). "Long-term motor cortex plasticity induced by an electronic neural implant." Nature **444**(7115): 56-60.

Krizsan-Agbas, D., M. K. Winter, L. S. Eggimann, J. Meriwether, N. E. Berman, P. G. Smith and K. E. McCarson (2014). "Gait Analysis at Multiple Speeds Reveals Differential Functional and Structural Outcomes in Response to Graded Spinal Cord Injury." Journal of Neurotrauma **31**(9): 846-856.

Levy, W. B. and O. Steward (1983). "Temporal contiguity requirements for long-term associative potentiation/depression in the hippocampus." Neuroscience **8**(4): 791-797.

Lewicki, M. S. (1998). "A review of methods for spike sorting: the detection and classification of neural action potentials." Network **9**(4): R53-78.

Lisman, J. (1989). "A mechanism for the Hebb and the anti-Hebb processes underlying learning and memory." Proc Natl Acad Sci U S A **86**(23): 9574-9578.

Markram, H., J. Lubke, M. Frotscher and B. Sakmann (1997). "Regulation of Synaptic Efficacy by Coinicidence of Postsynaptic APs and EPSPs." Science **275**: 213-215.

Matsuyama, K., F. Mori, B. Kuze and S. Mori (1999). "Morphology of Single Pontine Reticulospinal Axons in the Lumbar enlargement of the Cat: A Stud Using the Anterograde Tracer PHA-L." The Journal of Comparative Neurology **410**: 413-430.

McPherson, J. G., R. R. Miller and S. I. Perlmutter (2015). "Targeted, activity-dependent spinal stimulation produces long-lasting motor recovery in chronic cervical spinal cord injury." Proc Natl Acad Sci U S A **112**(39): 12193-12198.

Mitchell, E. J., S. McCallum, D. Dewar and D. J. Maxwell (2016). "Corticospinal and Reticulospinal Contacts on Cervical Commissural and Long Descending Propriospinal Neurons in the Adult Rat Spinal Cord; Evidence for Powerful Reticulospinal Connections." PLoS One **11**(3): e0152094.

Nishimura, Y., S. I. Perlmutter, R. W. Eaton and E. E. Fetz (2013). "Spike-timing-dependent plasticity in primate corticospinal connections induced during free behavior." Neuron **80**(5): 1301-1309.

Scheff, S. W., A. G. Rabchevsky, I. Fugaccia, J. A. Main and J. E. Lumpp, Jr. (2003). "Experimental modeling of spinal cord injury: characterization of a force-defined injury device." J Neurotrauma **20**(2): 179-193.

Schucht, P., O. Raineteau, M. E. Schwab and K. Fouad (2002). "Anatomical Correlates of Locomotor Recovery Following Dorsal and Ventral Lesions of the Rat Spinal Cord." Experimental Neurology **176**(1): 143-153.

Stent, G. S. (1973). "A physiological mechanism for Hebb's postulate of learning." Proc Natl Acad Sci U S A **70**(4): 997-1001.

CHAPTER FIVE: Spike-Triggered Intraspinal Microstimulation Improves Motor Performance in an Ambulatory Rat Model of Spinal Cord Injury

Abstract

The purpose of this study was to determine if spike-triggered intraspinal microstimulation (ISMS) results in improved motor performance in an ambulatory rat model of spinal cord injury (SCI). Experiments were carried out in adult, male, Sprague Dawley rats with 175 kdyn moderate T8 contusion injury. Rats were randomly assigned to one of two groups: Control or Activity Dependent Stimulation (ADS) therapy. Four weeks post-SCI, all rats were implanted with a recording electrode in the left hindlimb motor cortex and a fine-wire, custom-made stimulating electrode in the contralateral lumbar spinal cord. Intracortical and intraspinal microstimulation were used to find sites of similarly evoked hip movements, which were paired together for ADS therapy. In the ADS therapy group, spike-stimulus conditioning was administered for 4 hours/day, 4 days/week, for 4 weeks via a tethered cable in a testing chamber. During therapy sessions, single-unit spikes were discriminated in real time in the hindlimb motor cortex and used to trigger stimulation in the spinal cord ventral horn. The optimal stimulus intensity (50% ISMS movement threshold) and spike-stimulus delay (10ms) determined in preliminary anesthetized preparations were used during ADS. Control rats were similarly implanted with electrodes but did not receive stimulation therapy. Motor performances of each rat were evaluated before SCI contusion, once a week post-SCI for four weeks (prior to electrode implantation), and once a week post-conditioning for four weeks. Behavioral testing included BBB scoring, Ledged Beam walking, Horizontal Ladder walking, treadmill kinematics via the DigiGait and TreadScan system, and open field walking using OptiTrack kinematic analysis. BBB scores were significantly improved in ADS rats compared to Control rats after 1 week of therapy. In the ADS therapy rats, BBB scores were significantly improved after three weeks of ADS therapy when compared to pre-therapy ADS. Foot fault scores on the Horizontal Ladder were significantly lower in ADS rats compared to pre-therapy ADS and Control rats after 1 week of therapy and returned to pre-injury measures after three weeks of ADS therapy. The

Ledged Beam test and kinematic analysis using the DigiGait and TreadScan system showed deficits after SCI in both ADS and Control rats but there were no significant differences between groups after 4 weeks of ADS therapy. These results show that activity dependent stimulation using spike-triggered ISMS can enhance behavioral recovery of locomotor function, as measured by the BBB score and the Horizontal Ladder task after spinal cord injury.

Introduction

An injury to the central nervous system causes a disconnect between distant populations of neurons which results in chronic motor deficits. As a result, impairment severity is related to the function of remaining viable neurons. By focusing on remaining neurons and their pathways after injury, a primary goal of current researchers is to leverage the nervous system's intrinsic capacity for reorganization. One innovative device-based approach utilizes activity-dependent stimulation (ADS) paradigms that record and digitize extracellular neural activity from an implant microelectrode, discriminates individual action potentials in real time, and delivers small amounts of electrical current to another microelectrode implanted in a distal population of neurons (Guggenmos, Azin et al. 2013, Nishimura, Perlmutter et al. 2013, Zimmermann and Jackson 2014, McPherson, Miller et al. 2015, Capogrosso, Milekovic et al. 2016). This approach is based on mechanisms underlying neuroplasticity (Hebb 1949, Jackson and Zimmermann 2012). ADS paradigms look to strengthen the remaining pathways after injury by inducing neuroplasticity in order to restore or improve motor function that was lost due to injury.

A spinal cord injury (SCI) causes damage to descending motor pathways by disrupting the signals between the brain and spinal cord. This lack of input from the brain to neurons below the injury in the spinal cord can result in some level of paralysis. However, even without input from the brain, research has shown that circuits located below the injury, specifically in the lumbar segments of mammals, can fabricate coordinated patterns of leg motor activity (Sherrington 1892, Kiehn 2006). As a result, researchers have developed various neuromodulatory approaches to reconnect the brain to the spinal cord by "closing the loop" with brain-machine interfaces (Zimmermann and Jackson 2014). For example, closed-loop interfaces between the brain and spinal cord have been shown to improve locomotion (Capogrosso, Milekovic et al. 2016) and functional upper limb movement (Nishimura, Perlmutter

et al. 2013) in monkeys with unilateral spinal cord lesions, which is thought to strengthen connections or drive plasticity of the descending motor pathways after SCI.

These efforts encouraged us to develop an understanding of the connection between the brain and spinal cord after a thoracic bilateral spinal cord contusion which mimics those seen in the clinic (Krizsan-Agbas, Winter et al. 2014, Frost, Dunham et al. 2015, Borrell, Krizsan-Agbas et al. 2018, Frost, Borrell et al. 2018). By developing neuromodulation techniques using SCI models similar to injuries typically seen in the clinic, we can create neuromodulation protocols that can translate to the clinic for rehabilitation. This framework guided the design of a brain-machine-spinal cord interface (BMSI) that looks to utilize activity dependent stimulation (ADS) to strengthen motor pathways that may still exist after SCI (Shahdoost, Frost et al. 2016). ADS, administered in a closed-loop manner, uses neural activity to trigger stimulation. In our ADS paradigm, an implanted recording microelectrode in the hindlimb motor cortex records and digitizes extracellular neural activity, discriminates individual action potentials in real time, and delivers small amounts of electrical current to another stimulating microelectrode implanted in the ventral horn of the lumbar spinal cord.

However, in order to strengthen the brain input to spinal cord motoneurons, we first had to show that we could cortically evoke activity in some descending motor pathways that may remain intact after a spinal cord contusion (Frost, Borrell et al. 2018). Once pathways were identified, we applied an acute administration of ADS between the hindlimb motor cortex and hindlimb spinal cord in order to show that ADS could cause a plastic change in the intact pathways of rats with a thoracic contusion to the spinal cord (Borrell, Krizsan-Agbas et al. 2018). Finally, we want to determine whether ADS (i.e., spike-triggered intraspinal microstimulation) results in improved motor performance in an ambulatory rat model of SCI. The goal of this rehabilitation intervention is to facilitate and direct intrinsic synaptic plasticity in spared motor pathways and circuits that would result in improved motor performance. The resulting data

show a significant improvement in motor performance via various behavioral tasks. More importantly, the results gave insight into the descending motor pathways that may have been strengthened after ADS therapy.

Materials and Methods

Experimental Design

To determine if spike-triggered intraspinal microstimulation (ISMS) results in improved motor performance in an ambulatory rat model of spinal cord injury (SCI), extracellular neuronal activity was recorded from the hindlimb motor cortex and used to trigger ISMS in the ventral horn of the lumbar spinal cord (Figure 5.1). Rats' motor performance was recorded and scored on various behavioral tasks before SCI contusion, once a week post-SCI for four weeks (prior to electrode implantation), and once a week post-conditioning for four weeks. Behavioral scores were analyzed and compared to determine any improvement in motor performance.

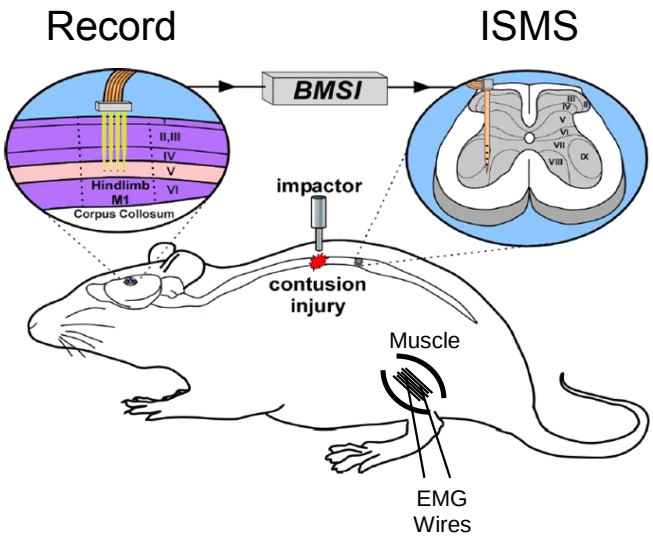

Figure 5.1. Overview of experimental design. A 175 kDyn spinal cord contusion was administered at T8 vertebral segment. Four weeks after injury, rats were implanted with a recording electrode in the hindlimb motor cortex and a fine wire electrode in the ventral horn of the lumbar spinal cord. Activity dependent stimulation was administered for four weeks post-implant.

Subjects

A total of 20 adult, male, Sprague Dawley rats were randomly selected for this study. At the beginning of the study, body weights ranged from 305 to 416 g (mean ± SE = 360.21 ± 9.23 g). Ages ranged from 64 to 106 days old (mean ± SE = 82.89 ± 3.36 days old). Rats were randomly assigned to one of two groups: ADS group and Control group. Each group

underwent the same surgical procedures and behavioral analysis described below. Seven rats were removed from the study due to complications during surgical procedures (SCI surgery, n = 3; implant surgery, n = 4) while one rat was removed after refusing to perform the behavioral tasks (n = 1), resulting in a total of six rats in the ADS group (n = 6) and six rats in the Control group (n = 6). This study was performed in accordance with all standards in *Guide for the Care and Use of Laboratory Animals* (Institute for Laboratory Animal Research, National Research Council, Washington, DC: National Academy Press, 1996). The protocol was approved by the University of Kansas Medical Center Institutional Animal Care and Use Committee.

Experimental Timeline

The experimental timeline is displayed in Figure 5.2. All behavioral tests were conducted once a week to evaluate motor performance in each rat pre-SCI (i.e., baseline), for 4 weeks post-SCI (i.e., prior to electrode and device implantation), and 4 weeks post-conditioning (i.e., after each week of ADS conditioning). Rats were acclimated to each behavioral task before baseline recordings were conducted. Baseline behavioral tests were conducted 1-3 days prior to SCI surgery. During ADS sessions, behavioral tests were always performed after each week of ADS therapy.

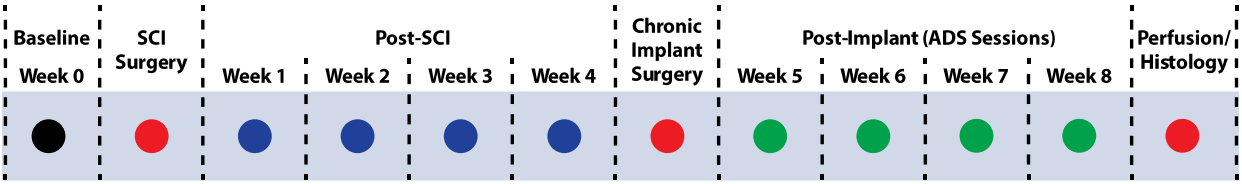

Figure 5.2. Experimental timeline of the study. Behavior tests were conducted before (i.e., baseline) SCI and once per week after each surgery for the duration of the study. ADS sessions occurred during weeks 5-8 (green dots) for 4 hours/day and 4 days/week. The behavior tests during weeks 5-8 were conducted at the end of the week after each week of ADS therapy.

General Surgical Procedures

The SCI surgery was performed after baseline recordings and the chronic implant surgery was performed at 4 weeks post-SCI. Both procedures followed the same general protocol. After an initial stable anesthetic state using isoflurane anesthesia was established and scalp and back shaved, isoflurane was withdrawn, and an initial dose of ketamine hydrochloride (100 mg /kg IP)/xylazine (5 mg /kg IP) was administered. The anesthetic state was maintained with subsequent doses of ketamine (10 mg IP or IM) and monitored via pinch and corneal responses. Additional doses of ketamine were administered if the rat reacted to a pinch of the forepaw/hindpaw, blinked after lightly touching the cornea, or exhibited increased respiration rate. At the conclusion of the surgery, 0.25% bupivacaine HCl was applied locally to the skin incision site. Buprenex (0.01 mg/kg, S.C.) was injected immediately after surgery and 1 day later. All animals were monitored daily until the end of the experiment. Before and after surgery, rats received a S.C. injection of 30,000 U of penicillin (Combi-Pen 48). Additionally, starting the first day after surgery, daily penicillin injections were given in 5 mL saline throughout the first week to prevent infections and dehydration. Bladders were expressed twice daily until animals recovered urinary reflexes. From the second week onward, animals were supplemented with vitamin C pellets (BioServ, Frenchtown, NJ) to avert urinary tract infection.

Spinal Cord Contusion

Spinal cord contusion procedures followed those described in previous experiments (Krizsan-Agbas, Winter et al. 2014, Borrell, Krizsan-Agbas et al. 2018, Frost, Borrell et al. 2018). Animals underwent a T8 laminectomy and 175 kDyn moderate impact contusion injury using an Infinite Horizon spinal cord impactor (Precision Systems and Instrumentation, LLC, Fairfax Station, VA). Displacement distance reported by the impactor software for each contusion was recorded at the time of surgery and was used as an initial quantitative marker for successful impact. Surgical procedure and rat care followed standard protocol.

Chronic Electrode Implantation

Rats were placed in a Kopf small-animal stereotaxic frame (David Kopf Instruments®, Tujunga, CA) and the incisor bar was adjusted until the heights of lambda and bregma were equal (flat skull position). The cisterna magna was punctured at the base of the skull to reduce edema during mapping and implantation. Before the craniectomy, 5 titanium screws were placed at various positions on the skull as shown in Figure 5.3: 1) Right frontal bone, rostral to bregma, and rostral to the coronal suture; 2) Right parietal bone, caudal to bregma but rostral to lambda, and just caudal to the coronal suture; 3) Right parietal bone, rostral to lambda but caudal to bregma, and just rostral to the lambdoid suture; 4) Right occipital bone, caudal to lambda, and caudal to the lambdoid suture; 5) Left occipital bone, caudal to lambda, and caudal to the lambdoid suture. These screws served as an anchor for the eventual head cap made of dental acrylic that encased the chronic recording and stimulating electrodes on the skull.

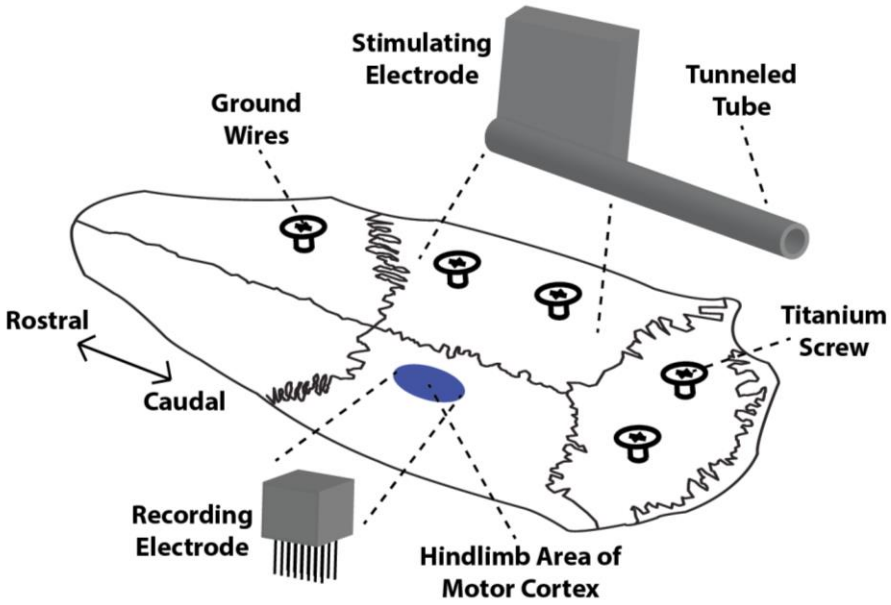

Figure 5.3. Placement of hardware and chronic electrodes on the skull of each rat. Dental acrylic was used to build a protective cap and anchor the electrodes to the skull via the five titanium screws. The recording electrode was implanted in the left hindlimb motor cortex. The headstage for the stimulating electrode was mounted on the right side of the skull while the microwires were tunneled via a tunneling tube to the lumbar spinal cord. The ground wires for both electrodes were wrapped around the front screw.

A craniectomy was performed over the hindlimb motor cortex in the left hemisphere. The general location of the craniectomy was based on previous motor mapping studies in the

rat (Frost, Iliakova et al. 2013, Frost, Dunham et al. 2015). After the dura over the cranial opening was incised, a small motor map was created using intracranial microstimulation (ICMS) to identify the hip area of the hindlimb motor cortex, which is bordered laterally by the trunk area and caudally by the forelimb area of the motor cortex (Figure 5.4 Left). ICMS mapping techniques were similar to those used in previous experiments (Frost, Iliakova et al. 2013, Frost, Dunham et al. 2015) (Site Aim 1 and 2 paper).

Hindlimb area (HLA) spikes (i.e., action potentials) were recorded with a chronic microwire array from TDT (Tucker-Davis Technologies, Alachua, FL). The recording electrode was a 16-channel (2 x 6 array) probe with wire diameter of 33 µm, wire length of 2 mm, wire spacing of 175 µm, row spacing of 500 µm, and tip angle of 60 degrees. Electrode depth was controlled using a Kopf hydraulic Microdrive (Kopf Instruments, Tujunga, CA) and was lowered to a depth of ~1700 µm (i.e., Layer V of the cortex). Kwik-Cast (World Precision Instruments Inc, Sarasota, FL), a silicone elastomer, was applied directly to the cortex around the inserted wires of the recording electrode to act as a sealant. The ground wire of the recording electrode was wrapped around the front rostral screw to ground the electrode.

A laminectomy was performed on the T13 vertebrae similar to previous studies (Borrell, Krizsan-Agbas et al. 2018, Frost, Borrell et al. 2018). The dura mater was not opened due to the very small subdural space in rats and to minimize cerebral spinal fluid leakage. A custom-made fine-wire stimulating electrode was fabricated as described by Bamford, *et. al.* (Bamford, Marc Lebel et al. 2017). Microwires were fabricated from 30-µm-diameter platinum/iridium (80%/20%) wire insulated with a 4 µm layer of polyimide (California Fine Wire, Grover Beach, CA). At least 4 microwires were soldered onto a custom-made electrode interface board which was soldered to an 18-pin male nano dual row Omnetics connector with guide post holes (Omnetics Connector Corporation, Minneapolis, MN). The interface board was encapsulated in UV-cured glue to ensure stability and electrical isolation of each wire. The ground wire was wrapped around the same screw as the ground wire from the recording electrode. The

microwires, not including the ground wire, were routed into a 1-mm diameter polyethylene tube (A-M Systems, Inc., Sequim, WA) to protect the wire from damage during implantation. Microwire tips were de-insulated by mechanically rubbing the polyimide layer between two glass slides. A length of 1 mm polyimide was initially removed, and the tips were sharpened by cutting at an ~45^0 angle leaving 30—60 µm of exposed metal from the tip. The wires were then gently bent to a 90^0 angle with a length of ~2.27 mm from tip to bend.

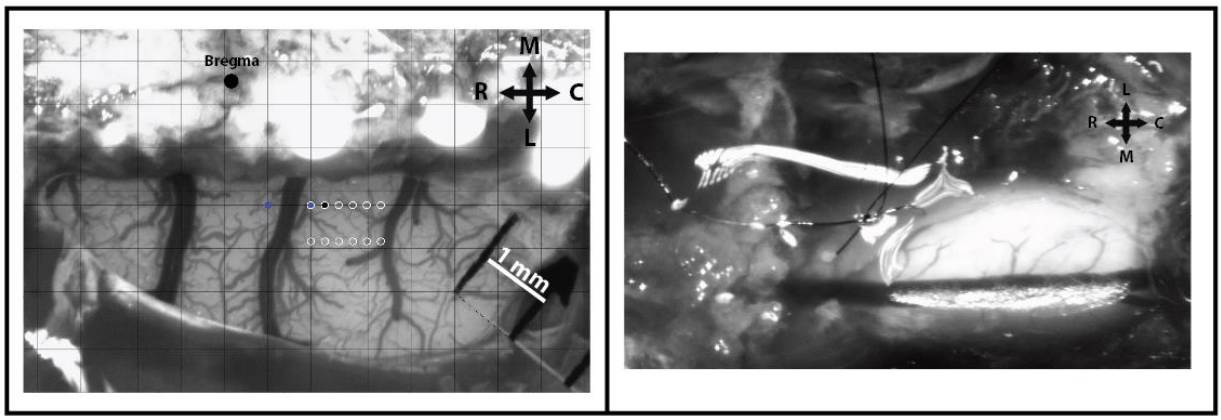

Figure 5.4. Overview of chronic electrode implantation. Left: Cranial opening over hindlimb motor cortex with superimposed grid for ICMS mapping. The bigger black dot represents Bregma; small blue dots represent ICMS-evoked forelimb movement; smaller black dot represents a no-response movement during ICMS; white outlined dots represent placement of chronic microarray. **Right:** Spinal cord opening over hindlimb spinal cord. The microwire was inserted into the spinal cord and sutured to the dura mater.

The microwire implantation procedure in the hindlimb spinal cord followed the procedure developed by Bamford, *et. al.* (Bamford, Marc Lebel et al. 2017). The microwire implant was sterilized using ethylene oxide (EtO) gas. The Omnetics connector (i.e., headpiece) of the microwire implant was positioned on the right hemisphere of the skull next to the recording electrode (Figure 5.3). The polyethylene tube and microwires were tunneled subcutaneously to the hindlimb spinal cord. Dental acrylic was used to anchor the recording and stimulating electrodes to the skull and screws. Once the acrylic was dry, the polyethylene tube of microwires was sutured to the T12 vertebral process with a 6-0 prolene, blue monofilament, taper point, C-1 (13 mm 3/8c), Ethicon suture and fixed further with a small amount of surgical glue (3M Vetbond Tissue Adhesive, St. Paul, MN) being careful to glue the polyethylene tube

directly to the bone and not the surrounding tissue. Additional dental acrylic was used if the suture and glue did not create a stable anchor. For this chronic ADS study, only one paired site between cortex and spinal cord was used. The paired site was a stimulation site that evoked any type of hip movement. The rostro-caudal placement of the microwire in the hindlimb spinal cord was directed by previously derived ISMS-evoked movement maps (Borrell, Frost et al. 2017). The medio-lateral placement of the microwire was 0.8—1.0 mm from the central blood vessel on the right side of the cord. Before microwire insertion, a small hole was made in the dura mater using the tip of a 30-gauge hypodermic needle. Microwire insertion began by gently holding the wire with fine forceps near the tip. When the tip penetrates the superficial dorsal layers of the cord, the remaining portion of the wire was inserted vertically until the 90^0 bend (~2.27 mm of wire which reaches the ventral horn of the rat hindlimb spinal cord). The inserted microwire can be seen in Figure 5.4 Right.

A small current (one biphasic pulse with 0.2 ms square-wave duration delivered at 300 Hz every 1 second) was used to test the evoked movement. The current was increased until movement threshold was met, and the current intensity was recorded. If the ISMS-evoked movement was not a hip movement, the wire was removed and reinserted in another rostro-caudal location avoiding major blood vessels. Every additional insertion of the microwire increases the risk of tissue damage; therefore, the number of reinsertions was limited to a maximum of three for any given location. If the maximum of reinsertions was reached, the microwire was left in the current location of the cord, and the rat was deemed a control rat (i.e., same injury, surgical procedures, chronic implants, and behavioral recordings with no stimulation therapy). The microwires laid flat on the epidural surface of the spinal cord and were sutured (8-0 nylon, black monofilament, taper point, BV130-5, 6.5 mm 3/8c, Ethilon suture) directly to the dura mater. Typically, the 8-0 suture was driven through the dura mater before microwire implantation to avoid pulling the microwire out of the spinal cord. A discreet drop of surgical glue was applied to the point of insertion and Kwik-Sil (World Precision Instruments Inc,

Sarasota, FL) was used to adhere the wire to the epidural surface and to act as a sealant. A layer of thin plastic film made of low polyethylene, cold sterilized in 100% Ethyl Alcohol and allowed to dry, was measured to the size of the exposed laminectomy and used to cover the implanted region of the spinal cord. The film was affixed to the vertebral edges of the opening with small drops of surgical glue in order to prevent the invasion of connective tissue into the laminectomy site during recovery. Muscle layers were then sutured over the opening before suturing the skin incision closed. The skin around the headpieces on the skull was pulled tight around the acrylic cap and sutured to create a snug fit. The rats were allowed to recover for a few days before the beginning of ADS therapy to avoid dislodging of the microwire implants.

ADS Paradigm

During ADS therapy, electrode leads/connectors of the headpieces were tethered to the TDT neurophysiolocal recording and stimulation system (Tucker-Davis Technologies, Alachua, FL). Rats were placed in a 30-cm x 30-cm x 52-cm Plexiglas chamber during each ADS session. Before each ADS session, a test stimulus was applied to measure movement threshold. A custom-made code was created using the TDT system to administer ADS. Individual spikes were detected, discriminated, and sorted in real time using principal component analysis. A consistent spiking profile was chosen from the site in the hindlimb motor cortex and used to trigger stimulation in the paired site in the ventral horn of the hindlimb spinal cord. The stimuli consisted of one, 200 μs biphasic cathodal leading pulse delivered at 300 Hz from an electrically isolated, charge-balanced (capacitively coupled) stimulation circuit. Stimulation amplitude was set at 50% movement threshold determined during the implantation surgery so that ISMS does not interfere with the rat's motor performance or induce muscle fatigue. A time delay of 10 ms between recorded spike and triggered stimuli was chosen from the conduction time results after SCI (Frost, Borrell et al. 2018) and acute ADS results (Borrell, Krizsan-Agbas et al. 2018) from previous experiments. Each ADS session occurred for 4 hours/day, 4 days/week, for 4 weeks (Figure 5.2).

BBB Behavioral Assessment

The Basso, Beattie, and Bresnahan (BBB) locomotor rating scale was used as a sensitive measure of locomotor ability after SCI (Basso, Beattie et al. 1995). Briefly, rats ran along a straight alley with the home cage and bedding at the end to encourage the rats to transverse the open field. Scores were recorded for the left and right sides of each animal. If SCI rats did not exhibit a deficit post-injury or did not have a BBB score between 13—15 at 4-weeks post-SCI, they were removed from the study.

OptiTrack Recording

Hindlimb kinematics were recorded using a high-speed OptiTrack motion capture system (NaturalPoint, Inc., Corvallis, OR), combining six Flex 3 cameras (100 Hz; three cameras per hindlimb). Rats traversed an open field (Figure 5.5 Top) for approximately 6 recordings. A total of 12 reflective markers (6 markers per hindlimb) were attached bilaterally overlying anatomical landmarks of the hindlimbs (Figure 5.5, Bottom). Markers were placed on the iliac crest, greater trochanter (hip), lateral femoral epicondyle (knee), lateral malleolus (ankle), fifth metatarsophalangeal joint (mtp), and digit end of the fourth digit (digit). The 3D position of the markers was reconstructed offline using Motive Optical motion capture software. Joint angles and kinematic analysis were calculated via custom-written code in Matlab (The Mathworks, Inc., Natick, MA). A minimum of 10 step cycles was extracted for each hindlimb during this task.

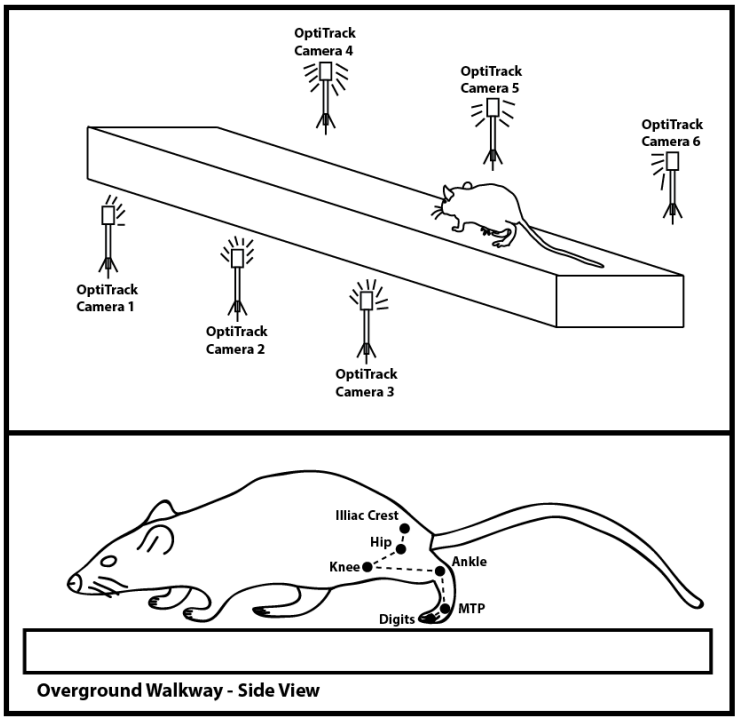

Figure 5.5. Set-up of the OptiTrack. Top: The OptiTrack cameras capture the markers at the hindlimb joints as the rat transverses an open field. **Bottom:** Reflective markers are placed on the iliac crest, hip joint, knee joint, ankle joint, fifth metatarsal joint, and fourth digit on both hindlimbs.

DigiGait Recording

Gait analysis was performed with the Mouse Specifics DigiGait System (Mouse Specifics, Inc., Quincy, MA). Computerized digital footprint images were generated by high-speed video recording from the ventral aspect of the animal (Figure 5.6). Rats were habituated to the DigiGait apparatus for 1 week before SCI. Baseline recordings were collected 1-3 days before SCI and repeated once a week for up to 4 weeks post-SCI. A predetermined speed of 11 cm/sec was used and remained consistent throughout the experiment. All gait dynamic indices, over 40 metrics, were calculated with version 12.1 of the Mouse Specifics analysis software. Specifically, paw angle is the angle that the paw makes with the long axis of the direction of motion of the animal. Propel duration is the moment of peak stance through full lifting off the belt. Swing duration is the amount of time the paw is not in contact with the belt. Stance duration is the amount of time the paw is in contact with the belt. Stride length is the

spatial length that a paw traverses through a given stride. Paw area is the maximal area of the paw seen by the camera at the time corresponding to peak stance. Paw overlap distance is the overlap extent of ipsilateral fore and hind paws. These gait parameters will quantify a deficit and possible recover during specific phases of the gait cycle. These types of parameters have been similarly used by other investigators for this purpose (Krizsan-Agbas, Winter et al. 2014).

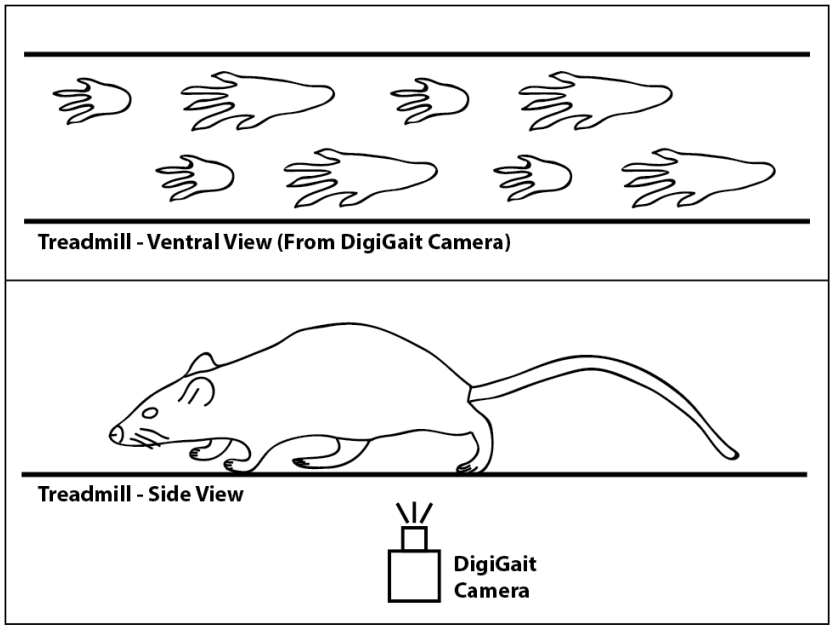

Figure 5.6. Set-up of the DigiGait. The DigiGait camera captures the paw placement from a ventral orientation. Gait analysis of foot placement is performed offline using DigiGait analysis software.

Horizontal Ladder Rung Walking Test

To quantify skilled locomotor movements, rats were trained on the horizontal ladder rung walking test apparatus (Otto Environmental, Greenfield WI) displayed in Figure 5.7. The horizontal ladder consisted of side walls made of clear Plexiglass and a metal rung (3 mm diameter) walkway. The metal rungs could be inserted to create a floor with a minimum distance of 1 cm between the rungs. The side walls were 1 m long and 19 cm high measured from the height of the rungs, while the width of the alley was adjusted to 1 cm wider than the rat to prevent the animal from turning around. The ladder was elevated well above the ground with two refuges at the end. The starting refuge was an open container, and the ending refuge was

a covered home cage. Two patterns were used during this experiment to prevent the rats from learning the pattern and to modify the difficulty of the task (Metz and Whishaw 2002). Pattern A consisted of a regular pattern with the rungs spaced at 2 cm intervals, while Pattern B consisted of an irregular pattern with the rungs spaced between 1 and 3 cm. All rats were recorded crossing the horizontal ladder five times per session for each pattern.

Rats were recorded traversing the horizontal ladder using a Sony digital camera. The camera was positioned at a slight ventral angle so that both right and left paw positions could be recorded simultaneously. The video recordings were scored using frame-by-frame analysis at 30 frames/sec and scored and analyzed using procedures previously described (Metz and Whishaw 2002). Only consecutive steps of each hindlimb were analyzed, so if the rat stops the last step before the stop and the first step after the stop were not scored. The last stepping cycle performed at the end of the ladder was not included in the scoring. The types of foot and paw placement on the rungs were rated using a 7-category scale. (0) Total miss: 0 points were given when the limb completely missed the rung and a fall occurred. (1) Deep slip: 1 point was given when the limb was placed on the rung and then slipped off when weight-bearing which caused a fall. (2) Slight slip: 2 points were given when the limb was placed on a rung, slipped off when weight bearing, but did not result in a fall and interrupt the walking. (3) Replacement: 3 points were given when the limb was paced on a rung, but before it was weight bearing it was quickly lifted and placed on another rung. (4) Correction: 4 points were given when the limb aimed for one rung but was then placed on another rung without touching the first one. (5) Partial placement: 5 points were given when the limb was placed on the rung with either heel or digits of a hindlimb. (6) Correct placement: 6 points were given when the midportion of the palm of the limb was place do a rung with full weight support. If different errors occurred at the same time, the lowest of the scores was recorded. Error rate in stepping was recorded as a percentage of the number of misplaced steps divided by the total number of steps on the ladder

[100 X (steps with error/total steps taken)]. Steps with error corresponded to values of 0 – 3 in the foot fault scoring system.

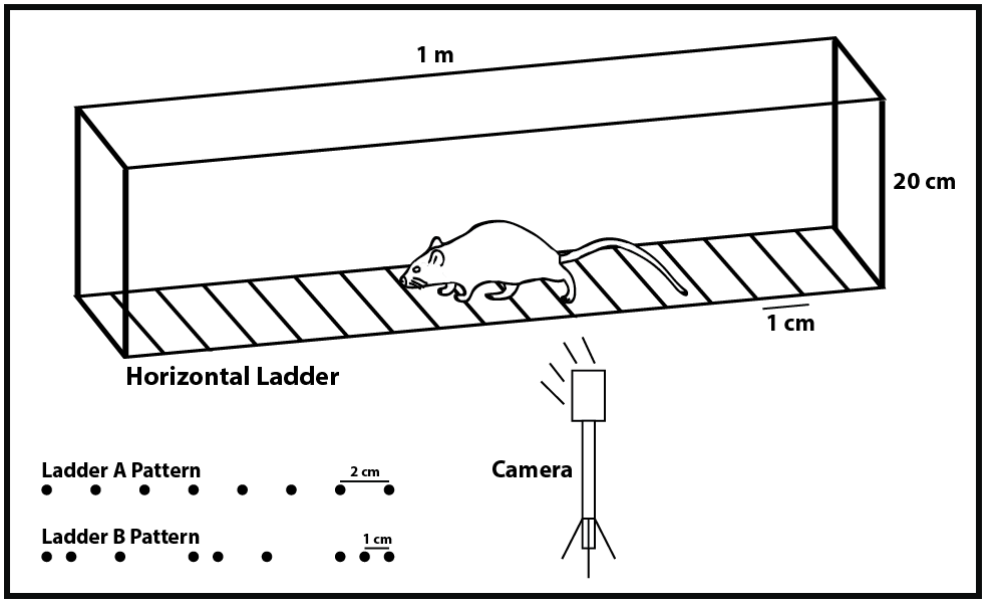

Figure 5.7. Set-up of the Horizontal Ladder Rung Apparatus. The camera captures the foot-faults of the paws as the rat transverses the horizontal ladder. The horizontal ladder is a sensitive test to show corticospinal tract connectivity.

Tapered/Ledged Beam Test

To assess deficits in balance and fine motor control, rats were trained on the tapered/ledged beam test displayed in Figure 5.8. The beam-walking apparatus consisted of a tapered beam with underhanging ledges (2 cm wide) on each side to permit foot faults without falling. The end of the beam was connected to a darkened safe (goal) box (20.5 cm x 25 cm x 25 cm). Rats had to cross the elevated tapered beam over 60 cm in length. The width of the beam began at 6.0 cm and narrowed to a width of 1.5 cm at the end. The rats were videotaped with a camera, and steps for each hindlimb were scored as a full slip or a half-slip if the limb touched the side of the beam. The slip ratio of each hindlimb (number of slips/number of total steps) was later calculated and averaged over three trials. Control/uninjured rats typically have no difficulties crossing the beam in its entire length, whereas SCI rats tend to step down onto

the fixed ledge underneath. Steps onto the ledge were scored as described by Schallert *et. al.* (Shallert, Woodlee et al. 2002).

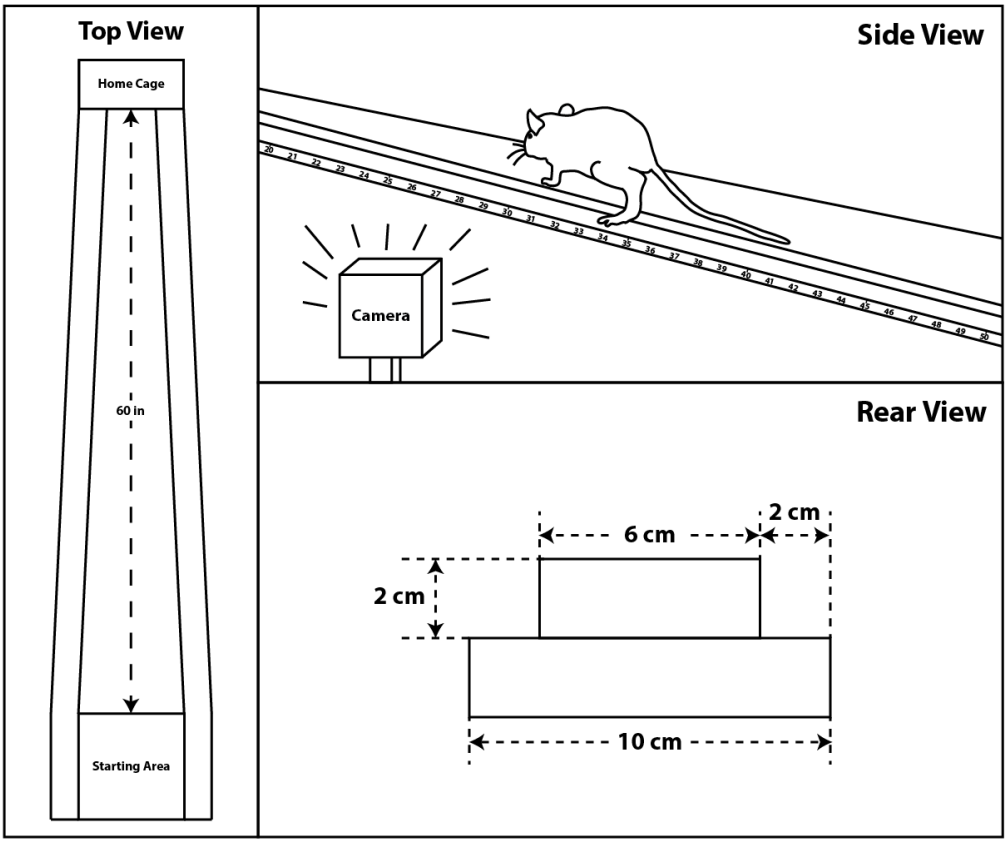

Figure 5.8. Set-up of the Tapered/Ledged Beam Test. Foot-fault scores were recorded for each slip of both hindlimbs as the rat transverse the narrowing beam.

Perfusion & Histology

At the conclusion of the study (after Week 8), rats were euthanized with an intraperitoneal injection of beuthanasia (100 mg/kg), then transcardially perfused with fixative (4% paraformaldehyde in 0.1 M PBS) and the spinal cord removed. The spinal cord was transversely sectioned at 30 µm on a cryostat and sections stained with cresyl violet for histological verification of the lesion and microwire placement.

Statistical Analysis

Statistical analyses of motor performance measures were conducted using JMP 11 software (SAS Institute Inc., Cary, NC). A 2x2 repeated measures analysis of variance

(ANOVA) was used to show a significant effect of ADS therapy over time on the various behavioral tasks. If a significant effect was obtained ($p < 0.05$), between-group and within-group post-hoc comparisons were further conducted at several time points using Fisher's Least Significant Difference (Fisher's LSD) and the student's t-test. Data are presented as average ± standard error of the mean unless otherwise stated.

Results

SCI and Microwire Implant Verification

All rats received a 175 kDyn impact at the level of the T8 vertebrae. The average displacement value of the impactor was 1082.83 ± 23.80 µm (mean ± SE) for all rats. Separately, the average displacement value was 1069.67 ± 31.38 µm for the ADS group and 1096.00 ± 37.92 µm for the Control group. An exemplar transverse histological section through the center of the injury and microwire tract are shown in Figure 5.9. After SCI, the spinal grey matter at the epicenter was severely damaged. The ventral (location of the ventral CST and RtST) and some dorsolateral (location of the RbST and dorsolateral CST) spinal cord white matter tracts appear to remain intact while the dorsal column white matter tracts (location of the dorsomedial CST) appears to be severely damaged (Figure 5.9A). After microwire implantation, the microwire creates a small dorsoventral tract which helps verify the location of the microwire (Figure 5.9B).

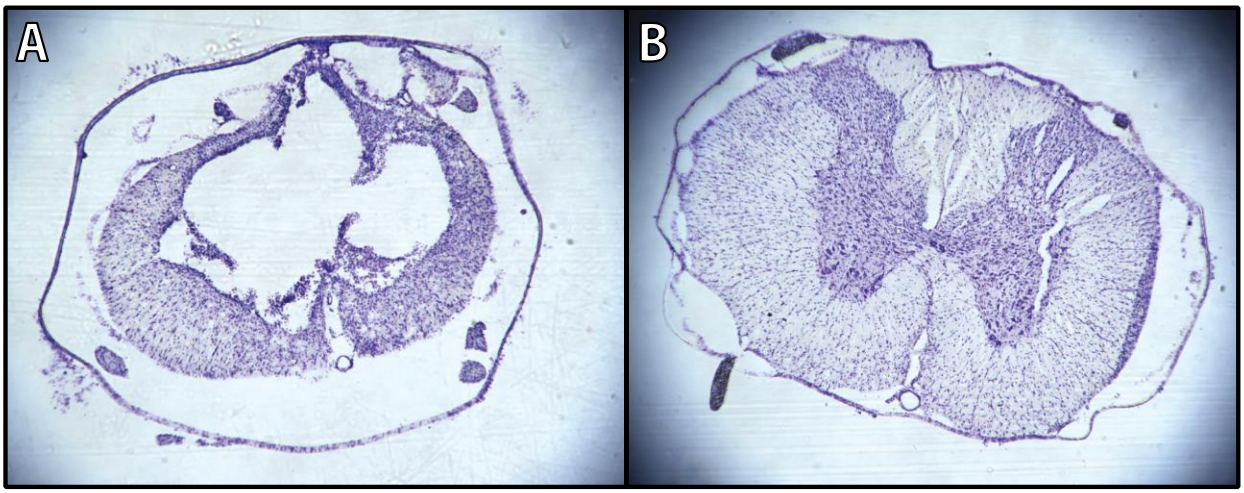

Figure 5.9. Verification of spinal cord injury and microwire implantation. A) Representative image of spinal cord injury epicenter under T8 vertebrae stained with cresyl violet 8 weeks after injury. **B)** Representative image of microwire implant under T13 vertebrae stained with cresyl violet 4 weeks after implantation.

HLA Microarray Impedances

The microarray impedances were recorded pre- and each week post-implant and are displayed in Table 5.1. In the control group, the impedances of all 16 recording channels of the cortical microarray significantly increased after the 1st week post-implantation (Week 5, $p < 0.0001$), returned to pre-implant measures after 2 weeks post-implant ($p = 0.8339$), and significantly increased after 3 and 4 weeks post-implant (Weeks 7 and 8, $p < 0.0001$). In the ADS group (within-group comparisons), the microarray impedances were significantly increased when compared to pre-implant measures after all 4 weeks post-implant (Week 5, $p < 0.0001$; Week 6, $p = 0.0002$; Weeks 7 and 8, $p < 0.0001$). This significant increase in microarray impedances was similarly seen when grouping the control and ADS groups together (Combined) and comparing pre-implant measures to each week post-implant (Weeks 5—8, $p < 0.0001$).

Table 5.1. Average microarray impedances (mean ± SE) pre-implant and after each week post-implant. * = Significant increase when compared to pre-implant recordings (within-group comparison of the respective week; $p < 0.05$).

HLA Microarray Impedances (kOhms)					
Rat Group	**Pre-Implant**	**Week 5**	**Week 6**	**Week 7**	**Week 8**
Control	31.7 ± 3.6	68.4 ± 5.4*	33.9 ± 1.3	67.2 ± 2.9*	70.3 ± 3.4*
ADS	41.3 ± 3.4	73.6 ± 4.8*	66.8 ± 4.8*	73.7 ± 7.6*	69.2 ± 6.1*
Combined	36.5 ± 2.5	71.6 ± 3.6*	58.6 ± 4.0*	70.9 ± 4.5*	69.7 ± 3.5*

HLA Spiking Frequency During ADS

For the ADS rats, the average spike frequency for each hour of ADS regardless of day and week was as follows: Hour 1 is 8.67 ± 0.55 spikes/sec, Hour 2 is 8.17 ± 0.72 spikes/sec, Hour 3 is 8.01 ± 0.54 spikes/sec, and Hour 4 is 8.34 ± 0.53 spikes/sec. When compared to Hour 1, there was no significant change in spike frequency (Hour 2, $p = 0.5537$; Hour 3, $p = 0.4388$; Hour 4, $p = 0.7032$) over the 4-hour ADS sessions.

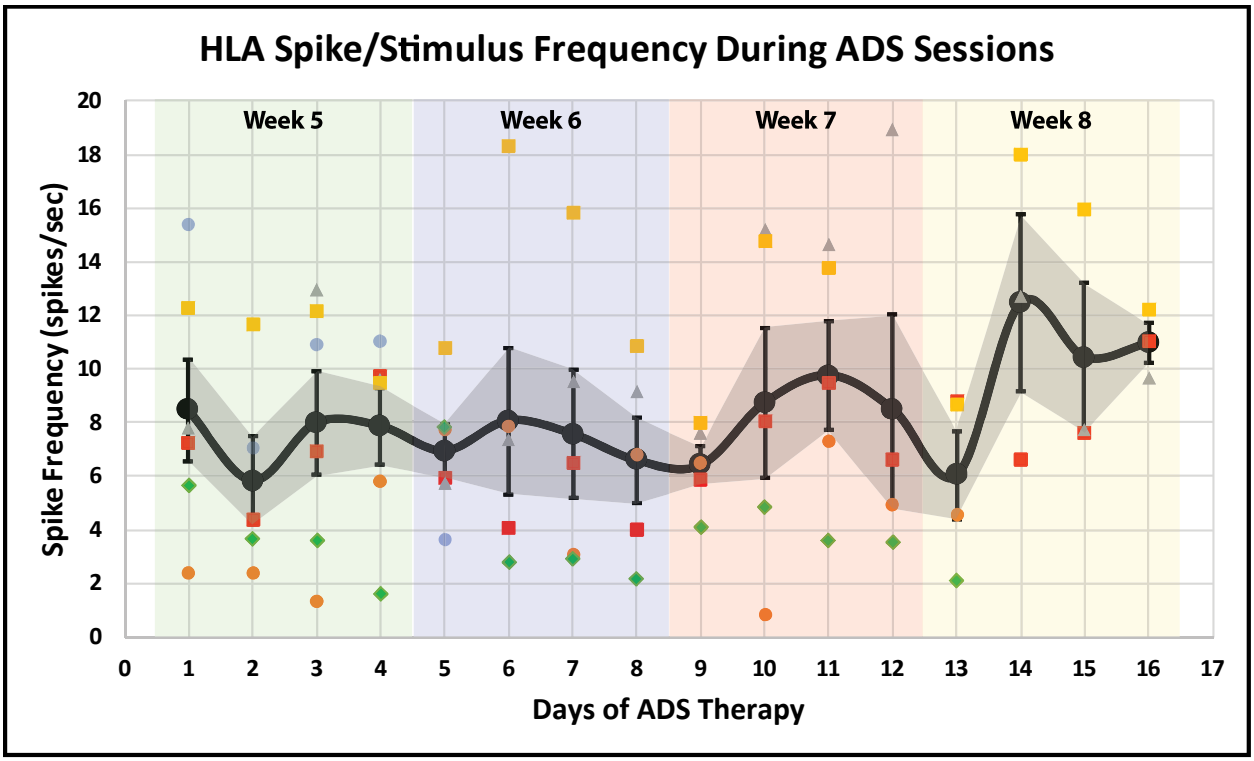

Figure 5.10. Average HLA spike/stimulus frequency (mean ± SE) during each day of ADS for the ADS rat group. The average is shown in black with error bars and grey shading representing standard error of the mean. Diamonds, squares, and circles of various colors represent individual animal data points.

The recorded spike frequencies were further calculated for each day of ADS (Figure 5.10). When comparing each day of ADS, the average spike frequencies were non-statistically different ($p > 0.05$). In the second week of ADS (Week 6), there is a general qualitative trend of increasing spiking frequency after the second day of ADS that tends to decrease by the fourth day of ADS for the week. After four weeks of ADS (Week 8), the HLA spike frequency tends to remain increased but not at a statistically significant level.

ISMS Current During ADS

The minimum current needed to evoke movement (i.e., movement threshold) via the implanted microwire in the hindlimb spinal cord was recorded directly after the implantation surgery and after each week of ADS. After the implantation surgery, the average current for both groups recorded at movement threshold was 36.0 ± 7.3 µA (mean ± SE). The average

current recorded at movement threshold immediately after the implantation surgery was 24.0 ± 4.3 μA for the ADS group and 55.5 ± 15.6 μA for the Control group. After each week of ADS, we were unable to evoke a movement via the implanted microwire in the hindlimb spinal cord. As a result, the threshold used during ADS for each rat in the ADS group was equal to the minimum current needed to evoke movement after the implantation surgery of each rat.

ISMS Microwire Impedances During ADS

The microwire impedances were recorded pre- and each week post-implant and are displayed in Table 5.2. When compared to pre-implant measures (Pre-Implant; within-group comparisons) from the control group, the microwire impedances were non-statistically different after each week post-implantation (Week 5, $p = 0.4238$; Week 6, $p = 0.2636$; Week 7, $p = 0.3595$; Week 8, $p = 0.3958$). When compared to pre-implant measures (Pre-Implant; within-group comparisons) from the ADS group, the microwire impedances were non-statistically different after each week post-implantation (Week 5, $p = 0.9617$; Week 6, $p = 0.4716$; Weeks 7, $p = 0.6561$; Week 8, $p = 0.3399$). Similarly, when combining rat groups, the microwire impedances were non-statistically different when compared to pre-implant measures after 4 weeks post-implant (Week 5, $p = 0.5529$; Week 6, $p = 0.1748$; Weeks 7, $p = 0.3174$; Week 8, $p = 0.1698$).

Table 5.2. Average spinal cord microwire impedances (mean ± SE) pre-implant and after each week post-implant.

Spinal Cord Microwire Impedances (kOhms; Mean ± SE)					
Rat Group	**Pre-Implant**	**Week 5**	**Week 6**	**Week 7**	**Week 8**
Control	39.0 ± 18.5	45.5 ± 19.9	48.6 ± 31.0	65.1 ± 8.5	63.2 ± 7.0
ADS	50.4 ± 8.3	51.4 ± 12.2	66.8 ± 23.2	59.7 ± 8.5	72.2 ± 27.0
Combined	46.1 ± 8.1	54.5 ± 9.8	70.0 ± 11.8	61.5 ± 9.0	68.6 ± 11.9

BBB Scores

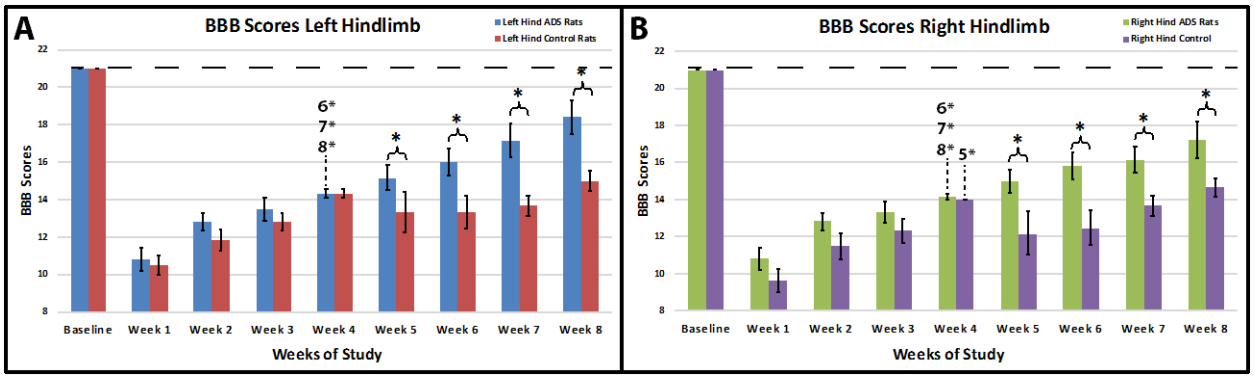

Figure 5.11. Average BBB scores (mean ± SE) in ADS and Control rats. A) Average BBB scores of the left hindlimb in ADS and Control rats. **B)** Average BBB scores of the right hindlimb in ADS and Control rats. Error bars are ± SE. ***** = Significant difference between groups (between-group comparison of the respected week; $p < 0.05$). **5*, 6*, 7*, 8*** = Significant increase when compared to Week 4 (pre-implant) measures (within-group comparison of the respective week; $p < 0.05$).

For the left hindlimb (Figure 5.11A), BBB scores were significantly higher in the ADS group as compared to the Control group after all 4 weeks of ADS (Week 5, $p = 0.0146$; Week 6, $p = 0.0005$; Week 7, $p < 0.0001$; Week 8, $p < 0.0001$). In the ADS group (within-group comparisons), BBB scores became significantly higher than pre-implant scores (Week 4) after 2 weeks of ADS (Week 6, $p = 0.0259$) and remained significantly higher than pre-implant scores after 3 weeks of ADS (Week 7, $p = 0.0002$) and 4 weeks of ADS (Week 8, $p < 0.0001$). The BBB scores of the left hindlimb in the ADS group remained significantly lower ($p < 0.05$) than baseline scores after each week of ADS (i.e., did not return to baseline measures). In the Control Group (within-group comparisons), BBB scores did not significantly change ($p > 0.05$) after 4 weeks post-implant (Week 5, $p = 0.1768$; Week 6, $p = 0.1768$; Week 7, $p = 0.3664$; Week 8, $p = 0.3664$) as compared to pre-implant measures (Week 4). The BBB scores of the left hindlimb in the Control group remained significantly lower ($p < 0.05$) than baseline scores for up to 4 weeks after electrode implantation (Weeks 5, 6, 7, and 8; $p < 0.0001$).

For the right hindlimb (Figure 5.11B), BBB scores were significantly higher in the ADS group compared to the Control group after 4 weeks of ADS (Week 5, $p = 0.0004$; Week 6, $p < 0.0001$; Week 7, $p = 0.0016$; Week 8, $p = 0.0016$). In the ADS group (within-group

comparisons), BBB scores became significantly higher than pre-implant scores (Week 4) after 2 weeks of ADS (Week 6, p = 0.0326) and remained significantly higher than pre-implant scores (Week 4) after 3 weeks of ADS (Week 7, p = 0.0108) and 4 weeks of ADS (Week 8, p = 0.0007). The BBB scores of the right hindlimb in the ADS group remained significantly lower (p < 0.05) than baseline scores after each week of ADS (i.e., did not return to baseline measures). In the Control group (within-group comparisons), BBB scores became significantly lower than pre-implant scores (Week 4) after 1 week (Week 5, p = 0.0191) but increased to a non-significant level after 2 weeks (Week 6, p = 0.0537) and remained unchanged after 3 weeks (Week 7, p = 0.6646) and 4 weeks (Week 8, p = 0.3868). The BBB scores of the right hindlimb in the Control group remained significantly lower (p < 0.05) than baseline scores for up to 4 weeks post-implant (Weeks 5, 6, 7, and 8; p < 0.0001).

OptiTrack Results

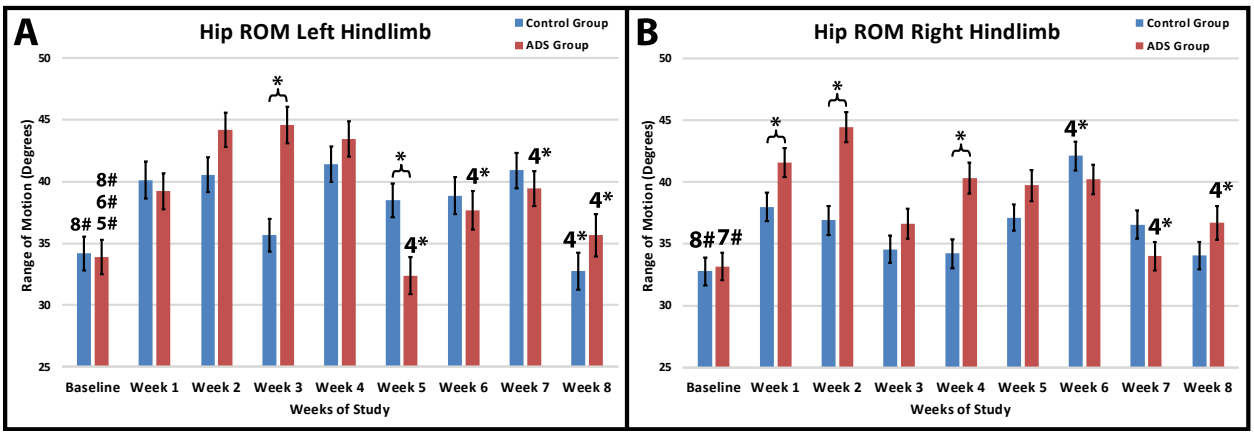

Figure 5.12. Average range of motion of the left (A) and right (B) hip joint (mean ± SE) in ADS and Control rats. Error bars are ± SE. ***** = Significant difference between groups when comparing groups (between-group comparison of the respected week; p < 0.05). **4*** = Significant difference when compared to Week 4 (pre-implant) measures (within-group comparison of the respective week; p < 0.05). ***5*#, 6#, 7#, 8#** = p > 0.05 when comparing (within-group comparison) baseline to the respective week number.

For the left hindlimb (Figure 5.12A), the range of motion of the hip joint was significantly different in the ADS group as compared to the Control group after 3 weeks post-injury (Week 3, p < 0.0001) and after 1 week of ADS (Week 5, p = 0.0024). In the ADS group (within-group comparisons), the hip range of motion was significantly decreased when compared to pre-

implant measures (Week 4) after 1 week of ADS (Week 5, $p < 0.0001$) and remained significantly decreased after 2 weeks (Week 6, $p = 0.0069$), 3 weeks (Week 7, $p = 0.0453$), and 4 weeks (Week 8, $p = 0.0005$) of ADS. The hip range of motion of the left hindlimb in the ADS group was not significantly different ($p > 0.05$) than baseline measures after 1 week of ADS (Week 5, $p = 0.4554$) and remained so after 2 weeks (Week 6, $p = 0.0707$) and 4 weeks (Week 8, $p = 0.4238$) of ADS; however, the hip range of motion was significantly increased after 3 weeks (Week 7, $p = 0.0050$) of ADS when compared to baseline. In the Control group (within-group comparisons), the hip range of motion was not significantly different when compared to pre-implant measures (Week 4) after the first 3 weeks post-implant (Week 5, $p = 0.1339$; Week 6, $p = 0.2206$; Week 7, $p = 0.8002$) but was significantly decreased after 4 weeks (Week 8; $p < 0.0001$) post-implant. The hip range of motion of the left hindlimb in the Control group remained significantly higher ($p < 0.05$) than baseline scores for the first 3 weeks post-implant (Weeks 5, $p = 0.0237$; Week 6, $p = 0.0191$; Week 7, $p = 0.0006$) and was not significantly different after 4 weeks post-implant (Week 8, $p = 0.4783$).

For the right hindlimb (Figure 5.12B), the range of motion of the hip joint was significantly different in the ADS group as compared to the Control group after the first 2 weeks post-injury (Week 1, $p = 0.0280$; Week 2, $p < 0.0001$) and after 4 weeks post-injury (Week 4, $p = 0.0004$). In the ADS group (within-group comparisons), the hip range of motion was significantly decreased when compared to pre-implant measures (Week 4) after 3 weeks (Week 7, $p = 0.0002$) and remained significantly decreased after 4 weeks (Week 8, $p = 0.05$) of ADS. The hip range of motion of the left hindlimb in the ADS group was significantly larger ($p > 0.05$) than baseline scores after the first 2 weeks of ADS (Weeks 5 and 6, $p < 0.0001$), became non-significantly different after 3 weeks of ADS (Week 6, $p = 0.6044$), and became significantly increased after 4 weeks (Week 8, $p = 0.0452$) of ADS. In the Control group (within-group comparisons), the hip range of motion was non-significantly different as compared to pre-

implant measures (Week 4) after the first week post-implant (Week 5, $p = 0.0679$), became significantly increased after 2 weeks post-implant (Week 6, $p < 0.0001$), and returned to a non-significant difference after 3 and 4 weeks post-implant (Week 7, $p = 0.1537$; Week 8, $p = 0.9126$). The hip range of motion of the left hindlimb in the Control group remained significantly higher ($p < 0.05$) than baseline measures for the first 3 weeks post-implant (Weeks 5, $p = 0.0052$; Week 6, $p < 0.0001$; Week 7, $p = 0.0186$) and became non-significantly different after 4 weeks post-implant (Week 8, $p = 0.4246$).

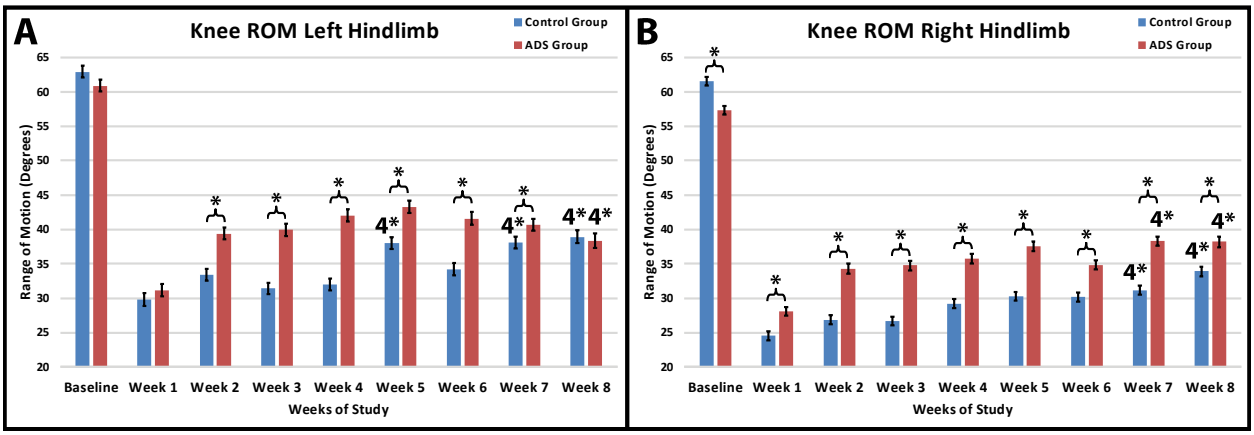

Figure 5.13. Average range of motion of the left (A) and right (B) knee joint (mean ± SE) in ADS and Control rats. Error bars are ± SE. ***** = Significant difference between groups when comparing groups (between-group comparison of the respected week; $p < 0.05$). **4*** = Significant increase when compared to Week 4 (pre-implant) measures (within-group comparison of the respective week; $p < 0.05$).

For the left hindlimb (Figure 5.13A), the range of motion of the knee joint was significantly different in the ADS group as compared (between-group comparisons) to the Control group from 2 to 7 weeks post-injury (Week 2 – 6, $p < 0.0001$; Week 7, $p = 0.0381$) and became non-significantly different after week 8 of the study (Week 8, $p = 0.6978$). In the ADS group (within-group comparisons), the knee range of motion was non-significantly different when compared to pre-implant measures (Week 4) after the first three weeks of ADS (Week 5, $p = 0.3241$; Week 6, $p = 0.7459$; Week 7, $p = 0.2766$) and became significantly lower after 4 weeks of ADS (Week 8, $p = 0.0086$). The knee range of motion of the left hindlimb in the ADS group was significantly smaller ($p < 0.05$) than baseline scores after all 4 weeks of ADS (Weeks

5—8, $p < 0.0001$) and did not return to pre-injury measures. In the Control group (within-group comparisons), the knee range of motion was significantly increased when compared to pre-implant measures (Week 4) after the 1st week post-implant (Week 5, $p < 0.0001$), decreased to a non-statistical difference after 2 weeks post-implant (Week 6, $p = 0.0848$), and significantly increased after weeks 3 and 4 of ADS (Weeks 7 and 8, $p < 0.0001$). The knee range of motion of the left hindlimb in the Control group remained significantly lower ($p < 0.05$) than baseline scores after all 4 weeks of ADS (Weeks 5—8, $p < 0.0001$) and did not return to pre-injury measures.

For the right hindlimb (Figure 5.13B), the range of motion of the knee joint was significantly different in the ADS group as compared (between-group comparisons) to the Control group for all eight weeks post-injury (Week 1 – 8, $p < 0.0001$). In the ADS group (within-group comparisons), the knee range of motion was non-significantly different when compared to pre-implant measures (Week 4) after the first two weeks of ADS (Week 5, $p = 0.0716$; Week 6, $p = 0.3333$) and became significantly higher after 3 and 4 weeks of ADS (Week 7, $p = 0.0087$; Week 8, $p = 0.0196$). The knee range of motion of the right hindlimb in the ADS group was significantly smaller ($p < 0.05$) than baseline scores after all 4 weeks of ADS (Weeks 5—8, $p < 0.0001$) and did not return to pre-injury measures. In the Control group (within-group comparisons), the knee range of motion of the right hindlimb was non-significantly different when compared to pre-implant measures (Week 4) after the first two weeks of ADS (Week 5, $p = 0.2078$; Week 6, $p = 0.3042$) and became significantly increased after 3 and 4 weeks of ADS (Week 7, $p = 0.0322$; Week 8, $p < 0.0001$). The knee range of motion of the right hindlimb in the Control group remained significantly lower ($p < 0.05$) than baseline scores after all 4 weeks of ADS (Weeks 5—8, $p < 0.0001$) and did not return to pre-injury measures.

DigiGait Parameters

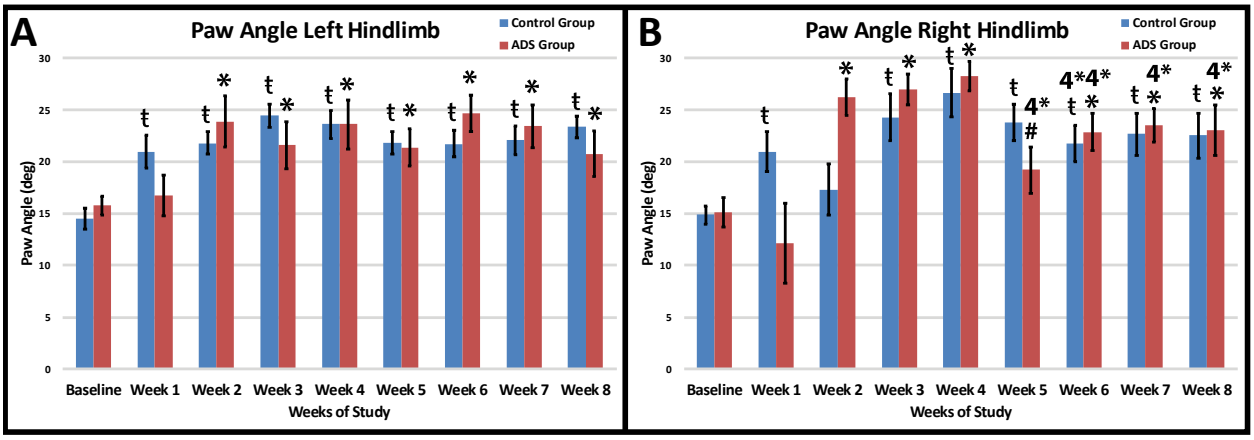

Figure 5.14. Average paw angle (mean ± SE) recorded on the DigiGait for the A) left and B) right hindlimb. A and B) * = Significant increase of paw angle when compared to baseline recordings (within-group comparison of ADS group; $p < 0.05$). ŧ = Significant increase of paw angle when compared to baseline recordings (within-group comparison of control group; $p < 0.05$). **4*** = Significant decrease of paw angle when compared to Week 4 recordings (within-group comparison of the respective week; $p < 0.05$).

Paw angle is displayed in Figure 5.14. Compared to baseline (i.e., within-group comparison), the paw angle significantly increased at 4 weeks post-SCI for both rat groups in both the left (Control, $p < 0.0001$; ADS, $p = 0.0006$) and right (Control, $p < 0.0001$; ADS, $p < 0.0001$) hindlimbs. After 4 weeks of ADS (i.e., Week 8), the paw angle was unchanged within-group in the left hindlimb (Control, p = 0.9150; ADS, p = 0.2381) when compared within-group to pre-implant (i.e., Week 4) measures.

Improvement of motor performance after ADS was only observed in one gait parameter on the DigiGait (i.e., paw angle); however, the paw angle did not return to baseline measures. After each week of ADS (i.e., Weeks 5, 6, 7, and 8), the paw angle of the right hindlimb was significantly decreased in the ADS group (Week 5, $p < 0.0001$; Week 6, $p = 0.0188$; Week 7, $p = 0.0378$; Week 8, $p = 0.0301$) when compared within-group to pre-implant (i.e., Week 4) measures.

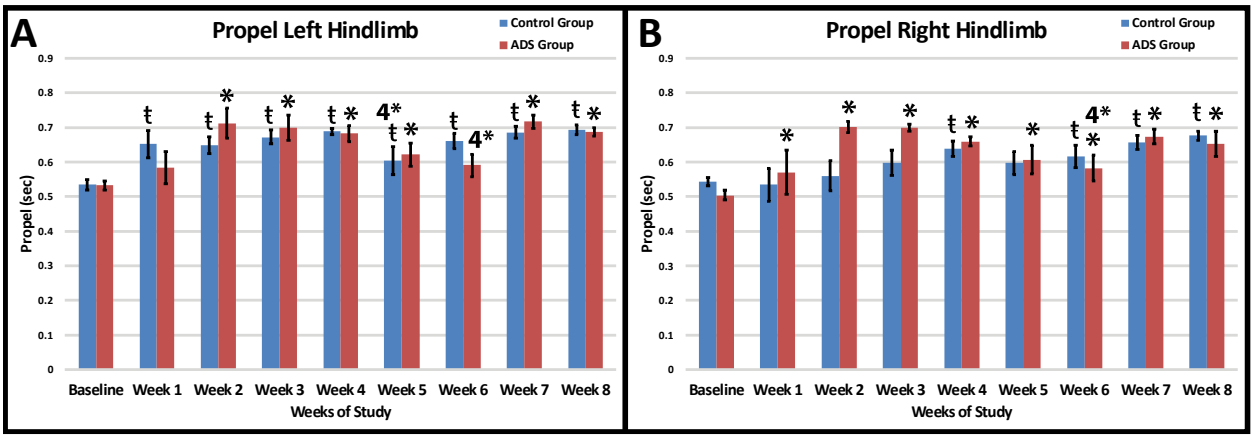

Figure 5.15. Average propel duration (mean ± SE) recorded on the DigiGait for the A) left and B) right hindlimb. A and B) * = Significant increase of propel duration when compared to baseline recordings (within-group comparison of ADS group; $p < 0.05$). ŧ = Significant increase of propel duration when compared to baseline recordings (within-group comparison of control group; $p < 0.05$). **4*** = Significant decrease of propel duration when compared to Week 4 recordings (within-group comparison of the respected group; $p < 0.05$).

Propel duration is displayed in Figure 5.15. Compared to baseline (i.e., within-group comparison), the propel duration significantly increased at 4 weeks post-SCI for both rat groups in both the left (Control, $p < 0.0001$; ADS, $p < 0.0001$) and right (Control, $p < 0.0001$; ADS, $p < 0.0001$) hindlimbs. After 4 weeks of ADS (i.e., Week 8), the propel duration was unchanged within-group in both the left (Control, $p = 0.2318$; ADS, $p = 0.8471$) and right (Control, $p = 0.8844$; ADS, $p = 0.8913$) hindlimbs when compared within-group to pre-implant (i.e., Week 4) measures.

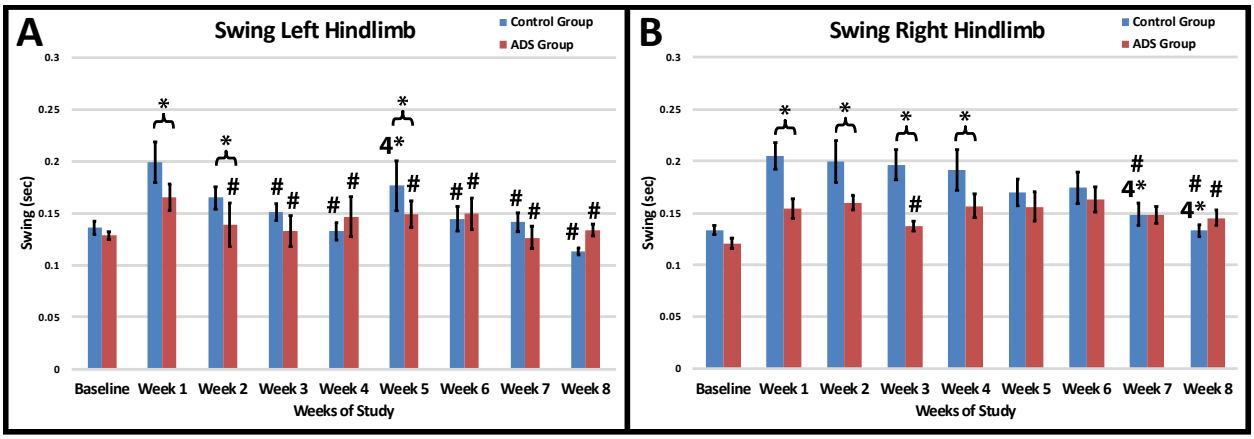

Figure 5.16. Average swing time (mean ± SE) recorded on the DigiGait for the A) left and B) right hindlimb. A and B) * = Significant difference when comparing the respective week of each group (between-group comparison; $p < 0.05$). # = Non-significant difference of swing time when compared to baseline recordings (within-group comparison of the respective group; $p < 0.05$). **4*** = Significant difference of swing time when compared to Week 4 recordings (within-group comparison of the respected group; $p < 0.05$).

Swing duration is displayed in Figure 5.16. Compared to baseline (i.e., within-group comparison), the stance time of the left hindlimb returned to a non-statistical difference after 2 weeks post-SCI (Week 2, $p = 0.3964$) and remained at baseline measures for the duration of the study in the ADS group. Similarly, the Control group returned to a non-statistical difference after 3 weeks post-SCI (Week 3, $p = 0.2233$); however, the swing time significantly increased after the first week post-implant (Week 5, $p = 0.0011$) but returned to baseline measures after 2 weeks post-implant (Week 6, $p = 0.4872$). Contrarily, there was a deficit seen in swing time in the right hindlimb (i.e., within-group comparison) pre-implant (ADS Week 4, $p = 0.0033$; Control Week 4, $p < 0.0001$). In the Control group, the swing time in the right hindlimb remained non-statistically different compared to pre-implant (Week 4) measures for the first two weeks post-implant (Week 5, $p = 0.0802$; Week 6, $p = 0.1607$) but returned to pre-injury (Baseline) measures after 3 weeks post-implant (Week 7, $p = 0.2320$) and remained at pre-injury measures 4 weeks post-implant (Week 8, $p = 0.9425$). In the ADS group, the swing time in the right hindlimb remained non-statistically different compared to pre-implant (Week 4) measures all four weeks post-implant (Week 5, $p = 0.9604$; Week 6, $p = 0.6133$; Week 7, $p = 0.4929$; Week 8, $p = 0.3751$) but returned to pre-injury (Baseline) measures after 4 weeks post-implant (Week 8, $p = 0.0548$).

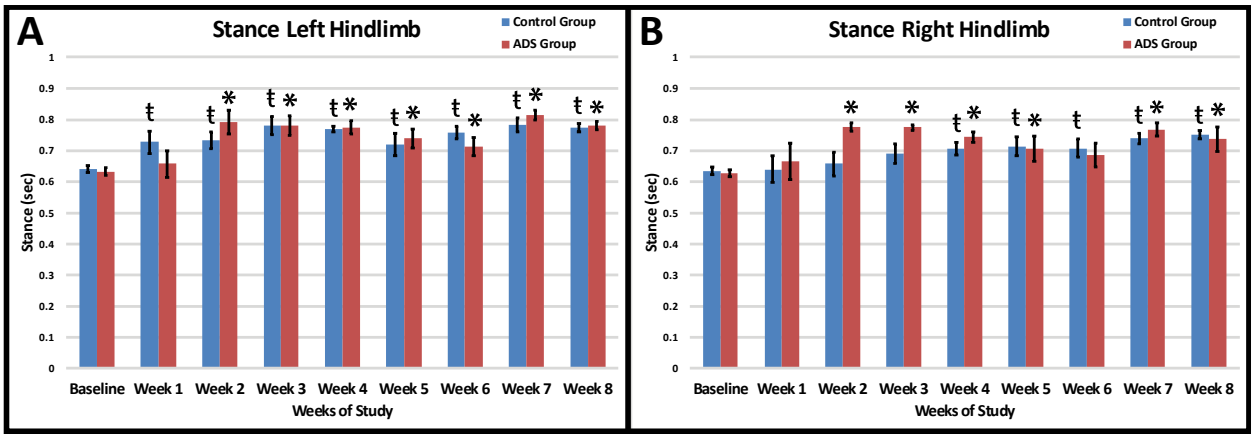

Figure 5.17. Average stance time (mean ± SE) recorded on the DigiGait for the A) left and B) right hindlimb. A and B) * = Significant increase of stance time when compared to baseline recordings (within-group comparison of ADS group; $p < 0.05$). ŧ = Significant increase of stance time when compared to baseline recordings (within-group comparison of control group; $p < 0.05$).

Stance duration is displayed in Figure 5.17. Compared to baseline (i.e., within-group comparison), the stance duration significantly increased at 4 weeks post-SCI for both rat groups in both the left (Control, $p = 0.0001$; ADS, $p < 0.0001$) and right (Control, $p = 0.0328$; ADS, $p = 0.0005$) hindlimbs. After 4 weeks of ADS (i.e., Week 8), the stance duration was unchanged within-group in both the left (Control, p = 0.9062; ADS, p = 0.8362) and right (Control, p = 0.1831; ADS, p = 0.8364) hindlimbs when compared within-group to pre-implant (i.e., Week 4) measures.

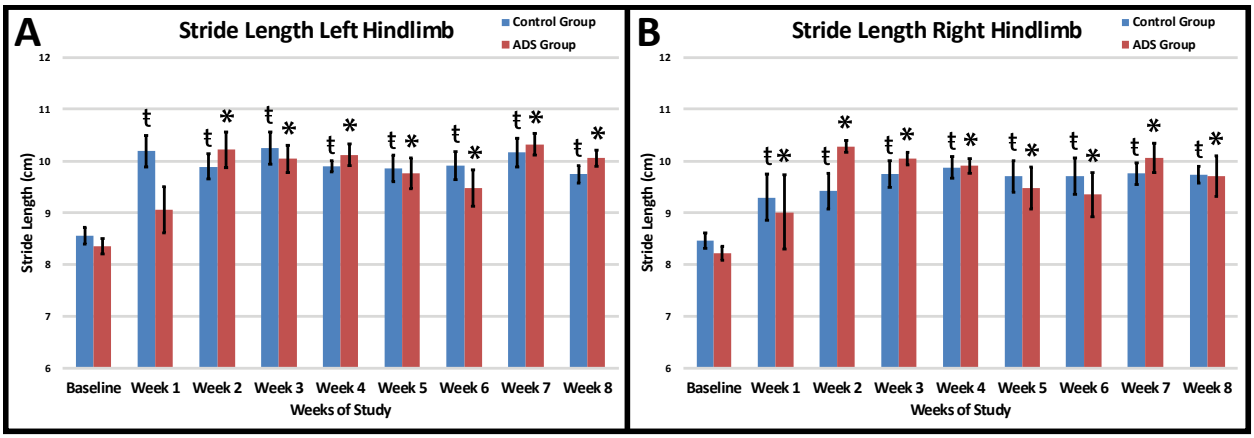

Figure 5.18. Average stride length (mean ± SE) recorded on the DigiGait for the A) left and B) right hindlimb. A and B) * = Significant increase of stride length when compared to baseline recordings (within-group comparison of ADS group; $p < 0.05$). ŧ = Significant increase of stride length when compared to baseline recordings (within-group comparison of control group; $p < 0.05$).

Stride length is displayed in Figure 5.18. Compared to baseline (i.e., within-group comparison), the stride length significantly increased at 4 weeks post-SCI for both rat groups in both the left (Control, $p = 0.0004$; ADS, $p < 0.0001$) and right (Control, $p = 0.0002$; ADS, $p < 0.0001$) hindlimbs. After 4 weeks of ADS (i.e., Week 8), the stride length was unchanged within-group in both the left (Control, p = 0.6704; ADS, p = 0.8865) and right (Control, p = 0.7028; ADS, p = 0.6184) hindlimbs when compared within-group to pre-implant (i.e., Week 4) measures.

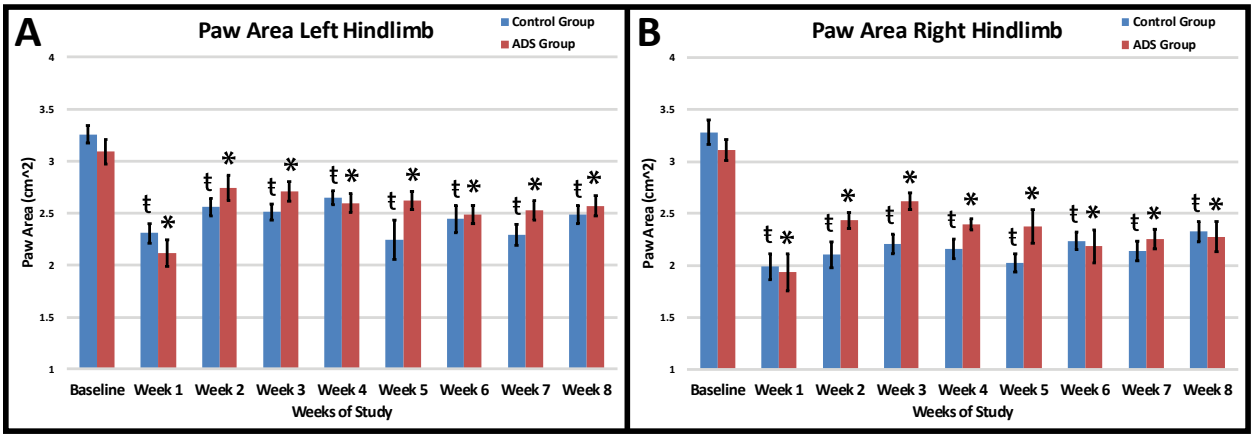

Figure 5.19. Average paw area (mean ± SE) recorded on the DigiGait for the A) left and B) right hindlimb. A and B) * = Significant decrease of paw area when compared to baseline recordings (within-group comparison of ADS group; $p < 0.05$). ŧ = Significant decrease of paw area when compared to baseline recordings (within-group comparison of control group; $p < 0.05$).

Paw area is displayed in Figure 5.19. Compared to baseline (i.e., within-group comparison), the paw area significantly increased at 4 weeks post-SCI for both rat groups in both the left (Control, $p < 0.0001$; ADS, $p < 0.0001$) and right (Control, $p < 0.0001$; ADS, $p < 0.0001$) hindlimbs. After 4 weeks of ADS (i.e., Week 8), the paw area was unchanged within-group in both the left (Control, p = 0.2109; ADS, p = 0.8206) and right (Control, p = 0.1846; ADS, p = 0.3679) hindlimbs when compared within-group to pre-implant (i.e., Week 4) measures.

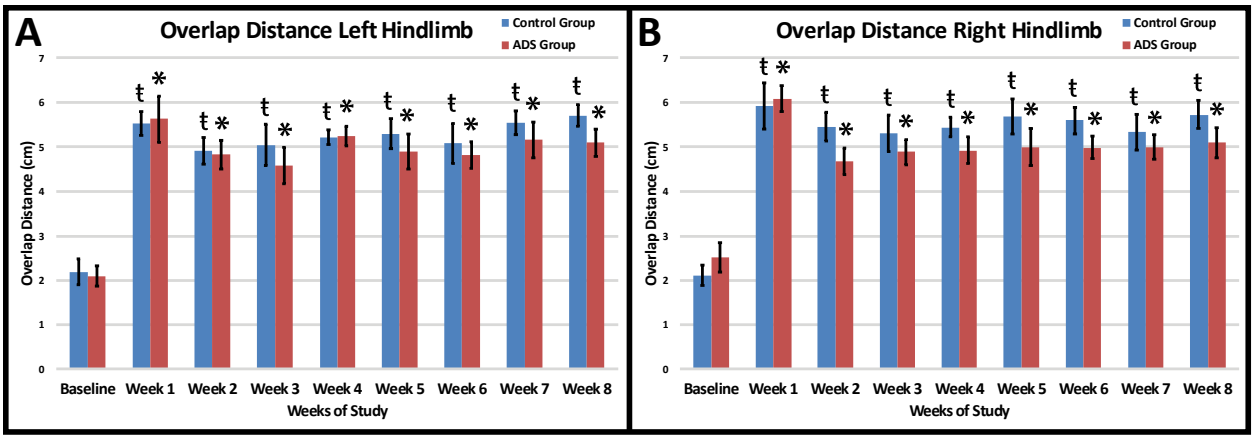

Figure 5.20. Average overlap distance between hind paws (mean ± SE) recorded on the DigiGait for the A) left and B) right hindlimb. A and B) * = Significant increase of paw overlap distance when compared to baseline recordings (within-group comparison of ADS group; $p < 0.05$). ŧ = Significant increase of paw overlap distance when compared to baseline recordings (within-group comparison of control group; $p < 0.05$).

Paw overlap is displayed in Figure 5.20. Compared to baseline (i.e., within-group comparison), the paw overlap distance significantly increased at 4 weeks post-SCI for both rat groups in both the left (Control, $p < 0.0001$; ADS, $p < 0.0001$) and right (Control, $p < 0.0001$; ADS, $p < 0.0001$) hindlimbs. After 4 weeks of ADS (i.e., Week 8), the paw overlap distance was unchanged within-group in both the left (Control, p = 0.2822; ADS, p = 0.7580) and right (Control, p = 0.5269; ADS, p = 0.7066) hindlimbs when compared within-group to pre-implant (i.e., Week 4) measures.

Foot-Faults on Horizontal Ladder Rung Walking Test

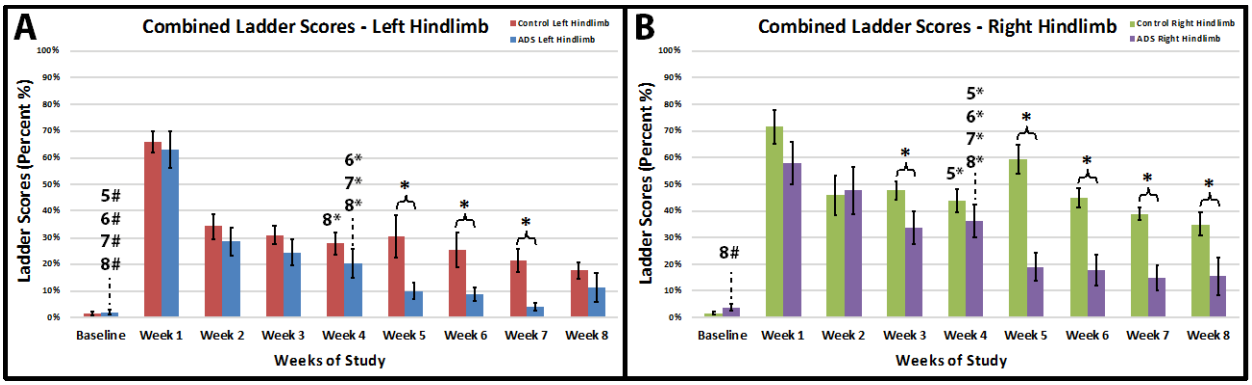

Figure 5.21. Average foot-fault scores (mean ± SE) on both horizontal ladder patterns for ADS and Control rats. A) Average foot-fault scores of the left hindlimb for ADS and Control rats. **B)** Average foot-fault scores of the right hindlimb for ADS and Control rats. Error bars are ± SE. ***** = $p < 0.05$. **5*, 6*, 7*, 8*** = $p < 0.05$ when comparing (within-group comparison) Week 4 to the respective week number. ***5*#, 6#, 7#, 8#** = $p > 0.05$ when comparing (within-group comparison) baseline to the respective week number.

For the left hindlimb (Figure 5.21A), foot-fault scores on the Horizontal Ladder were significantly lower in the ADS group compared to the Control group after 1 week of ADS (Week 5, $p < 0.0001$), 2 weeks of ADS (Week 6, $p = 0.0005$), and 3 weeks of ADS (Week 7, $p = 0.0008$) but returned to a non-significant difference after 4 weeks of ADS (Week 8, $p = 0.0554$). In the ADS group (within-group comparisons), foot-faults were significantly lower than pre-implant scores (Week 4) after 2 weeks of ADS (Week 6, $p = 0.0289$) and remained significantly lower than pre-implant scores (Week 4) after 3 weeks of ADS (Week 7, $p = 0.0039$) and after 4 weeks of ADS (Week 8, $p = 0.0311$). When compared to pre-injury (Baseline) measures, foot-fault scores were non-statistically different after all 4 weeks of ADS (Week 5, $p = 0.1175$; Week 6, $p = 0.2303$; Week 7, $p = 0.6004$; Week 8, $p = 0.2835$), essentially foot-fault scores returned to pre-injury measures after 1 week of ADS and remained at pre-injury measures after all 4 weeks of ADS. In the Control group (within-group comparisons), foot-fault scores remained non-statistically different ($p > 0.05$) than pre-implant scores (Week 4) after 3 weeks post-implant (Weeks 5, $p = 0.6683$; Week 6, $p = 0.5825$; Week 7, $p = 0.1616$) and became significantly lower than pre-implant measures after 4 weeks (Week 8, $p = 0.0292$). When compared to pre-injury

scores (Baseline), foot-fault scores after all 4 weeks (Weeks 5, 6, and 7, $p < 0.0001$; Week 8, $p = 0.0007$) remained significantly higher ($p < 0.05$) and did not return to pre-injury measures.

For the right hindlimb (Figure 5.21B), foot-fault scores on the Horizontal Ladder were significantly lower (between-group comparisons) in the ADS group compared to the Control group after all 4 weeks of ADS (Week 5, $p < 0.0001$; Week 6, $p < 0.0001$; Week 7, $p < 0.0001$; Week 8, $p < 0.0001$). In the ADS group (within-group comparisons), foot-fault scores became significantly lower than pre-implant scores (Week 4) after all 4 weeks of ADS (Week 5, $p = 0.0002$; Week 6, $p < 0.0001$; Week 7, $p < 0.0001$; Week 8, $p < 0.0001$). When compared to pre-injury scores (Baseline), foot-fault scores were non-statistically different after 4 weeks of ADS (Week 8, $p = 0.1466$), essentially returning to pre-injury measures. In the Control group (within-group comparisons), foot-fault scores were significantly lower than pre-implant scores (Week 4) after 1 week post-implant (Week 5, $p = 0.0045$) but returned to a non-statistical difference after 2 weeks post-implant (Week 5, $p = 0.8201$) and remained unchanged after 3 weeks (Week 7, $p = 03228$) and 4 weeks (Week 8, $p = 0.0853$) post-implant. When compared to pre-injury scores (Baseline), foot-fault scores remained significantly higher after all 4 weeks post-implant (Weeks 5—8, $p < 0.0001$) and did not return to pre-injury measures.

Foot-Faults on Tapered/Ledged Beam Test

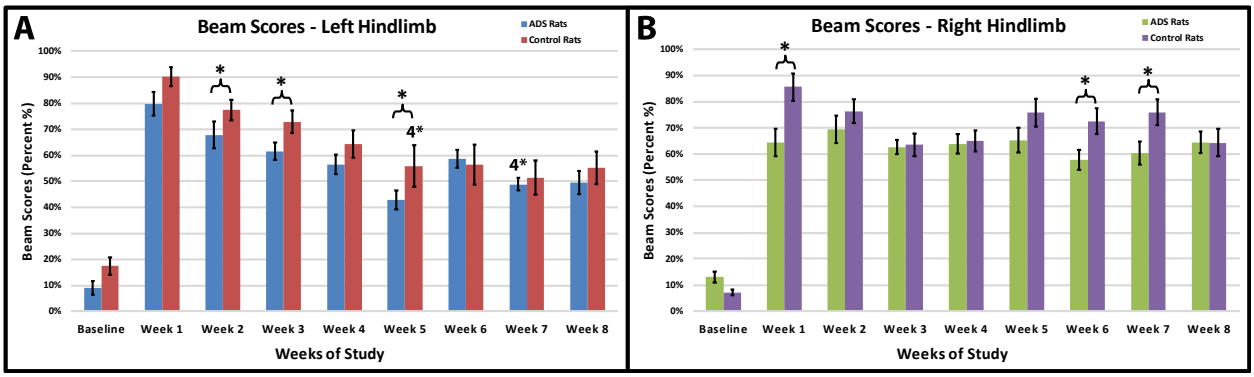

Figure 5.22. Average foot-fault scores (mean ± SE) on the narrowed beam task in ADS and Control rats. A) Average foot-fault scores of the left hindlimb in ADS and Control rats. **B)** Average foot-fault scores of the right hindlimb in ADS and Control rats. Error bars are ± SE. ***** = $p < 0.05$. **4*** = $p < 0.05$ when comparing (within-group comparison) to the respective week to Week 4.

For the left hindlimb (Figure 5.22A), foot-fault scores were only significantly different ($p > 0.05$) after week 2 ($p = 0.0446$), week 3 ($p = 0.0228$), and week 5 ($p = 0.0101$) of the study when comparing rats in the ADS and Control groups (between-group comparisons). In the ADS group (within-group comparisons), foot-fault scores became significantly lower than pre-implant scores (Week 4) after 1 week of ADS (Week 5, $p = 0.0131$) but returned to a non-significant difference ($p > 0.05$) after 2 weeks (Week 6, $p = 0.6761$) of ADS and remained unchanged after 3 weeks (Week 7, $p = 0.1636$) and 4 weeks (Week 8, $p = 0.4006$) of ADS. When comparing each week of ADS (Weeks 5 – 8) to pre-injury (Baseline) measures, foot-fault scores remained significantly increased ($p < 0.0001$) and did not return to pre-injury measures after each week of ADS. In the Control group (within-group comparisons), foot-fault scores were significantly lower 1-week (Week 5, $p = 0.0131$) post-implant but returned to pre-implant (Week 4) measures 2 weeks (Week 6, $p = 0.6761$) post-implant and remained unchanged after 3 and 4 weeks post-implant (Week 7, $p = 0.1636$; Week 8, $p = 0.4006$). When comparing each week of the study (Weeks 5 – 8) to pre-injury (Baseline), foot-fault scores remained significantly increased ($p < 0.0001$) measures and did not return to pre-injury measures.

For the right hindlimb (Figure 5.22B), foot-fault scores were significantly different (between-group comparisons; $p < 0.05$) after 2 weeks of ADS (Week 6; $p = 0.0157$) and 3

weeks of ADS (Week 7; $p = 0.0106$) but returned to a non-significant difference ($p > 0.05$) after 4 weeks of ADS (Week 8). In the ADS group (within-group comparisons), foot-fault scores were not significantly different ($p > 0.05$) after all 4 weeks of ADS (Week 5, $p = 0.8025$; Week 6, $p = 0.2970$; Week 7, $p = 0.5430$; Week 8, $p = 0.8950$) when compared to pre-implant (Week 4) measures. When comparing each week of ADS (Weeks 5—8) to pre-injury (Baseline) measures, foot-fault scores remained significantly increased ($p < 0.0001$) and did not return to pre-injury measures after each week of ADS. In the Control group (within-group comparisons), foot-fault scores were not significantly different ($p > 0.05$) after all 4 weeks of ADS (Week 5, $p = 0.0572$; Week 6, $p = 0.1893$; Week 7, $p = 0.0576$; Week 8, $p = 0.9096$) when compared to pre-implant (Week 4) measures. When comparing each week of the study (Weeks 5 – 8) to pre-injury (Baseline), foot-fault scores remained significantly increased ($p < 0.0001$) and did not return to pre-injury measures.

Discussion

This proof-of-concept study demonstrations that activity dependent stimulation (ADS) using spike-triggered intraspinal microstimulation (ISMS) can enhance behavioral recovery of locomotor function, as measured by various behavioral tasks after spinal cord injury (SCI). The use of ADS to enhance functional connectivity between distant neuronal populations has been similarly conducted in various injury models resulting in behavioral recovery (Moritz, Perlmutter et al. 2008, Guggenmos, Azin et al. 2013, Zimmermann and Jackson 2014, McPherson, Miller et al. 2015). Most importantly, behavioral recovery was seen after ADS was applied across a bilateral spinal cord contusion and a clearly polysynaptic connection. The present study demonstrates that the ADS approach is translatable to rat models of spinal cord contusion specific to hindlimb control.

Mechanisms Mediating Functional Recovery From ADS

The mechanisms underlying the therapeutic effects of ADS after injury in the present model of SCI are still somewhat theoretical. The functional state of spinal network excitability of interneurons (Bannatyne, Liu et al. 2009) and motor neurons was modulated by the sub-threshold ISMS (i.e., 50% movement threshold), presumably driving them closer to their appropriate activation threshold, enabling intentional/voluntary movement. As a result, loss of voluntary control of movement may be attributed to not only a physical interruption of descending connections but also to a physiological change of the normal/baseline state of excitability of the spinal circuitry.

Following the notion of Hebbian plasticity (Hebb 1949), it was shown previously that the strength of two synaptically connected neurons, still intact after a bilateral spinal cord contusion between the hindlimb motor cortex and lumbar spinal cord, could be strengthened after 3 hours of ADS (Borrell, Krizsan-Agbas et al. 2018). The increased excitability seen previously could have resulted in the behavioral recovery seen in this study. In prior experiments, we have

demonstrated enhanced functional connectivity and lasting improvements to grasp function using a neural prosthesis that connected premotor and somatosensory cortex in a rodent model of focal brain injury (Guggenmos, Azin et al. 2013). The behavioral recovery reported here suggests that the Hebbian process is translatable to various injury models. Similarly, Zimmermann and Jackson (Zimmermann and Jackson 2014) have demonstrated in monkeys with muscimol inactivation of primary motor cortex that closed-loop stimulation between cortex and spinal cord could strengthen surviving descending pathways. This was previously shown in healthy monkeys but via closed-loop cortical stimulation which resulted in strengthened cortical connectivity by a Hebbian process (Jackson, Mavoori et al. 2006). Finally, Nishimura et al. (Nishimura, Perlmutter et al. 2013) have demonstrated that similar Hebbian mechanisms may also act at corticospinal connections in the monkey, and McPherson et al. (McPherson, Miller et al. 2015) have shown increased efficacy of damaged but spared neural circuits in a rodent model of SCI in a manner consistent with that shown here.

Additional mechanisms (Raineteau and Schwab 2001, Darian-Smith 2009) that were not shown but could be involved in the behavioral recovery seen here include one or a combination of the following: 1) structural plasticity which could include dendritic changes (increased length), axonal sprouting, and increased spine density, 2) electrophysiological plasticity which could include motor map reorganization, synaptic strengthening, and synaptic weakening, and 3) neurotransmitter plasticity which could include a change in GABAergic neurons, receptor subunit expression, and neurotrophic factors.

Potential Motor Pathways Conditioned by ADS

There are three descending motor pathways that mainly influence hindlimb motor function in the rat: corticospinal tract (CST), rubrospinal tract (RbST), and reticulospinal tract (RtST). It has been shown that corticospinal axons are severely damaged, regardless of spinal cord contusion severity (Basso, Beattie et al. 2002). Additionally, based on the qualitative level of white matter remaining after injury, the RbST in the dorsolateral funiculus and the RtST in the

ventrolateral funiculus appear to be relatively intact after the bilateral spinal cord contusion used in this study.

With the spinal cord contusion used in this study, it has been shown that hindlimb spinal cord activity can still be evoked via cortico-reticulo-spinal pathways that remain intact after injury (Frost, Borrell et al. 2018). Using the BBB locomotor score, spared RtST fibers have been shown to result in the recovery of 7 to 8 points, as compared to a recovery of 1 to 2 points due to spared CST fibers, and indicated that the RtST has a major influence on the initiation and control of open-field locomotion (Schucht, Raineteau et al. 2002). Significant increases in BBB scores (roughly 3—4 points) in the ADS group were observed in this study for both hindlimbs. This recovery in BBB scores alone suggests that ADS may have strengthened the cortico-reticulo-spinal pathways which resulted in improved control of open-field locomotion.

Furthermore, forelimb-hindlimb (FL-HL) and left-right coordination (i.e., interlimb coordination) is controlled via long descending propriospinal pathways (Frigon 2017). The amount of propriospinal sparing was uncertain, but it has been shown that long descending propriospinal axons are almost completely lost in the cervical cord with this type of injury (Basso, Beattie et al. 2002), which would lead one to assume that FL-HL coordination would be lost. Conversely, it has been shown that long descending propriospinal pathways are located in the ventrolateral funiculus, which appears to remain undamaged after injury in this study (Reed, Shum-Siu et al. 2006). Nonetheless, FL-HL coordination was recovered before electrode implantation (BBB score of ~14 after Week 4) and remained present after ADS therapy which suggests that some propriospinal axons remained intact. Since propriospinal pathways have been shown to receive a large number of terminals from reticulospinal neurons (Mitchell, McCallum et al. 2016), this suggests that coordination is strongly controlled via the RtST and further backs the notion that ADS strengthened cortico-reticulo-spinal fibers. However, if propriospinal pathways were disrupted after injury, it has been shown that recovery of FL-HL coordination is also associated with the number of rubrospinal axons spared after injury,

especially if long descending propriospinal axon sparing is insufficient (Basso, Beattie et al. 2002). Similarly, in Celsr3/EMx1 (i.e., CST absent) mice, it has been shown that the red nuclei and RbST increased in size in the absence of the entire CST but does not affect the RtST (Han, Cao et al. 2015). This suggests that the RbST may compensate after CST ablation and help restore FL-HL coordination. In addition to a strengthened cortico-reticulo-spinal pathway due to ADS, plasticity most likely occurs with the RbST depending on the remaining number of long descending propriospinal neurons after injury.

When measuring intralimb coordination, there was recovery of the ROM of the hip and improvement of the ROM of the knee. These changes in ROM measures could have simply been compensatory due to the trunk instability obtained from the injury in the thoracic cord, especially since the circuitry involving rhythmic hindlimb locomotion (i.e., the circuitry below the injury) remains intact after injury (Kiehn 2006). Trunk instability was still present after ADS which suggests there are still compensatory deficits seen in the ROM, especially with the knee. However, the amount of remaining descending pathways innervating hip and knee motoneurons after injury is still uncertain. It has been shown in cats that the RbST tract excites hindlimb flexor motoneurons via polysnaptic pathways (Hongo, Jankovska et al. 1969) which are modulated in phase with the locomotor cycle, with maximal discharge at the swing phase when flexors are active (Orlovsky 1972). Additionally, it has been shown in cats that injury to the RtST caused an increase in the variability of the step cycle duration but no major changes in the step cycle structure or in the intralimb coupling of the joints suggesting that the RtST plays no role in intralimb coupling (Brustein and Rossignol 1998). In addition to intralimb coordination, deficits were seen in various phases of the locomotor cycle (i.e., propel, stance, etc.) which agree with previous studies involving CST damage (Krizsan-Agbas, Winter et al. 2014); however, there was recovery of swing phase after ADS. These deficits in the locomotor cycle and intralimb coordination and return to pre-injury swing time measures suggest an undamaged

or plastic RbST while the deficits that remained after ADS suggest a damaged CST that wasn't recovered or strengthened.

The ladder rung walking task was used to assess skilled walking (i.e., aiming, fine-adjustment, limb coordination, and balanced weight supported stepping), which is assumed to rely more strongly on CST function (Metz and Whishaw 2002). The narrowed beam task was used to test weight bearing and fine motor adjustments during gait as well as to remove compensatory strategies that provide balance to non-impaired limbs (Schallert, Woodlee et al. 2002). Surprisingly, foot fault scores on the horizontal ladder walking task returned to pre-injury measures in both hindlimbs after ADS therapy; however, no improvement was observed in either hindlimb on the narrowed beam task after ADS therapy. No improvement on the narrowed beam task was expected as trunk stability never returned after ADS therapy, as observed in the final BBB scores and the severity of the injury in the gray matter of the thoracic spinal cord. Thus, rats would not be able to balance themselves appropriately on the beam. However, aiming, fine-adjustment, and limb coordination seemed to improve, as noted on the ladder rung walking task. This suggests that there may be some recovery of the CST, especially since the CST has been shown to play a major role in the precise control over paw placement and limb trajectory (Drew, Jiang et al. 2002). Due to the extent of the injury on the descending corticospinal fibers, this seems highly unlikely and suggests that the RbST may have played a role in the recovery seen on the ladder rung walking task (Basso, Beattie et al. 2002); however, a strengthened cortico-reticulospinal tract cannot be ruled out as it has the capacity to deliver information from the cortex to the spinal cord in the absence of direct CST input (Mitchell, McCallum et al. 2016).

Finally, the ventral CST has been shown to sprout and parallel functional recovery after a dorsal transection in the cervical enlargement of the rat (Weidner, Ner et al. 2001). It is unknown if this sprouting occurs after a thoracic contusion. Nonetheless, it was assumed that the dorsolateral (with possible minor damage) and ventral CSTs remain relatively intact after

injury in this study. The recovery seen after ADS therapy could additionally involve plasticity of the dorsolateral and ventral CSTs in chorus with rubrospinal and reticulospinal fibers.

Limitations of Study

The main limitation to this study was the inability to evoke motor movement 1—3 days post-implant. This could have been due to one or a combination of the following factors: 1) The microwire was pushed out of the cord; 2) Extensive scar tissue formed around the microwire thus driving the maximum current needed to evoke movement (i.e., movement threshold) well above the maximum current that was used in this study (i.e., 100 μA with 1 biphasic pulse); 3) The microwire shifted in the spinal cord but was not removed from the spinal cord. Future studies involving implantable microwires directly into the spinal cord would benefit from being able to evoke a hindlimb movement well after the implantation procedure and would act as an additional verification that the microwire is still implanted correctly. It is uncertain from the histological cross-section of the microwire tract how long the microwire remained in the cord; however, the narrow medio-lateral width of the tract indicates that it remained relatively stationary. Nonetheless, the recorded impendences of the microwire throughout the study indicate that we were able to drive the correct current during ADS. Finally, the behavioral recovery seen after each week of ADS suggests that the microwire was still able to produce a neuromodulatory effect that aided in the behavioral recovery seen in this study.

Conclusion

Spike-triggered intraspinal microstimulation was shown to significantly improve hindlimb motor performance after a moderate spinal cord contusion. The behavioral recovery shown here indicates that activity dependent stimulation may have strengthened cortico-reticulospinal fibers in parallel with plasticity of rubrospinal, dorsolateral corticospinal, and ventral corticospinal fibers. These data will inform the future development of activity-dependent based therapies which have been shown to be translatable across mono- and multi-synaptic pathways as well as various injuries related to the central nervous system.

Acknowledgments

This work was supported by the Paralyzed Veterans of America Research Foundation #3068, The Ronald D. Deffenbaugh Family Foundation, NIH/NINDS R01 NS030853, T32 Neurological Rehabilitation Sciences Training Program, and NIH/NINDS F31 NS105442. The authors thank Erica Hoover and Matthew Jaeschke for exceptional technical support.

References

Bamford, J. A., R. Marc Lebel, K. Parseyan and V. K. Mushahwar (2017). "The Fabrication, Implantation, and Stability of Intraspinal Microwire Arrays in the Spinal Cord of Cat and Rat." IEEE Trans Neural Syst Rehabil Eng **25**(3): 287-296.

Bannatyne, B. A., T. T. Liu, I. Hammar, K. Stecina, E. Jankowska and D. J. Maxwell (2009). "Excitatory and inhibitory intermediate zone interneurons in pathways from feline group I and II afferents: differences in axonal projections and input." J Physiol **587**(2): 379-399.

Basso, D. M., M. S. Beattie and J. C. Bresnahan (1995). "A sensitive and reliable locomotor rating scale for open field testing in rats." J Neurotrauma **12**(1): 1-21.

Basso, D. M., M. S. Beattie and J. C. Bresnahan (2002). "Descending systems contributing to locomotor recovery after mild or moderate spinal cord injury in rats: experimental evidence and a review of literature." Restor Neurol Neurosci **20**(5): 189-218.

Borrell, J. A., S. B. Frost, J. Peterson and R. J. Nudo (2017). "A 3D map of the hindlimb motor representation in the lumbar spinal cord in Sprague Dawley rats." J Neural Eng **14**(1): 016007.

Borrell, J. A., D. Krizsan-Agbas, R. J. Nudo and S. B. Frost (2018). Optimal spike-stimulus delay for increasing synaptic efficacy in descending motor pathways using an actiivty dependent stimulation paradigm in an acute, anesthetized rat model of spinal cord injury. Society for Neuroscience. San Diego, Abstract.

Brustein, E. and S. Rossignol (1998). "Recovery of locomotion after ventral and ventrolateral spinal lesions in the cat. I. Deficits and adaptive mechanisms." J Neurophysiol **80**(3): 1245-1267.

Capogrosso, M., T. Milekovic, D. Borton, F. Wagner, E. M. Moraud, J. B. Mignardot, N. Buse, J. Gandar, Q. Barraud, D. Xing, E. Rey, S. Duis, Y. Jianzhong, W. K. Ko, Q. Li, P. Detemple, T. Denison, S. Micera, E. Bezard, J. Bloch and G. Courtine (2016). "A brain-

spine interface alleviating gait deficits after spinal cord injury in primates." Nature **539**(7628): 284-288.

Darian-Smith, C. (2009). "Synaptic plasticity, neurogenesis, and functional recovery after spinal cord injury." Neuroscientist **15**(2): 149-165.

Drew, T., W. Jiang and W. Widajewicz (2002). "Contributions of the motor cortex to the control of the hindlimbs during locomotion in the cat." Brain Res Rev **40**(1-3): 178-191.

Frigon, A. (2017). "The neural control of interlimb coordination during mammalian locomotion." J Neurophysiol **117**(6): 2224-2241.

Frost, S. B., J. A. Borrell, D. Krizsan-Agbas and R. J. Nudo (2018). Effects of contusive spinal cord injury on spinal motor neuron activity, corticospinal coupling, and conduction time in rats. Society for Neuroscience. San Diego, Abstract.

Frost, S. B., C. L. Dunham, S. Barbay, D. Krizsan-Agbas, M. K. Winter, D. J. Guggenmos and R. J. Nudo (2015). "Output Properties of the Cortical Hindlimb Motor Area in Spinal Cord-Injured Rats." J Neurotrauma **32**(21): 1666-1673.

Frost, S. B., M. Iliakova, C. Dunham, S. Barbay, P. Arnold and R. J. Nudo (2013). "Reliability in the location of hindlimb motor representations in Fischer-344 rats: laboratory investigation." J Neurosurg Spine **19**(2): 248-255.

Guggenmos, D. J., M. Azin, S. Barbay, J. D. Mahnken, C. Dunham, P. Mohseni and R. J. Nudo (2013). "Restoration of function after brain damage using a neural prosthesis." PNAS **110**(52): 21177-21182.

Han, Q., C. Cao, Y. Ding, K. F. So, W. Wu, Y. Qu and L. Zhou (2015). "Plasticity of motor network and function in the absence of corticospinal projection." Exp Neurol **267**: 194-208.

Hebb, D. O. (1949). The Organization of Behavior. Wiley, New York.

Hongo, T., E. Jankovska and A. Lundberg (1969). "The rubrospinal tract. I. Effects on alpha-motoneurons innervating hindlimb muscles in cats." Exp. Brain Res. **7**: 344-364.

Jackson, A., J. Mavoori and E. E. Fetz (2006). "Long-term motor cortex plasticity induced by an electronic neural implant." Nature **444**(7115): 56-60.

Jackson, A. and J. B. Zimmermann (2012). "Neural interface for brain and spinal cord - restoring motor function." Nat Rev Neurol **8**: 690-699.

Kiehn, O. (2006). "Locomotor Circuits in the Mammalian Spinal Cord." Annual Review of Neuroscience **29**(1): 279-306.

Krizsan-Agbas, D., M. K. Winter, L. S. Eggimann, J. Meriwether, N. E. Berman, P. G. Smith and K. E. McCarson (2014). "Gait Analysis at Multiple Speeds Reveals Differential Functional and Structural Outcomes in Response to Graded Spinal Cord Injury." Journal of Neurotrauma **31**(9): 846-856.

McPherson, J. G., R. R. Miller and S. I. Perlmutter (2015). "Targeted, activity-dependent spinal stimulation produces long-lasting motor recovery in chronic cervical spinal cord injury." Proc Natl Acad Sci U S A **112**(39): 12193-12198.

Metz, G. A. and I. Q. Whishaw (2002). "Cortical and subcortical lesions impair skilled walking in the ladder rung walking test: a new task to evaluate fore- and hindlmb stepping, placing, and co-ordination." Journal of Neuroscience Methods **115**: 169-179.

Mitchell, E. J., S. McCallum, D. Dewar and D. J. Maxwell (2016). "Corticospinal and Reticulospinal Contacts on Cervical Commissural and Long Descending Propriospinal Neurons in the Adult Rat Spinal Cord; Evidence for Powerful Reticulospinal Connections." PLoS One **11**(3): e0152094.

Moritz, C. T., S. I. Perlmutter and E. E. Fetz (2008). "Direct control of paralysed muscles by cortical neurons." Nature **456**(7222): 639-642.

Nishimura, Y., S. I. Perlmutter, R. W. Eaton and E. E. Fetz (2013). "Spike-timing-dependent plasticity in primate corticospinal connections induced during free behavior." Neuron **80**(5): 1301-1309.

Nishimura, Y., S. I. Perlmutter and E. E. Fetz (2013). "Restoration of upper limb movement via artificial corticospinal and musculospinal connections in a monkey with spinal cord injury." Front Neural Circuits **7**: 57.

Orlovsky, G. N. (1972). "Activity of Rubrospinal Neurons during Locomotion." Brain Research **46**(Nov13): 99-&.

Raineteau, O. and M. E. Schwab (2001). "Plasticity of motor systems after incomplete spinal cord injury." Nat Rev Neurosci **2**(4): 263-273.

Reed, W. R., A. Shum-Siu, S. M. Onifer and D. S. Magnuson (2006). "Inter-enlargement pathways in the ventrolateral funiculus of the adult rat spinal cord." Neuroscience **142**(4): 1195-1207.

Schallert, T., M. T. Woodlee and S. M. Fleming (2002). "Disentangling multiple types of recovery from brain injury." In: Krieglstein J, Klumpp S, editors. Pharmacology of cerebral ischemia. Stuttgart: Medpharm Scientific Publishers: 201-216.

Schucht, P., O. Raineteau, M. E. Schwab and K. Fouad (2002). "Anatomical Correlates of Locomotor Recovery Following Dorsal and Ventral Lesions of the Rat Spinal Cord." Experimental Neurology **176**(1): 143-153.

Shahdoost, S., S. Frost, D. J. Guggenmos, J. A. Borrell, S. Barbay, R. Nudo and P. Mohseni (2016). "A Miniaturized Brain-Machine-Spinal Cord Interface (BMSI) for Closed-Loop Intraspinal Microstimulation." IEEE Biomedical Circuits and Systems Conference: 364-367.

Shallert, T., M. T. Woodlee and S. M. Fleming (2002). "Disentangling multiple types of recovery from brain injury." Pharmacology of Cerebral Ischemia: 201-216.

Sherrington, C. S. (1892). "Notes on the arrangement of some motor fibres in the lumbo-sacral plexus." J Physiol **13**(6): 621-772.617.

Weidner, N., A. Ner, N. Salimi and M. H. Tuszynski (2001). "Spontaneous corticospinal axonal plasticity and functional recovery after adult central nervous sytem injury." PNAS **98**(6): 3513-3518.

Zimmermann, J. B. and A. Jackson (2014). "Closed-loop control of spinal cord stimulation to restore hand function after paralysis." Front Neurosci **8**: 87.

CHAPTER SIX: Summary

Summary of Study

The primary goal of this dissertation was to test the central hypothesis that precisely-timed activity dependent stimulation (ADS) in a rat model of spinal cord contusion will result in potentiation of corticospinal and corticobulbar connections as well as enhanced motor recovery after SCI. The results of this dissertation indicate that ADS therapy, in as early as 1-week, can improve hindlimb locomotion in spinal cord injured rats and continue to improve hindlimb locomotion after subsequent weeks of ADS therapy for up to 4 weeks.

The first study determined the effects of a contusive spinal cord injury on spinal motor neuron activity, corticospinal coupling, and conduction time in rats. The results showed that spinal cord responses could still be evoked after injury. After a moderate T8 spinal cord contusion, the retention of the short-latency responses indicated that spared descending spinal fibers, most likely via the cortico-reticulospinal pathway, can still depolarize spinal cord motor neurons after a dorsal midline contusion injury.

The second study determined the a spike-stimulus delay for increasing synaptic efficacy in descending motor pathways using an ADS paradigm in an acute, anesthetized rat model of SCI. The results showed that after 3 hours of ADS conditioning, using a 10 ms time delay and one stimulation pulse, ICMS-evoked spiking activity was significantly increased in the ventral horn at 10 ms post-onset ICMS. After 2 hours of ADS conditioning, using a 25 ms time delay and one or three stimulation pulses, resulted in significant increases in ICMS-evoked spiking activity in the dorsal/intermediate layers of the spinal gray matter at 10 ms post-onset ICMS. This activity continued to increase after 3 hours of ADS conditioning. These results showed that bouts of ADS conditioning can increase synaptic efficacy in intact descending motor pathways, as measured by cortically evoked activity in the spinal cord, after SCI.

The third study determined whether spike-triggered intraspinal microstimulation, using optimized spike-stimulus delays, results in improved motor performance in an ambulatory rat

model of SCI. ADS therapy enhanced the behavioral recovery of locomotor function after spinal cord injury, as measured by improved BBB scores, decreased foot faults on the Horizontal Ladder task, and improved intralimb coordination of the hip and knee.

Possible Mechanisms of Recovery

Currently, the mechanistic explanation as to how activity dependent stimulation promotes recovery is not known, but theories exist for investigation. First, Hebbian plasticity is most likely the primary mechanism involved in the behavioral recovery seen after ADS. With the use of ADS, it is assumed that Hebbian plasticity plays a major role in strengthening the connection between two neurons. This may be a way that ADS influences recovery: Neuronal connections are strengthened by constantly stimulating the ventral horn of the lumbar spinal cord when hindlimb motor cortex is active in a time-dependent manner; these anatomical connections may become stronger and influence the interaction between hindlimb motor cortex and hindlimb spinal cord. This has been shown between two neurons with a monosynaptic connection; however, it is uncertain how well the theory of Hebbian plasticity holds true between two neurons with a polysynaptic connection. In this study, enhanced synaptic efficacy and improved hindlimb motor performance was shown after ADS via a polysynaptic pathway, most likely the cortico-reticulo-spinal tract; however, these improvements will only occur under the rules of spike-timing dependent plasticity.

Secondly, axonal sprouting could serve as a mechanism for recovery. It has been shown that axonal sprouting can occur after injury alone. Understanding these newly created pathways that occur after injury could help direct the application of ADS to strengthen these new pathways. However, axonal sprouting could also be produced after the use of ADS therapy and could serve as an additional substrate for functional recovery. It is important to understand the temporal nature of axonal sprouting in relation to injury and ADS, as different time points of

axonal sprouting could parallel strengthened pathways to aid in behavioral recovery or be detrimental for recovery.

Finally, there are other mechanisms that could be involved in the behavioral recovery seen after ADS therapy that most likely occur alongside Hebbian plasticity and axonal sprouting. First, structural change could occur throughout the central nervous system. This could include changes in dendritic length and spine density. Second, electrophysiological change could occur in the pathways of interest. This could include motor map reorganization, changes in synaptic strength, and deviations in evoked potentials. Third, modulation of neurotransmitters could occur in essential neurons. This could include changes in the release of glutamate, GABAergic expression, and function of receptor subunits.

Future Studies

Anatomical Analysis

One fundamental question that remains after this study is: Does activity-dependent stimulation induce any changes in the anatomical projections following a spinal cord contusion? This is an anatomical study that can be achieved via tract tracing of the descending pathways of interest. However, in order to answer this question, there are a few subset questions that need to be answered beforehand.

First, which descending pathways remain intact after spinal cord contusion? Previous tract tracing studies have been conducted using different contusion models. It was assumed in this study that the reticulospinal and rubrospinal tracts remain relatively intact after the 175 kDyn, T8 contusion used in this study, but it should be verified anatomically in a tract tracing study after injury. This question could be applied to the dorsolateral and ventral corticospinal tracts as well.

Second, does axonal sprouting occur after spinal cord contusion? This is an important question because axonal sprouting could also occur as a result of ADS therapy. Hence, there

are two time periods in which axonal sprouting could occur: 1) After injury and 2) after ADS. It is important to understand when axonal sprouting occurs and at which stages of the study (i.e., the observed axonal sprouting is due to injury or ADS therapy).

Electrophysiological Analysis

Another fundamental question that remains after this study is: What is the functional role of the strengthened pathways after ADS therapy? It is assumed that the cortico-reticulo-spinal tract has been strengthened and assumes the role of the injured corticospinal tract after ADS. After injury, hindlimb responses can no longer be evoked from the hindlimb motor cortex via intracortical microstimulation. If the cortico-reticulo-spinal tract has assumed the role of the CST, we should be able to evoke hindlimb movement again from the hindlimb motor cortex. Accessing the hindlimb motor cortex would require removing the dental acrylic cap that housed the chronic recording electrode in the hindlimb motor cortex, which proved to be a difficult. Additionally, we were unable to drive a large enough current through the recording electrode to evoke a hindlimb movement. The development of a chamber that houses the chronic electrode microarray as well as permits easy removal of the electrode would allow for easy access to the hindlimb motor cortex for further electrophysiological study after a long-term study. Evoking a hindlimb response, either physical movement or EMG, via ICMS in the hindlimb motor cortex would validate the functional connectivity of this strengthened pathway.

Comparative Analysis

The last fundamental question that remains after this study is: How does activity dependent stimulation compare to other stimulation therapies? The first step to answer this question would be to test this set-up with a 10 ms time delay against a control stimulation therapy. However, there is debate on the proper control stimulation therapy that should be used to test against ADS therapy. The correct answer is probably variable depending on the parameters that are used for ADS. In this case, the main parameter of ADS is the time delay

between recorded spike and triggered stimuli. Control stimulation therapies could include a different time delay with regards to spike-timing dependent plasticity or random stimulation which would involve determining the proper stimulation frequency. Even though a non-therapy, control group was included in this study, it is important to compare the behavioral recovery from the ADS therapy used in this study to the behavioral recovery from other forms of stimulation therapy. This would help determine if ADS is the proper form of stimulation therapy to use to promote functional locomotor recovery in this rat model of spinal cord contusion.

Conclusions

The results from this study indicate that activity-dependent stimulation is an effective treatment for behavioral recovery following a moderate spinal cord contusion in the rodent. The implications of these results have the potential to lead to a novel treatment for a variety of neurological disease and disorders. We have the ability to reconnect two areas of the central nervous system after injury, as long as we understand how these areas are connected. With this study, we now have the ability to improve lower limb function by *strengthening spared descending pathways* to reconnect the brain to the spinal cord which in turn can *enhance voluntary control of movement* after incomplete spinal cord injuries. Most importantly, this therapeutic approach seems to be translatable across various injuries of the central nervous system and shows promise for future clinical studies. Such a treatment approach could augment concomitant physical and occupational therapy, *potentially reducing rehabilitation time*. Ultimately, patients *might regain some voluntary movement* due to the increased synaptic efficacy in remaining descending fibers after injury.